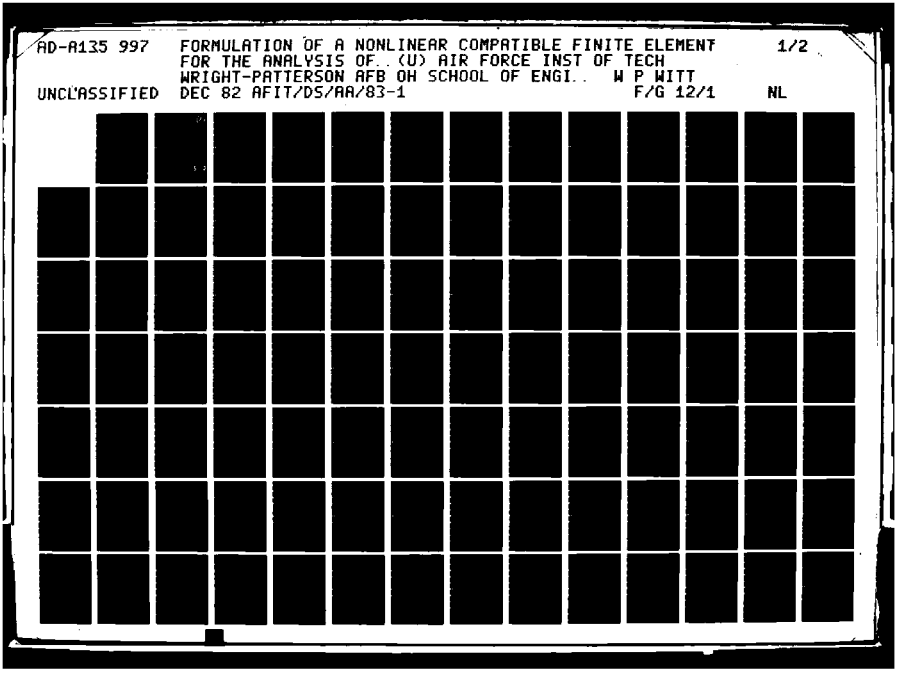
AD-A135 997
FORMULATION OF A NONLINEAR COMPATIBLE FINITE ELEMENT
FOR THE ANALYSIS OF.. (U) AIR FORCE INST OF TECH
WRIGHT-PATTERSON AFB OH SCHOOL OF ENGI.. W P WITT
UNCLASSIFIED
DEC 82 AFIT/DS/AA/83-1
F/G 12/1
1/2
NL

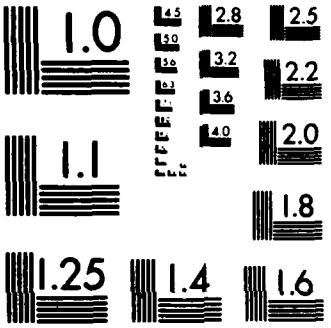

AFIT/DS/AA/~~80-4~~ 83-1

FORMULATION OF A NONLINEAR, COMPATIBLE FINITE ELEMENT FOR THE ANALYSIS OF LAMINATED COMPOSITES

DISSERTATION

AFIT/DS/AA/~~80-4~~ 83-1

William P. Witt, III
Major USAF

UNCLASSIFIED

SECURITY CLASSIFICATION OF THIS PAGE *(When Data Entered)*

REPORT DOCUMENTATION PAGE	READ INSTRUCTIONS BEFORE COMPLETING FORM
1. REPORT NUMBER AFIT/DS/AA/83-1 (~~80-4~~)	2. GOVT ACCESSION NO. AD-A131 997
3. RECIPIENT'S CATALOG NUMBER	
4. TITLE *(and Subtitle)* FORMULATION OF A NONLINEAR, COMPATIBLE FINITE ELEMENT FOR THE ANALYSIS OF LAMINATED COMPOSITES	5. TYPE OF REPORT & PERIOD COVERED Doctoral Dissertation
	6. PERFORMING ORG. REPORT NUMBER
7. AUTHOR(s) William P. Witt, III Major USAF	8. CONTRACT OR GRANT NUMBER(s)
9. PERFORMING ORGANIZATION NAME AND ADDRESS Air Force Institute of Technology(AFIT-EN) Wright-Patterson AFB, Ohio 45433	10. PROGRAM ELEMENT, PROJECT, TASK AREA & WORK UNIT NUMBERS
11. CONTROLLING OFFICE NAME AND ADDRESS	12. REPORT DATE December 1982
	13. NUMBER OF PAGES 125
14. MONITORING AGENCY NAME & ADDRESS*(if different from Controlling Office)*	15. SECURITY CLASS. *(of this report)* Unclassified
	15a. DECLASSIFICATION DOWNGRADING SCHEDULE

16. DISTRIBUTION STATEMENT *(of this Report)*

Approved for Public release; distribution unlimited.

17. DISTRIBUTION STATEMENT *(of the abstract entered in Block 20, if different from Report)*

18. SUPPLEMENTARY NOTES

Approved for public release IAW AFR 190-17.
LYNN E. WOLAVER
Dean for Research and Professional Development
Air Force Institute of Technology (AIC)
Wright-Patterson AFB OH 45433
9 SEP 1983

19. KEY WORDS *(Continue on reverse side if necessary and identify by block number)*

NONLIEAR FINITE ELEMENTS
LAMINATED COMPOSITES
TRANSVERSE SHEAR
NONLINEAR PLATE ANALYSIS

20. ABSTRACT *(Continue on reverse side if necessary and identify by block number)*

Increased use of laminated composites has pointed out the need for better analytic tools. These tools must be able to correctly account for normal shear in the laminates and should be able to solve nonlinear problems. The finite element method can be applied to analyze laminated composites, and this research presents a new and unique method to include nonlinear effects and normal shear effects. The finite element is formulated from basic elasticity equations. The most unique characteristic of the element is the

DD FORM 1 JAN 73 1473 EDITION OF 1 NOV 65 IS OBSOLETE UNCLASSIFIED

SECURITY CLASSIFICATION OF THIS PAGE *(When Data Entered)*

(Block 20 continued)

manner in which normal shear is handled. The normal to a reference surface is allowed to not only rotate but also change shape. Not only is displacement continuity imposed at lamina interfaces, but also slope continuity is guaranteed. After a complete general formulation of the finite element is presented, the method is specialized to plates so that the convergence characteristics, the accuracy, and the applicability of the element can be studied. The finite element does an excellent job of analyzing laminated composites, alt hough there is some degradation in accuracy as the plates become thinner. This finite element gives the analyst the ability to do nonlinear analysis of laminated composites under a variety of loading and boundary conditions.

AFIT/DS/AA/~~80-4~~ 83-1

FORMULATION OF A NONLINEAR, COMPATIBLE FINITE ELEMENT FOR THE ANALYSIS OF LAMINATED COMPOSITES

DISSERTATION

Presented to the Faculty of the
School of Engineering of the Air
Force Institute of Technology in
Partial Fulfillment of the Requirements
For the Degree of Doctor of Philosophy

by

William P. Witt, III, M.S.
Major USAF
PhD Aerospace Engineering
December 1982

AFIT/DS/AA/83-1

FORMULATION OF A NONLINEAR, COMPATIBLE FINITE ELEMENT FOR THE ANALYSIS OF LAMINATED COMPOSITES

by

William P. Witt, III, B.S., M.S.
Major USAF

Approved:

Anthony N. Palazotto Chairman	16 Dec 1982
B Van Kuyk	16 Dec 1982
Narendra Sekhar	16 Dec 1982
Peter J Torvik	16 Dec 1982
John Jones Jr.	16 Dec 1982
Hugh C Briggs	16 Dec 1982

Accepted:

J S Przemieniecki Dean, School of Engineering	22 Dec 1982

CONTENTS

PREFACE

Thank you to the U. S. Air Force for the opportunity.

Thank you to my committee for their patience.

Thanks to my advisor, Dr. Palazotto, for sticking with me.

Eternal thankfulness to my family for always being there

List of Figures

List of Tables

List of Symbols

$\bar{A}_i$ - Basis vectors.

A - Lame', constant for major radius of curvature.

$\bar{a}_\alpha$ - Basis vectors of reference surface.

$a_i, \{a\}$ - Degree of freedom vector.

a - Planar dimension of a plate.

B - Lame' constant for minor radius of curvature.

$b_i, \{b\}$ - Body force vector.

C_{ijkl} - Fourth order constituitive tensor.

C_u, C_v - Integration constants.

D_{rs} - Second order constituitive tensor.

$\bar{d}$ - Director vector; unit normal vector which passes through arbitrary point in reference structure.

E_L - Young's modulus in the direction parallel to the fibers.

E_T - Young's modulus in the direction perpendicular to the fibers.

$\bar{e}_1, \bar{e}_2$ - Unit vectors in primary directions of reference surface.

$e_i, \{e\}$ - Physical components of strain.

$f_i, \{f\}$ - Surface force vector.

G_{LT} - Shear modulus for shear in a plane parallel to fibers.

G_{TT} - Shear modulus for shear in a plane perpendicular to fibers.

g_{ij} - Metric of undeformed surface.

g^*_{ij} - Metric of deformed surface.

h - Total thickness of structure.

$[K^e_L]$ - Linear part of element stiffness matrix.

$[K^e_{NL}]$ - Nonlinear part of element stiffness matrix.

$\bar{K}_{ij}, [K_L]$ - Linear part of global stiffness matrix.

$\bar{\bar{K}}_{ij}, [K_{nl}]$ - Nonlinear part of global stiffness matrix.

$[L]$ - Operator matrix relating $\{e\}$ and $\{u\}$.

$[L_0]$ - Linear part of $[L]$.

$[\tilde{L}_1]$ - Nonlinear part of $[L]$ that is dependent on the deformations of the reference surface.

$[\hat{L}_1]$ - Nonlinear part of $[L]$ that is dependent on the deformations of the director.

l - Planar dimension of plate.

N_1, N_2, N_3 - Finite element shape functions which depend only on the surface coordinates.

n, n - Number of layers in thickness direction.

p - Proportional load factor.

$\bar{Q}$ - Normalized loading parameter.

q - Loading parameter.

$\{q^E\}$ - Element generalized external force vector.

$\{q\}$ - Global generalized external force vector.

$\bar{R}$ - Position vector of arbitrary point in undeformed structure.

$\bar{R}^*$ - Position vector of arbitrary point in deformed structure.

R_1 - Major radius of reference surface curvature.

R_2 - Minor radius of reference surface curvature.

$\bar{r}$ - Position vector of point on reference surface where the normal through arbitrary point intersects with the reference surface in undeformed structure.

S_{ij} - Second Piola-Kirchoff stress tensor.

S_p - Current stiffness parameter.

S - Thickness ratio, $\frac{h}{a}$, thicker plates have smaller ratios.

dS - Surface area differential.

T_{ij} - Finite element shape function which is dependent only on the normal coordinate.

$\mathcal{T}$ - Kinetic energy.

t_i - Thickness of the ith layer.

$\vec{u}$ - Total displacement vector.

$\bar{\vec{u}}$ - Displacement vector of a point on the reference surface.

$\hat{\vec{u}}$ - Displacement vector of a point on the director with respect to the same point on the undeformed director.

$\tilde{u}$ - Displacement of a point on the reference surface in direction 1.

$\hat{u}$ - Displacement of a point on the director in direction 1.

$\bar{u}$ - Normalized displacement in x-direction.

dV - Volume differential.

$\tilde{v}$ - Displacement of a point on the reference surface in direction 2.

$\hat{v}$ - Displacement of a point on the director in direction 2.

$\mathcal{W}$ - Potential Energy.

$\mathcal{W}_e$ - External work.

w - Displacement of a point on the reference surface in the normal direction.

$\bar{w}$ - Normalized displacement in the z-direction.

x^1, x^2, x^3 - Coordinates of arbitrary point in the structure in arbitrary coordinate system.

z - Coordinate of arbitrary point in the structure measured normal to the reference surface.

$\bar{z}$ - Normalized z coordinate.

γ_{ij} - Lagrangian strain tensor.

$_{,\Theta}$ - Derivative of $\hat{u}$ at $z=z_i$.

ν_{LT}, ν_{TT} - Poisson's ratio corresponding to the planes parallel to the fibers and perpendicular to the fibers respectively.

ξ^1, ξ^2, ξ^3 - Coordinates of arbitrary point in the structure in structural coordinate system.

$\bar{\sigma}_x$ - Normalized normal stress in the x-direction

$\bar{\tau}_{xz}$ - Normalized shear stress in the x z=plane.

$_i\phi$ - Derivative of $\hat{v}$ at $z = z_i$.

Ψ_i - Residual force vector.

ABSTRACT

Increased use of laminated composites has pointed out the need for better analytic tools. These tools must be able to correctly account for normal shear in the laminates and should be able to solve nonlinear problems. The finite element method can be applied to analyze laminated composites, and this research presents a new and unique method to include nonlinear effects and normal shear effects. The finite element is formulated from basic elasticity equations. The most unique characterisitc of the element is the manner in which normal shear is handled. The normal to a reference surface is allowed to not only rotate but also to change shape. Not only is displacement continuity imposed at lamina interfaces, but also slope continuity is guaranteed. After a complete general formulation of the finite element is presented, the method is specialized to plates so that the convergence characteristics, the accuracy, and the applicability of the element can be studied. The finite element does an excellent job of analyzing laminated composites, although there is some degradation in accuracy as the plates become thinner. This finite element gives the analyst the ability to do nonlinear analysis of laminated composites under a variety of loading and boundary conditions.

1. Introduction

PROBLEM STATEMENT

The general objective of this dissertation is to formulate a numerical procedure for the large-displacement analysis of laminated composite structures with general loading and boundary conditions. The specific numerical procedure is the finite element technique. The translational displacements may be large, but the rotations of the reference surface normal will be infinitesimal. The strains will remain in the elastic range. To examine a wider range of boundary and loading conditions, only laminated plates will be considered. Several loading and boundary conditions will be considered, but primary emphasis will be on normal shear behavior and those conditions which have a large influence on shear.

Laminated, fibrous composites have some unique advantages over isotropic materials, but they also present some additional analysis considerations. The most obvious advantage is in the strength-to-weight ratio of high strength composites (1). The advantages to be gained through weight savings are obvious. The other advantage, which is being exploited in the design of the forward swept wing (2), is the coupling which occurs between bending and extension in unsymmetrically, laminated composites. The coupling makes it possible to adjust the stiffness properties of the material to meet design limits rather than only adjusting geometrical sizes of the structure.

To fully capitalize on the weight advantage of composites, the designer should optimize the size of the structure. Optimized structures are sensitive to collapse; therefore, a complete analysis tool should include at least geometrically non-linear analysis.

A unique characteristic of composites which presents a challenge to the analyst is the heterogeneous character of the fiber and matrix constituents. Smearing the properties of these two constituents and treating a lamina as an orthotropic material in the plane of the lamina adequately describe the planar response of the lamina, but other methods must be used to handle the out-of-plane heterogeneity of laminates.

These other methods should account for normal shear effects since these out-of-plane effects are important not only for thick structures, but also for what would classically be considered thin structures (3).

An analytical method must include nonlinear geometrical effects and normal shear effects if laminated composites are to be used effectively. By including these two effects in a generalized computer program, structural designers and analysts can exploit the full potential of composites.

GENERAL PROCEDURE

The procedure to be followed in achieving the objective of this research can be divided into four steps. First, previous work in composite materials, nonlinear geometrical effects, normal shear effects, and finite element analysis is examined. This area is covered in the background chapter. Next, the theory and methods to be used as the basis for a numerical analysis of the large displacements of laminated composite structures with general loading and boundary conditions are developed. This development is in the Theory chapter. To test the theory, it is necessary to apply it to specific cases. For this dissertation the behavior of plates under a variety of boundary and loading conditions is examined. The Results chapter presents this examination. Last, the degree to which the dissertation objective is met is covered in the Conclusions chapter.

In addition, three appendices are included. The first appendix presents the derivation of the strain-displacement equations for the unique displacement function which is presented in this work. The results are similar to those obtained for other large-displacement analyses, but are derived in a unique manner. The second appendix contains the derivations of the stiffness matrix for a constant strain triangular plate element which includes not only in plane translations but also compatible variations in displacements through the thickness. This material is related to the information in the Theory Chapter, but is not included there due to the magnitude of the manipulation required. The last appendix contains an explantion and derivation of the current stiffness parameter which is used in the nonlinear analysis.

2. Background

In this chapter, previous work in composite materials, nonlinear geometrical effects, normal shear effects, and finite element analysis is examined as it relates to this research. To effectively and clearly cover these areas, the following approach is used. First, the methods used to include three-dimensional effects in plate and shell theory are considered. This consideration will concentrate on how normal shear is included in the analysis of isotropic structures and laminated structures. Next the methods used to include these three-dimensional effects in finite element analysis are examined Last, the previous work in non-linear structural analysis is reviewed.

THREE-DIMENSIONAL EFFECTS

To fully appreciate the implications of three-dimensional effects, the basic theories must be understood. A recent review of the basic theory of shells can be found in Gould's book (4). One of the earliest works on orthotropic shells was by Hildebrand, Reissner, and Thomas (5). This paper developed thin shell theory from the three-dimensional small displacement elasticity equations, and then examined the effect of various assumptions on the formulation. Laminated plate and shell theory was examined extensively in Amburtsumyan's books(6,7). Most of the development used the theory of thin shells and the Kirchoff-Love assumption. The last chapter does contain a plane stress type of development in which transverse shear effects are included. His book on anisotropic plates includes a large section on analyzing shear in a specific case. Books by Calcote (8), and Jones (9) contain reviews of

current laminated, composite, plate and shell theory. The basic development in both books still includes thin plate and shell theory assumptions and the Kirchoff-Love assumption; although Jones does mention that transverse stress effects can have a larger impact in composite laminates than is experienced with shells made of isotropic materials.

To examine the effect of transverse shear in composites, it is first necessary to look at what was done with isotropic materials to include the transverse stress effects. One of the earliest works was presented by Reissner (10). In his analysis of the bending plates, the normal was allowed to rotate, but not deform. To account for the nonsatisfaction of equilibrium, shear correction factors were used. In 1949, Reissner took a similar approach in analyzing sandwich-type shells (11). Another shortcoming of earlier theories was accounted for by Mindlin (12) when he included the effect of transverse inertia terms on the bending of plates.

Another way to account for transverse effects is through the use of an oriented continuum. There are three ways to formulate oriented continuum theories. Various authors have applied Cosserat surface theory to shells to include couple stresses and transverse stress effects (13-16). In this theory all action of the shell is simulated by a surface to which directors are associated. These directors cause particles to not only have translational displacements, but also rotational displacements. A second directed continuum theory is that of micromorphic continua(17,18).In this theory, the assumption is made that the continuum is composed of microelements which have their own microdisplacements about the macroelement center of mass which in addition has macrodisplacements relative to the global system. An approach that incorporates elements of both Cosserat surface theory and micromorphic

continuum theory is that proposed by Mindlin (19). He divided the continuum into characteristic parts such as crystals, grains or lamina. The motion of the entire surface was described by the displacement of the center of mass of these characteristic parts and microdisplacements which could be equivalently described by rotation of directors assigned to the center of mass.

Although there is experimental evidence that this type of continuum behavior exists when an elastic layer is imbedded between two more rigid layers and experiences a shear type force (20), there are practical problems in obtaining the constituitive equations. Some of the constituitive properties are represented by fifth and sixth order tensors and cannot be directly obtained from experiments. The usual practice to obtain these material properties is to obtain the strain energy density for an equivalent three dimensional problem and equate this strain energy with that obtained using a directed continuum theory (16). Rather than use a directed continuum theory, one could use an equivalent three-dimensional problem where deformations, which vary with the thickness, are described by deformation of directors attached to the reference surface. This will be the approach followed in this research.

One of the earliest attempts to include the shear stress effects for anisotropic laminated plates was made by Amburtsumyan (7). His approach was complicated and could only be applied to plates. Yang, Norris, and Stavsky also developed a theory for heterogeneous plates (21) in which they assumed that the in-plane displacements varied linearly with the thickness coordinate. They had to use correction factors to satisfy boundary conditions and equilibrium. The next significant work was by Pagano (3). He analyzed the cylindrical bending of a semi-infinite plate using elasticity. His work has been used by many others to guage the accuracy of their solutions. Whitney recently

applied the work of both Amburtsumyan and Yang to specific symmetric and antisymmetric laminated composite plate problems (22-28).

The next logical step after assuming a linear variation in the tangental displacement through the thickness was to assume the displacements varied linearly within each layer of a laminate. Grot used this approach for laminated composites and divided the laminate into fiber and matrix layers (29). Each layer was treated as isotropic and the entire formulation was worked out in terms of the matrix and fiber properties and displacements. Srinivas let the displacements vary linearly within an orthotropic layer composed of both fiber and matrix (30) and used his formulation to analyze the vibrations of laminated plates. An approach similar to that developed by Srinivas was used to formulate the equations for the nonlinear analysis of multilayered shells (31). In this paper, the similarities between this approach and the results obtained using directed continuum theories were also examined. Most recently Pagano developed a theory using Reissner's variational principle and assumed stress fields (32). As a result of his formulation, he obtained 13N field equations and 7N edge conditions (where N is the number of layers) which required simultaneous solution.

All of these approaches except the most recent presented by Pagano introduced discontinuities in the displacement derivatives at the layer interfaces. As a result shear correction factors had to be used to guarantee satisfaction of the equilibrium equations. Although Pagano did guarantee satisfaction of equilibrium, his approach results in a large system of linear equations which must be solved simultaneously. The solution of this system would be even more difficult if the equations were nonlinear, as they are when collapse is analyzed. This initial analytical development has now moved into finite element analysis.

FINITE ELEMENT ANALYSIS

The basic theory behind finite element analysis is well documented (33-35) and will not be covered here. Rather, the methods used to do three-dimensional finite element analysis will be examined.

The earliest attempts at including shear in finite elements were in two categories. These areas were sandwich shell analysis (36) and three dimensional continuum analysis (37). The sandwich shell type elements usually analyzed the outer coverings as membranes and the core material as if it would only carry transverse shear. The solid hexahedra is the usual element chosen for three-dimensional continuum analysis (34). The eight node trilinear element and the twenty-one node serendipity type of element are the predominant choice among analysts (35).

Another application of shear in finite element analysis is the Mindlin bending elements (35). In these elements the nodal degrees of freedom are the transverse displacement, w, and two rotations of the normal to the reference surface.

Although satisfactory results are obtained with these types of elements for thick structures, they could not be used to analyze thin structures without modification (38). The problems with thin structures came about because of the phenomena called "locking" in which the shear energy predominated rather than going to zero as theoretically required. The locking also occurred in elements which used linear or quadratic shape functions, but disappeared when higher order shape functions were used. There are various ways of reducing the effect of locking (39).

The simplest method which has been presented for improving thin structure analysis is reduced integration (40, 41). Other methods adjust the geometrical

properties of the element (39). Recently, penalty functions have been used successfully (42). The result of all methods is to reduce the magnitude of shear stiffness and, hence, significantly reduce the magnitude of the shear energy.

Since shear is more dominant in anisotropic materials than isotropic materials (3), it was logical to conclude that the finite elements which are used for composites must include the effects of transverse shear. The first finite elements for composites which included shear were based on the theory formulated by Amburtsumyan (7) and applied by Whitney (22). This theory is a Mindlin type of theory. In these elements (43, 44), the nodal degrees of freedom were the three translational displacements u, v, w, and two rotations, ϕ_x and ϕ_y, which describe the rotation of the normal. The normal for these elements remained straight, but the classical Kirchoff-Love assumption for normals was relaxed. This type of analysis resulted in a constant value of shear per layer. This meant that neither compatibility nor equilibrium were satisfied at the lamina interfaces.

An extension of this theory was to include the transverse shears at each node as two additional degrees of freedom (35, 45). This approach did give somewhat more accurate results, but still was not able to model the additional deformation of the normal which occurs in a laminated structure (45).

The next extension was by Mau, Tong, and Pian (46). They allowed the normal to have a different rotation within each layer. This approach has also been used by others for a variety of problems (47-49). In this approach, the shear is only approximated in an average sense per layer and displacement continuity, but not strain compatibility is satisfied at lamina interfaces.

Since shear is more dominant in composites, these analyses did not suffer

from locking as much as would occur for isotropic analysis, but the phenomena still existed. The effects of reduced integration and higher order shape functions was studied by Reddy (41). He showed that reduced integration and higher order shape functions did improve solution accuracy.

In all of these methods, both for isotropic and anisotropic materials, in which the normal is allowed to rotate, but remains straight, a shear correction factor had to be used. Several authors have derived formulas for this correction factor, which adjusts for the non-satisfaction of equilibrium by the constant shears. These formulas are not universally applicable (50), and therefore, the confidence is low for the usage of these elements in varied loading and boundary conditions.

Another recent approach for laminated finite element analysis is the hybrid stress element (51). This element uses the stresses as degrees of freedom along with the usual degrees of freedom. It also employs the use of Lagrangian multipliers to ensure the satisfaction of equilibrium at layer interfaces. It then uses 20 stress degrees of freedom per layer plus displacement degrees of freedom. As a consequence, the number of required computations is extensive. Although one stress type element has been applied to nonlinear analysis (52), the application is extremely complicated and requires additional computational efforts.

NONLINEAR ANALYSIS

As Koiter mentioned in a paper, linear theory cannot adequately describe the collapse behavior of structures (53). Since solutions of nonlinear equations are not readily available, numerical methods must be used. In this research, the finite element method will be incorporated. Good reviews of the finite element method and the application to nonlinear shell problems

can be found in two texts, one by Brebbia and Connor (54) and one by Zienkiewicz (33). Brebbia and Connor have a section on shell analysis which covers the inclusion of curvilinear conditions in the shape function and the causes of the problems associated with rigid body displacements. Zienkiewicz covers the solution procedures which can be used to solve the nonlinear shell equations. Zienkiewicz recently collaborated on the use of nonlinear finite elements to study one dimensional type problem (55). A larger and more complete work on the use and formulation of finite elements for solving nonlinear equations was recently published by Dodds (56). Following is a synopsis of previous research in nonlinear finite element analysis.

There are two main areas to consider in geometrically nonlinear structural analysis. First, is the formulation of the nonlinear equations. The second area is the collection of methods that are used to solve these equations. In addition to these two main areas, the work that has applied these formulations and solution technique must be examined.

All formulations of nonlinear structural analysis have their basis in three-dimensional continuum mechanics (57). These formulations are either built with a Lagrangian or Eulerian frame of reference. In the Eulerian formulation, the equilibrium equations are more simply expressed (57). In addition, using the Eulerian formulation, nonlinear problems can be solved as if they are piecewise linear. Since the Lagrangian formulation is based on the undeformed configuration, the material properties in the undeformed configuration can be used independent of the deformations (55). This property is extremely convenient for anisotropic analysis. There are several derivations of suitable equations for shells and plates based on the three dimensional equations, using both Lagrangian and Eulerian systems; these are also

well known, and detailed derivations can be found in elasticity textbooks (58-60).

There have been some applications of an Eulerian type approach for solving nonlinear problems using finite elements (61). The disadvantage of this approach is that coordinates, strains, stresses and material properties must be transformed at each load step. This greatly increases the number of required calculations, especially for large structures.

The Lagrangian method seems to have become the most favored for nonlinear finite elements. This is especially true for anisotropic and laminated structures.

The various methods which are used to solve nonlinear equations have been studied extensively (57, 62-65). These include the following methods: incremental stiffness, predictor corrector, Newton-Raphson iteration, first-order and second order, self-correcting and perturbation (66). Although all have been used successfully, it has been demonstrated that the most powerful method are the Newton-Raphson iteration and the first-order self-correcting methods (66). The Newton-Raphson method usually has been employed due to its simplicity.

In all methods, force incrementation has been used in the pre-collapse portion of the analysis (57,65). Post-collapse analysis has usually required displacement incrementation (66). In most cases collapse has been determined by examining the rank of the structural stiffness matrix (57, 64). When this matrix becomes singular a collapse point is reached. Recently, Bergan and others proposed the use of a current stiffness parameter to determine collapse points (64). This method has recently been successfully applied by Noor (65). The current stiffness parameter is a global measure of the structural stiffness and eliminates the need for determining the rank of the large finite element

stiffness matrix. This method and its application will be more thoroughly explained in the theory chapter and Appendix 3.

Nonlinear analysis has been applied to isotropic materials for many years. The two most common methods have been determination of the complete nonlinear behavior (67) and an eigenvalue analysis to determine buckling loads. Nonlinear analysis has been reviewed in many articles (57, 68, 69). A general review of buckling and collapse analysis can be found in the text by Brush and Almroth (70). Collapse analysis of shells is covered in Gould's text (4). Gould emphasizes the importance of the effect of transverse stresses on shell stability.

The collapse and nonlinear analysis of laminated composite structures has only been studied thoroughly in recent years. Calcote discussed the stability analysis of laminated composite shells (8), but his analysis used the Kirchoff-Love assumption. Khot wrote a series of reports which analyzed the influence of fiber orientation, non-homogenieties, and initial imperfections on the buckling of laminated composite shells (71-74). More recently, Bauld analyzed the collapse of laminated, composite panels using finite differences (75). Missing from most of these papers is experimental data to compare with the analyses. There has been some recently published experimental data (76).

The literature on complete nonlinear analysis of laminated composites is relatively small (48, 55, 77-81). The results presented have been of complete plates or of one dimensional type structures. Epstein and Glockner have recently presented a theory which includes thickness variations in transverse shear, but they did not present results (80). The other papers used either a Mindlin type theory (78, 81), or nonlinear classical laminated plate theory (77, 79).

SUMMARY

Although there has been extensive previous work in composite materials, nonlinear geometrical effects, normal shear effects, and finite element analysis, there has not been a great deal of research into combining these four areas. In those instances where these areas are combined, compatibility was not completely satisfied in the transverse direction. Presented in the following section is the theory for a nonlinear finite element for the analysis of laminated composites which is based on general three dimensional continuum theory and does completely satisfy compatibility in the transverse direction.

3. Theory

The theory behind the finite element solution of nonlinear problems involving laminated fibrous composites can best be understood by separating it into three areas. First is the development of the basic equations of strain and displacement and stress and strain. Next is the finite element formulation. Last is the solution procedure.

BASIC EQUATIONS

There are several criteria which must be considered when establishing relations for this problem. The choice of these criteria is influenced by the solution method, finite elements, the type of problem, geometrically nonlinear, and the type of material, laminated, fibrous composites. Since a geometrically nonlinear problem is studied, the strain-displacement relations must include large displacements. As has been shown, accurate analysis of composites must include the effects of normal shear (31). To include these stresses, the displacements must be dependent on the thickness coordinate. An additional consideration is the reduction of the adverse effect of rigid body displacements in satisfying equilibrium (82). To minimize this effect, three items should be included in the analysis. First, the elements must be curved elements for curved surfaces, therefore, the displacements should be functions of the curvilinear coordinates. Second, the displacements must be continuous at the edge of the elements. Third, the displacements and their first derivatives should be continuous within the domain of the element.

These measures can be met if the displacements are divided into two portions, the displacement of the reference surface and the displacement of a director which is initially normal to the undeformed reference surface. By using a linear shape function for the reference surface displacements and

letting normals deform, the displacements at the edge of the elements will be continuous.

To handle large displacements either a Lagrangian or an Eulerian formulation must be used. Since composite material properties are anisotropic, the calculation of material properties for an Eulerian formulation would be complex. The properties of the material are known and established in the undeformed configuration. Therefore, a Lagrangian formulation will be carried out.

To develop the strains and displacements, one must establish the metrics in the undeformed and deformed systems. Let the position of a point in the undeformed shell be described by, $\vec{R}$ (fig 3.1), where,

$$\vec{R} = \vec{r}(\vec{\xi}^{\alpha}) + \xi^3 \vec{d}(\vec{\xi}^{\alpha}) \qquad \alpha = 1,2 \tag{3.1}$$

The position vector of a point on the reference surface is $\vec{r}$ and $\vec{d}$ is the director along the normal to the reference surface at position $\vec{r}$. The basis vectors are then given by,

$$\vec{A}_i = \vec{R}_{,i} \qquad i = 1,2,3 \tag{3.2}$$

where the comma stands for covariant differentiation. The metric of the undeformed surface, g_{ij}, is,

$$g_{ij} = \vec{A}_i \cdot \vec{A}_j = \vec{R}_{,i} \cdot \vec{R}_{,j} \tag{3.3}$$

The position of the same point in the deformed shell is $\vec{R}^*$, where

$$\vec{R}^* = \vec{R} + \vec{U} \tag{3.4}$$

where $\vec{u}$ describes the displacement field. The metric of the deformed body, g_{ij}^*, is then

$$g^*_{ij} = \vec{R}^*_{,i} \cdot \vec{R}^*_{,j}$$

$$= (\vec{R}_{,i} + \vec{U}_{,i}) \cdot (\vec{R}_{,j} + \vec{U}_{,j})$$

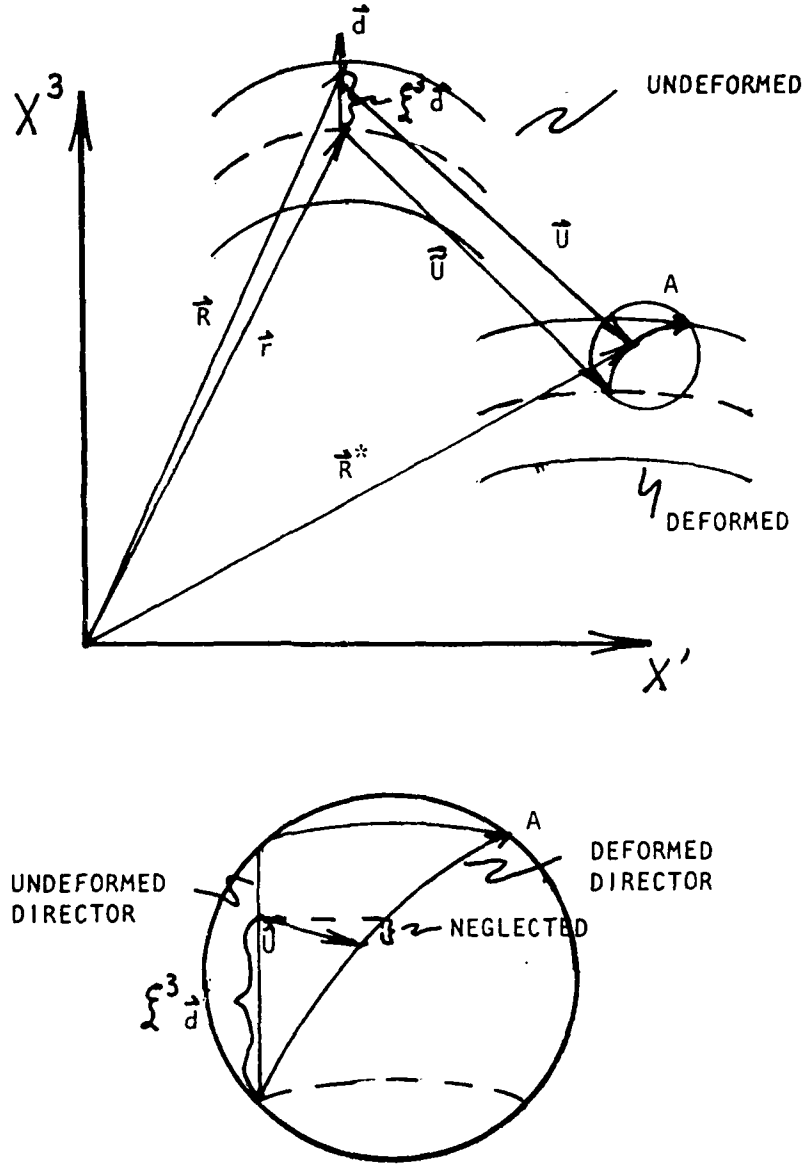

FIGURE 3.1: Deformation Terms and Geometry

$$g^*_{ij} = g_{ij} + \vec{R}_{,i} \cdot \vec{U}_{,j} + \vec{R}_{,j} \cdot \vec{U}_{,i} + \vec{U}_{,i} \cdot \vec{U}_{,j} \tag{3.5}$$

The Lagrangian strain is then defined as the difference between the metrics,

$$\gamma_{ij} = \frac{1}{2}\left(g_{ij}^* - g_{ij}\right)$$

$$\gamma_{ij} = \frac{1}{2}\left(\vec{R}_{,i} \cdot \vec{U}_{,j} + \vec{R}_{,j} \cdot \vec{U}_{,i} + \vec{U}_{,i} \cdot \vec{U}_{,j}\right) \tag{3.6}$$

The displacement field in its two parts can be represented by,

$$\vec{U} = \tilde{\vec{U}}(\xi^\alpha) + \hat{\vec{U}}(\xi^\alpha, \xi^3) \tag{3.7}$$

where $\tilde{\vec{U}}$ is associated with the deformation of the reference surface and $\hat{\vec{U}}$ is associated with the deformation of the director. Using equations (3.1) and (3.7) and letting $\vec{r}_{,\alpha} = \vec{a}_\alpha$, where the $\vec{a}_\alpha$ are the Lame' constants of the surface, the strain-displacement relations become,

$$\begin{aligned}
\gamma_{\alpha\beta} &= \frac{1}{2}\left[(\bar{a}_\alpha + \xi^3 \bar{d}_\alpha)\cdot(\tilde{\vec{U}}_{,\beta} + \hat{\vec{U}}_{,\beta}) + (\vec{a}_\beta + \xi^3 \vec{d}_\beta)\cdot(\tilde{\vec{U}}_{,\alpha} + \hat{\vec{U}}_{,\alpha}) + (\tilde{\vec{U}}_{,\alpha} + \hat{\vec{U}}_{,\alpha})\cdot(\tilde{\vec{U}}_{,\beta} + \hat{\vec{U}}_{,\beta})\right] \\
\gamma_{\alpha 3} &= \frac{1}{2}\left[(\vec{a}_\alpha + \xi^3 \vec{d}_{,\alpha}) + \hat{\vec{U}}_{,3} + \vec{d}\cdot(\tilde{\vec{U}}_{,\alpha} + \hat{\vec{U}}_{,\alpha}) + (\tilde{\vec{U}}_{,\alpha} + \hat{\vec{U}}_{,\alpha})\cdot\hat{\vec{U}}_{,3}\right] \\
\gamma_{33} &= \vec{d}\cdot\hat{\vec{U}}_{,3} + \frac{1}{2}\,\hat{\vec{U}}_{,3}\cdot\hat{\vec{U}}_{,3}
\end{aligned} \tag{3.8}$$

Now assuming the curvilinear coordinates are the principal directions and that the transverse displacement is independent of ξ^3 , the strain-displacement relations become, (see Appendix I)

$$\begin{aligned}
\gamma_{11} = A\left(1 + \tfrac{z}{R_1}\right)&\left[(\tilde{u} + \hat{u})_{,1} + \frac{A_{,2}}{B}(\tilde{v} + \hat{v}) + \frac{A}{R_1} w\right] + \frac{1}{2}\left\{\left[(\tilde{u} + \hat{u})_{,1} + \frac{A_{,2}}{B}(\tilde{v} + \hat{v})\right.\right. \\
&\left. + \frac{A}{R_1} w\right]^2 + \left[(\tilde{v} + \hat{v})_{,1} - \frac{A_{,2}}{B}(\tilde{u} + \hat{u})\right]^2 + \\
&\left.\left[w_{,1} - \frac{A}{R_1}(\tilde{u} + \hat{u}\right]^2\right\}
\end{aligned} \tag{3.9}$$

$$\begin{aligned}
\gamma_{22} = B\left(1 + \tfrac{z}{R_2}\right)&\left[(\tilde{v} + \hat{v})_{,2} + \frac{B_{,1}}{A}(\tilde{u} + \hat{u}) + \frac{B}{R_2} w\right] + \frac{1}{2}\left\{\left[(\hat{u} + \hat{u})_{,2} + \frac{B_{,1}}{A}(\tilde{v} + \hat{v})\right]^2 + \right. \\
&\left.\left[(\hat{v} + \hat{v})_{,2} + \frac{B_{,1}}{A}(\hat{u} + \hat{u}) + \frac{B}{R_2} w\right]^2 + \left[w_{,2} - \frac{B}{R_2}(\hat{v} + \hat{v})\right]^2\right\}
\end{aligned} \tag{3.10}$$

$$\gamma_{33} = \frac{1}{2}\left(\hat{u}_{,3}^2 + \hat{v}_{,3}^2\right) \tag{3.11}$$

$$\gamma_{23} = \frac{1}{2}\left\{B\left(1+\frac{z}{R_2}\right)\hat{v}_{,3} + \left[w_{,2} - \frac{B}{R_2}\left(\tilde{v}+\hat{v}\right)\right]\right\} + \frac{1}{2}\left\{\hat{u}_{,3}\left[\left(\tilde{u}+\hat{u}\right)_{,2} - \frac{B_{,1}}{A}\left(\tilde{v}+\hat{v}\right)\right]\right.$$
$$\left.\hat{v}_{,3}\left[\left(\tilde{v}+\hat{v}\right)_{,2} + \frac{B_{,1}}{A}\left(\tilde{u}+\hat{u}\right) + \frac{B}{R_2}w\right]\right\} \tag{3.12}$$

$$\gamma_{13} = \frac{1}{2}\left\{A\left(1+\frac{z}{R_1}\right)\hat{u}_{,3} + \left[w_{,1} - \frac{A}{R_1}\left(\tilde{u}+\hat{u}\right)\right]\right\} + \frac{1}{2}\left\{\hat{u}_{,3}\left[\left(\tilde{u}+\hat{u}\right)_{,1} + \frac{A_{,2}}{B}\left(\tilde{v}+\hat{v}\right) + \right.\right.$$
$$\left.\left.\frac{A}{R_1}w\right] + \hat{v}_{,3}\left[\left(\tilde{v}+\hat{v}\right)_{,3} - \frac{A_{,2}}{B}\left(\tilde{u}+\hat{u}\right)\right]\right\} \tag{3.13}$$

$$\gamma_{12} = \frac{1}{2}\left\{A\left(1+\frac{z}{R_1}\right)\left[\left(\tilde{u}+\hat{u}\right)_{,2} - \frac{B_{,1}}{A}\left(\tilde{v}+\hat{v}\right)\right] + B\left(1+\frac{z}{R_2}\right)\left[\left(\tilde{v}+\hat{v}\right)_{,1} - \frac{A_{,2}}{B}\left(\tilde{u}+\hat{u}\right)\right]\right\} +$$
$$\frac{1}{2}\left\{\left[\left(\tilde{u}+\hat{u}\right)_{,1} + \frac{A_{,2}}{B}\left(\tilde{v}+\hat{v}\right) + \frac{A}{R_1}w\right]\left[\left(\tilde{u}+\hat{u}\right)_{,2} - \frac{B_{,1}}{A}\left(\tilde{v}+\hat{v}\right)\right] + \left[\left(\tilde{v}+\hat{v}\right)_{,1} - \frac{A_{,2}}{B}\left(\tilde{u}+\hat{u}\right)\right]\right.$$
$$\left.\left[\left(\tilde{v}+\hat{v}\right)_{,2} + \frac{B_{,1}}{A}\left(\tilde{u}+\hat{u}\right) + \frac{B}{R_2}w\right] + \left[w_{,1} - \frac{A}{R_1}\left(\tilde{u}+\hat{u}\right)\right]\left[w_{,2} - \frac{B}{R_2}\left(\tilde{v}+\hat{v}\right)\right]\right\} \tag{3.14}$$

where

R_1 = principal radius of curvature for ξ^1 direction,

R_2 = principal radius of curvature for ξ^2 direction,

$\vec{a}_1 = A\vec{e}_1$, where $\vec{e}_1$ is unit vector in ξ^1 direction,

$\vec{a}_2 = B\vec{e}_2$, where $\vec{e}_2$ is unit vector in ξ^2 direction,

$\vec{\tilde{u}}(\xi^\alpha) = \tilde{u}(\xi^\alpha)\vec{e}_1 + \tilde{v}(\xi^\alpha)\vec{e}_2 + w(\xi^\alpha)\vec{d}$

$\vec{\hat{u}}(\xi^\alpha) = \hat{u}(\xi^\alpha, \xi^3)\vec{e}_1 + \hat{v}(\xi^\alpha, \xi^3)\vec{e}_2$

$\xi^3 = z$

These Lagrangian strain components then are equivalent to the Green strain tensor. The stress-strain law must relate a Lagrangian stress to these Lagrangian strains. Since it is Lagrangian and symmetric, the second Piola-Kirchoff stress is used in this work. This symmetry aids in establishing the constitutive law. The disadvantage in choosing this stress is that it does not have a physical meaning for large displacements. The constitutive law is, (3.15)

$$S_{ij} = C_{ijkl}\gamma_{kl}$$

where S_{ij} represents the second Piola-Kirchoff stress and C_{ijkl} represents a fourth order constitutive tensor.

Since the stress tensor is symmetric, its order can be reduced. This reduction is represented in the conventional notation by

$$\begin{aligned} S_{11} &= s_1 \\ S_{22} &= s_2 \\ S_{33} &= s_3 \\ S_{23} &= S_{32} = s_4 \\ S_{13} &= S_{31} = s_5 \\ S_{12} &= S_{21} = s_6 \end{aligned} \tag{3.16}$$

The order of the constitutive tensor and the strain tensor can be similarly reduced. In addition, the components of the strain tensor need to be changed from tensorial to physical components, so that the experimentally determined material constants can be used. This change is represented by

$$\begin{aligned} e_1 &= \frac{\gamma_{11}}{A^2(1+z/R_1)^2} \\ e_2 &= \frac{\gamma_{22}}{B^2(1+z/R_2)^2} \\ e_3 &= \gamma_{33} \\ e_4 &= 2\,\frac{\gamma_{23}}{B(1+z/R_2)} \\ e_5 &= 2\,\frac{\gamma_{13}}{A(1+z/R_1)} \\ e_6 &= 2\,\frac{\gamma_{12}}{A(1+z/R_1)(1+z/R_2)B} \end{aligned} \tag{3.17}$$

The new constitutive law then becomes

$$S_r = D_{rd} e_s \qquad r,s=1, \cdots, 6 \tag{3.18}$$

The constitutive law for a composite material takes on a specific form. For a material in which the principal material axes and the principal geometric axes coincide, this law in matrix form is

$$\begin{Bmatrix} S_1 \\ S_2 \\ S_3 \\ S_4 \\ S_5 \\ S_6 \end{Bmatrix} = \begin{bmatrix} D_{11} & D_{12} & D_{13} & 0 & 0 & 0 \\ D_{12} & D_{22} & D_{23} & 0 & 0 & 0 \\ D_{13} & D_{23} & D_{33} & 0 & 0 & 0 \\ 0 & 0 & 0 & D_{44} & 0 & 0 \\ 0 & 0 & 0 & 0 & D_{55} & 0 \\ 0 & 0 & 0 & 0 & 0 & D_{66} \end{bmatrix} \begin{Bmatrix} e_1 \\ e_2 \\ e_3 \\ e_4 \\ e_5 \\ e_6 \end{Bmatrix} \tag{3.19}$$

The law for a case where physical and geometric axes do not coincide becomes,

$$\begin{Bmatrix} S_1 \\ S_2 \\ S_3 \\ S_4 \\ S_5 \\ S_6 \end{Bmatrix} = \begin{bmatrix} D_{11} & D_{12} & D_{13} & 0 & 0 & D_{16} \\ D_{12} & D_{22} & D_{23} & 0 & 0 & D_{26} \\ D_{13} & D_{23} & D_{33} & 0 & 0 & D_{36} \\ 0 & 0 & 0 & D_{44} & D_{45} & 0 \\ 0 & 0 & 0 & D_{45} & D_{55} & 0 \\ D_{16} & D_{26} & D_{36} & 0 & 0 & D_{66} \end{bmatrix} \begin{Bmatrix} e_1 \\ e_2 \\ e_3 \\ e_4 \\ e_5 \\ e_6 \end{Bmatrix} \tag{3.20}$$

The physical components of strain can also be represented in matrix form,

$$\{e\} = [L]\{u\}$$

$$\text{where } \{u\} = \begin{Bmatrix} \tilde{u} + \hat{u} \\ \tilde{v} + \hat{v} \\ w \end{Bmatrix} \tag{3.21}$$

The L - operator matrix can be broken down into linear, L_0, and nonlinear, L_1, parts where

$$[L] = [L_0] + [\tilde{L}_1] + [\hat{L}_1] \tag{3.22}$$

$$[L_0] = \begin{bmatrix} \left[\frac{1}{A(1+z/R_1)}\frac{\partial}{\partial \xi^1}\right] & \left[\frac{1}{A(1+z/R_1)}\frac{A_{,2}}{B}\right] & \left[\frac{1}{A(1+z/R_1)}\frac{A}{R_1}\right] \\ \left[\frac{1}{B(1+z/R_2)}\frac{B_{,1}}{A}\frac{\partial}{\partial \xi^2}\right] & \left[\frac{1}{B(1+z/R_2)}\frac{\partial}{\partial \xi^2}\right] & \left[\frac{1}{B(1+z/R_2)}\frac{B}{R_2}\right] \\ 0 & 0 & 0 \\ 0 & \left[\frac{\partial}{\partial z} - \frac{1}{B(1+z/R_2)}\frac{B}{R_2}\right] & \left[\frac{1}{B(1+z/R_2)}\frac{\partial}{\partial \xi^2}\right] \\ \left[\frac{\partial}{\partial z} - \frac{1}{A(1+z/R_1)}\frac{A}{R_1}\right] & 0 & \left[\frac{1}{A(1+z/R_1)}\frac{\partial}{\partial \xi^1}\right] \\ \left[\frac{1}{B(1+z/R_2)}\frac{\partial}{\partial \xi^2} - \frac{1}{A(1+z/R_1)}\frac{A_{,2}}{B}\right] & \left[\frac{1}{A(1+z/R_1)}\frac{\partial}{\partial \xi^1} - \frac{1}{B(1+z/R_2)}\frac{B_{,1}}{A}\right] & 0 \end{bmatrix} \tag{3.23}$$

$$
[L] = \begin{bmatrix}
\text{[illegible]} & \text{[illegible]} \\
\text{[illegible]} & \text{[illegible]} \\
0 & 0 \\
\text{[illegible]} & \text{[illegible]} \\
\text{[illegible]} & \text{[illegible]} \\
\text{[illegible]} & \text{[illegible]} \\
\text{[illegible]} & \\
\text{[illegible]} & \\
0 & \\
0 & \\
0 & \\
w_{,}\ \frac{\partial}{\partial \zeta^2} &
\end{bmatrix} \qquad (3.24)
$$

$$[L_1] = \begin{bmatrix} \frac{1}{2A^2(1+2/k_1)}\left[\left(\hat{a}_{11}+\frac{B_1}{A}\hat{V}\right)\frac{B_1}{A}-\left(\hat{V}_{11}-\frac{B_1}{A}\hat{a}\right)\frac{B_1}{A}+\frac{B_1^2}{A^2}\hat{a}\right] & \frac{1}{2A^2(1+2/k_1)}\left[\left(\hat{a}_{11}+\frac{B_1}{A}\hat{V}\right)\frac{B_1}{A}+\left(\hat{V}_{11}-\frac{B_1}{A}\hat{a}\right)\frac{B_1}{A}\right] \\ \frac{1}{2B^2(1+2/k_2)}\left[\left(\hat{a}_{12}-\frac{B_1}{A}\hat{V}\right)\frac{B_2}{A}+\left(\hat{V}_{12}+\frac{B_1}{A}\hat{a}\right)\frac{B_2}{A}\right] & \frac{1}{2B^2(1+2/k_2)}\left[\left(\hat{V}_{12}+\frac{B_1}{A}\hat{a}+\frac{B_2}{A}\hat{a}\right)\frac{B_2}{A}-\left(\hat{a}_{12}-\frac{B_1}{A}\hat{V}\right)\frac{B_2}{A}+\frac{B_1B_2}{A^2}\hat{V}\right] \\ \frac{1}{2}\frac{\partial^2 L}{\partial a^2}\frac{\Delta a}{\Delta t} & \frac{1}{2}\frac{\partial^2 L}{\partial a^2}\frac{\Delta a}{\Delta t} \\ \frac{1}{B(1+2/k_2)}\left[\left(\hat{a}_{12}-\frac{B_1}{A}\hat{V}\right)\frac{B_2}{A}\right] & \frac{1}{A(1+2/k_1)}\left[\left(\hat{V}_{12}+\frac{B_1}{A}\hat{a}\right)\frac{B_2}{A}\right] \\ \frac{1}{A(1+2/k_1)}\left[\left(\hat{a}_{11}+\frac{B_1}{A}\hat{V}\right)\frac{B_1}{A}\right] & \frac{1}{A(1+2/k_1)}\left[\left(\hat{V}_{11}-\frac{B_1}{A}\hat{a}\right)\frac{B_1}{A}\right] \\ \frac{1}{A(1+2/k_1)B(1+2/k_2)}\left[\left(\hat{a}_{11}+\frac{B_1}{A}\hat{V}\right)\frac{B_2}{A}-\left(\hat{V}_{12}+\frac{B_1}{A}\hat{a}\right)\frac{B_1}{A}+\frac{B_1B_2}{A^2}\hat{V}\right] & \frac{1}{A(1+2/k_1)B(1+2/k_2)}\left[\left(\hat{V}_{12}+\frac{B_1}{A}\hat{a}\right)\frac{B_2}{A}-\left(\hat{a}_{11}+\frac{B_1}{A}\hat{V}\right)\frac{B_1}{A}\right] \end{bmatrix}$$

$$\begin{bmatrix} \frac{1}{2A^2(1+2/k_1)}\left[\left(\hat{a}_{11}+\frac{B_1}{A}\hat{V}\right)\frac{B_1}{A}-\frac{B_1^2}{A^2}\hat{a}\right] \\ \frac{1}{2B^2(1+2/k_2)}\left[\left(\hat{V}_{12}+\frac{B_1}{A}\hat{a}\right)\frac{B_2}{A}-\frac{B_2}{A}\hat{V}\right] \\ \bigcirc \\ \bigcirc \\ \bigcirc \\ \bigcirc \end{bmatrix}$$

(3.25)

The displacements $\tilde{U}$, $\tilde{V}$, W, $\hat{U}$, and $\hat{V}$ do not explicitly appear in the L_o matrix. The displacements $\tilde{U}$, $\tilde{V}$, and W appear to the first power in the $\tilde{L}_1$ matrix, which is independent of $\hat{U}$ and $\hat{V}$. The displacements $\hat{U}$ and $\hat{V}$ appear to the first power in the $\hat{L}_1$ matrix which is independent of $\tilde{U}$, $\tilde{V}$ and W. Equation (3.20) then becomes

$$\{s\} = [D][L_o + \tilde{L}_1 + \hat{L}_1]\{u\} \tag{3.26}$$

FINITE ELEMENT FORMULATION

The theory and philosophy behind finite element analysis are well established and can be found in several sources and will not be reproduced here (33 - 35). The finite element will be formulated using a variational method and a displacement model. First the nodal degrees of freedom and the type of interpolation function for these degrees of freedom must be selected.

The interpolation function must meet two criteria. It can be one degree less than the order of the governing differential equation, and it must be smooth within the domain of the element. From Equation (3.21), (3.23), (3.24), and (3.25), the order of the differential equations is two; therefore a first order interpolation is sufficient. For the function to be sufficiently smooth within the domain of the element, at least all first derivatives must be continuous. An additional consideration in the case of laminated composites is that the displacement function be able to change from layer to layer. This means that in order for the first derivatives to be continuous through the thickness, they must be at least linear within each layer.

To meet these criteria, $\tilde{U}$, $\tilde{V}$, and W must be at least linear with respect to the ξ^1 and ξ^2 coordinates, and $\hat{U}$ and $\hat{V}$ must be at least linear with respect to ξ^1, ξ^2, and Z.

Since the thrust of this work is the nonlinear analysis of plates and shells under varying loading and boundary conditions, the most convenient element to use is the triangular element. The use of triangular elements allows better matching of irregular geometric boundaries. The node numbering and geometric arrangements are as shown in Figure 3.2.

Then the interpolation function for the displacements associated with the deformation of the reference surface is,

$$\tilde{u} = \frac{1}{\Delta}\left(N_1 \tilde{u}_1 + N_2 \tilde{u}_2 + N_3 \tilde{u}_3 \right) \tag{3.27}$$

$$\tilde{v} = \frac{1}{\Delta}\left(N_1 \tilde{v}_1 + N_2 \tilde{v}_2 + N_3 \tilde{v}_3 \right) \tag{3.28}$$

$$w = \frac{1}{\Delta}\left(N_1 w_1 + N_2 w_2 + N_3 w_3 \right) \tag{3.29}$$

where

$$\Delta = \xi_1' \xi_2^2 - \xi_2' \xi_1^2 + \xi_2' \xi_3^2 - \xi_3' \xi_2^2 + \xi_3' \xi_1^2 - \xi_1' \xi_3^2 \tag{3.30}$$

$$N_1 = \left(\xi_2' \xi_3^2 - \xi_3' \xi_2^2 \right) + \left(\xi_2^2 - \xi_3^2 \right) \xi' + \left(\xi_3' - \xi_2' \right) \xi^2 \tag{3.31}$$

$$N_2 = \left(\xi_3' \xi_1^2 - \xi_1' \xi_3^2 \right) + \left(\xi_3^2 - \xi_1^2 \right) \xi' + \left(\xi_1' - \xi_3' \right) \xi^2 \tag{3.32}$$

$$N_3 = \left(\xi_1' \xi_2^2 - \xi_2' \xi_1^2 \right) + \left(\xi_1^2 - \xi_2^2 \right) \xi' + \left(\xi_2' - \xi_1' \right) \xi^2 \tag{3.33}$$

where ξ_i^j is the coordinate in the j direction at node i.

To meet the smoothness and continuity conditions at the lamina interfaces, the displacements are not only forced to be equal, but also the Z-derivatives of the displacements are forced to be equal. Defining the Z-coordinate of the bottom of the ith lamina as Z_{i-1} (Figure 3.2) and the Z-coordinate of the top as Z_i, the derivatives at the interfaces can be

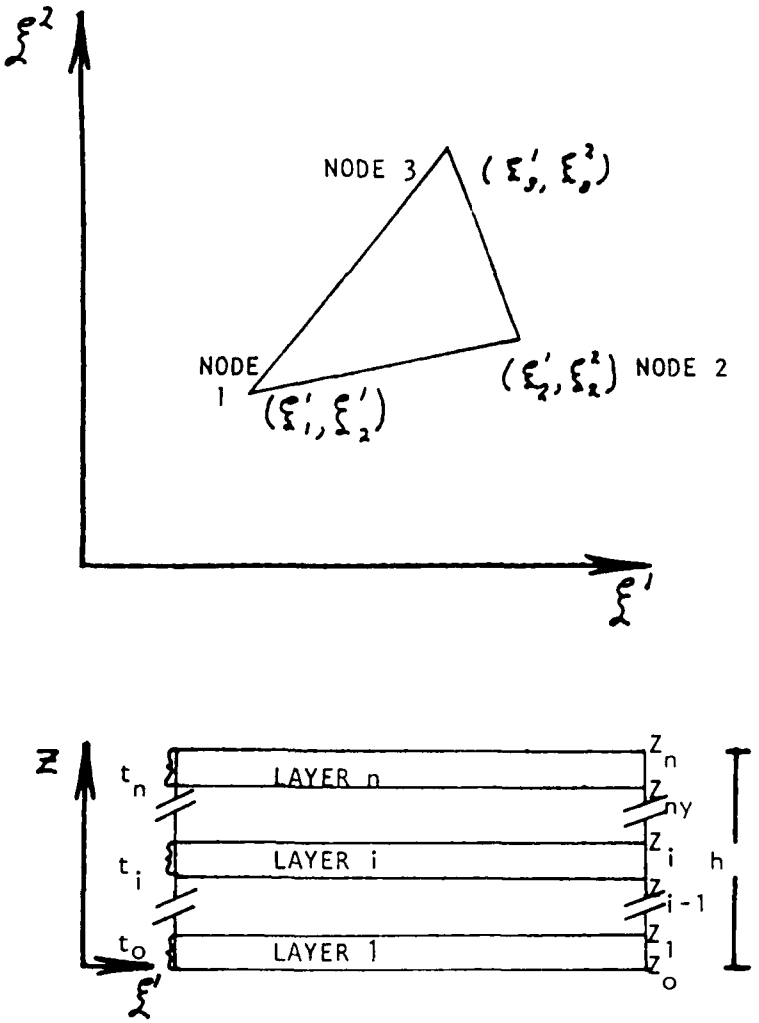

FIGURE 3.2: Element Configuration and Nomenclature

defined as,

$$\frac{\partial \hat{u}}{\partial z} = {}_{i-1}\phi \qquad @\ z = z_{i-1} \tag{3.34}$$

$$\frac{\partial \hat{u}}{\partial z} = {}_{i}\phi \qquad @\ z = z_{i} \tag{3.35}$$

$$\frac{\partial \hat{v}}{\partial z} = {}_{i-1}\theta \qquad @\ z = z_{i-1} \tag{3.36}$$

$$\frac{\partial \hat{v}}{\partial z} = {}_{i}\theta \qquad @\ z = z_{i} \tag{3.37}$$

Using equations (3.34) through (3.37), and using a linear interpolation function, the Z-derivative within each lamina is,

$$\left(\frac{\partial \hat{u}}{\partial z}\right)_i = {}_{i-1}\phi + \frac{{}_{i}\phi - {}_{i-1}\phi}{(z_i - z_{i-1})}(z - z_{i-1}) \tag{3.38}$$

$$\left(\frac{\partial \hat{v}}{\partial z}\right)_i = {}_{i-1}\theta + \frac{{}_{i}\theta - {}_{i-1}\theta}{(z_i - z_{i-1})}(z - z_{i-1}) \tag{3.39}$$

To obtain the interpolation function for the displacements, a Taylor series is expanded about the bottom of the layer and truncated after three terms.

$${}_{i}\hat{u} = \hat{u}(z_{i-1}) + (z - z_{i-1})\frac{\partial \hat{u}(z_{i-1})}{\partial z} + \frac{1}{2!}(z - z_{i-1})^2\frac{\partial^2 \hat{u}(z_{i-1})}{\partial z^2} + \cdots \tag{3.40}$$

$${}_{i}\hat{v} = \hat{v}(z_{i-1}) + (z - z_{i-1})\frac{\partial \hat{v}(z_{i-1})}{\partial z} + \frac{1}{2!}(z - z_{i-1})^2\frac{\partial^2 \hat{u}(z_{i-1})}{\partial z^2} + \cdots \tag{3.41}$$

Using equations 3.38 and 3.39, equations 3.40 and 3.41 become,

$${}_{i}\hat{u} = {}_{i-1}\phi(z - z_{i-1}) + \frac{{}_{i}\phi - {}_{i-1}\phi}{2(z_i - z_{i-1})}(z - z_{i-1})^2 + {}_{i}C_u \tag{3.42}$$

$${}_{i}\hat{v} = {}_{i-1}\theta(z - z_{i-1}) + \frac{{}_{i}\theta - {}_{i-1}\theta}{2(z_i - z_{i-1})}(z - z_{i-1})^2 + {}_{i}C_v \tag{3.43}$$

where the C's are constants which allow matching of displacements at layer boundaries. The constants can be evaluated by forcing $\hat{U}$ and $\hat{V}$ to be zero at the reference surface and $\hat{U}$ and $\hat{V}$ to be equal at interfaces. For this analysis, the reference surface will always be the interior surface which is determined by the direction of the surface normal. Using these criteria, equations (3.42) and (3.43) become,

$$i\hat{U} = {}_{i-1}\phi\, T^{i}_{i-1} + {}_{i}\phi T^{i}_{i} + \sum_{j=0}^{i-1} {}_{j}\phi\, T^{i}_{j} \tag{3.44}$$

$$i\hat{V} = {}_{i-1}\theta T^{i}_{i-1} + {}_{i}\theta T^{i}_{i} + \sum_{j=0}^{i-1} {}_{j}\theta\, T^{i}_{j} \tag{3.45}$$

where,

$$T^{i}_{j} = \begin{cases} \frac{1}{2}(t_j + t_{j+1}) & j < i-1 \\ \frac{1}{2}\left[t_{j-1} + 2(z - z_{i-1}) - \frac{1}{t_i}(z - z_{i-1})^2\right] & j = i-1 \\ \frac{1}{2} t_i (z - z_{i-1})^2 & j = i \\ 0 & j > 2i \end{cases} \tag{3.46}$$

where t_j is the thickness of the layer.

This manipulation accounts for the Z-dependence of U and V. The ξ' and ξ^2 dependence is carried in ϕ and θ, that is

$$i\phi = {}_{i}\phi(\xi^{\alpha})$$
$$i\theta = {}_{i}\theta(\xi^{\alpha}) \tag{3.47}$$

To meet the smoothness and continuity requirements, linear interpolation functions will be used for ϕ and θ. The functions are

$$i\phi = \frac{1}{\Delta}(N_{1i}\phi_1 + N_{2i}\phi_2 + N_{3i}\phi_3) \tag{3.48}$$

$$i\theta = \frac{1}{\Delta}(N_{1i}\theta_1 + N_{2i}\theta_2 + N_{3i}\theta_3) \tag{3.49}$$

The nodal degrees of freedom are the three displacements $\tilde{U}$, $\tilde{V}$, and W at each node and the rotations, ${}_i\phi$ and ${}_i\theta$, at the lamina interfaces on the director emanating from each node. The element degree of freedom vector is

$$\{a\} = \begin{Bmatrix} \tilde{u}_1 \\ \vdots \\ w_3 \\ {}_0\phi_1 \\ \vdots \\ {}_n\phi_3 \\ {}_0\theta_1 \\ \vdots \\ {}_n\theta_3 \end{Bmatrix} \quad \text{where } n = \text{number of layers} \tag{3.50}$$

Using equations (3.28) through (3.30), (3.44), (3.45), (3.48), and (3.49), the displacements in terms of the nodal degrees of freedom can be represented by

$$\begin{Bmatrix} u \\ v \\ w \end{Bmatrix} = [\tilde{N} + \hat{N}]\{a\} \tag{3.51}$$

$$[\tilde{N}] = \frac{1}{\Delta}\begin{bmatrix} N_1 N_2 N_3 & 0\,0\,0 & 0\,0\,0\,0 & 0 \\ 0\,0\,0 & N_1 N_2 N_3 & 0\,0\,0\,0 \ldots & 0 \\ 0\,0\,0 & 0\,0\,0 & N_1 N_2 N_3\,0 & 0 \end{bmatrix} \tag{3.52}$$

$$\hat{N}_i = \begin{bmatrix} 0 & 0 & T_0^i N_1 & T_m^i N_3 & 0 & 0 \\ 0 \ldots 0 & 0 & \ldots & 0 & T_0^i N_1 \ldots & T_m^i N_3 \\ 0 & 0 & 0 & 0 & 0 & 0 \end{bmatrix} \tag{3.53}$$

Equation (3.21) then becomes,

$$\{e\} = [L_0 + \tilde{L}_1 + \hat{L}_1][\tilde{N} + \hat{N}]\{a\} \tag{3.54}$$

Equation (3.26) then becomes,

$$\{s\} = [D][L_0 + \tilde{L}_1 + \hat{L}_1][\tilde{N} + \hat{N}]\{a\} \tag{3.55}$$

The variational principle that will be used to derive the element stiffness matrices is Hamilton's principle,

$$\delta \int_{t_o}^{t_i} (\mathcal{T} - \mathcal{W})\, dt + \int_{t_o}^{t_i} \delta \mathcal{W}_e\, dt = 0 \qquad (3.56)$$

where $\mathcal{T}$ is the kinetic energy, $\mathcal{W}$ is the potential energy, and $\mathcal{W}_e$ is the work done by external forces. This analysis will be a static analysis; therefore, the kinetic energy is zero and there is no time dependence. Equation (3.56) becomes, $-\delta \mathcal{W} + \delta \mathcal{W}_e = 0$ or

$$\delta \mathcal{W} = \delta \mathcal{W}_e \qquad (3.57)$$

Assuming only conservative forces are applied and letting $\vec{b}$ or b^i be the body forces and $\vec{f}$ or f^i be the surface forces,

$$\mathcal{W}_e = \int_V \{u\}^T \{b\}\, dV + \int_S \{u\}^T \{f\}\, dS \qquad (3.58)$$

then for an element

$$\delta \mathcal{W}_e^E = \int_V \delta \{u^E\}^T \{b\}\, dV + \int_S \delta \{u^E\}^T \{f\}\, dS \qquad (3.59)$$

From equation (3.51),

$$\delta \{u^E\}^T = \delta \{a^E\}^T [\tilde{N} + \hat{N}]^T \qquad (3.60)$$

Equation (3.59) can then be written as,

$$\delta \mathcal{W}_e^E = \delta \{a^E\} \left(\int_V [\tilde{N} + \hat{N}]^T \{b\}\, dV + \int_S [\tilde{N} + \hat{N}]^T \{f\}\, dS \right) \qquad (3.61)$$

Now let,

$$\{q^E\} = \int_V [\tilde{N} + \hat{N}] \{b\}\, dV + \int_S [\tilde{N} + \hat{N}] \{f\}\, dS \qquad (3.62)$$

Combining equations (3.61) and (3.62) the variation of the external work on one element is,

$$\delta \mathcal{W}_e^E = \delta \{a^E\}^T \{q^E\} \qquad (3.63)$$

The potential energy for an element can be represented by

$$\mathcal{W}^E = \frac{1}{2} \int_V \{e\}^T \{s\}\, dV \qquad (3.64)$$

The variation of the potential energy is

$$\delta \mathcal{W}^E = \int_V \delta \{e\}^T \{s\}\, dV \qquad (3.65)$$

Using equations (3.54) and (3.55), equations (3.65) becomes

$$\delta W^E = \delta \{a^E\}^T \int_V [\tilde{N}+\hat{N}]^T [L_0+\tilde{L}_1+\hat{L}_1]^T [D] [L_0+\tilde{L}_1+\hat{L}_1] [\tilde{N}+\hat{N}] dV \{a^E\} \quad (3.66)$$

The terms within the integration sign then become the element stiffness matrix. The stiffness matrix can be divided into linear and nonlinear parts, such that

$$\delta W^E = \delta \{a^E\}^T [K_L^E + K_{NL}^E] \{a^E\} \quad (3.67)$$

where

$$\begin{aligned} [K_L^E] &= \text{linear part of stiffness matrix} \\ &= \int_V [\tilde{N}+\hat{N}]^T [L_0]^T [D] [L_0] [\tilde{N}+\hat{N}] dV \end{aligned} \quad (3.68)$$

$$\begin{aligned} [K_{NL}^E] &= \text{nonlinear part of stiffness matrix} \\ &= \int_V [\tilde{N}+\hat{N}]^T [L_0]^T [D] [\tilde{L}_1+\hat{L}_1] [\tilde{N}+\hat{N}] dV + \\ &\quad \left(\int_V [\tilde{N}+\hat{N}]^T [L_0]^T [D] [\tilde{L}_1+\hat{L}_1] [\tilde{N}+\hat{N}] dV\right)^T + \\ &\quad \int_V [\tilde{N}+\hat{N}]^T [\tilde{L}_1+\hat{L}_1]^T [D] [\tilde{L}_1+\hat{L}_1] [\tilde{N}+\hat{N}] dV \end{aligned} \quad (3.69)$$

Using equations (3.57), (3.63), and (3.67), the basic variational equation is

$$\delta \{a^E\}^T \{q^E\} = \delta \{a^E\}^T [K_L^E + K_{NL}^E] \{a^E\} \quad (3.70)$$

Since the variations are arbitrary and independent, equation (3.70) becomes

$$\{q^E\} = [K_L^E + K_{NL}^E] \{a^E\} \quad (3.71)$$

Since the functions chosen to represent the degrees of freedom are continuous at element boundary interfaces, the equations for each element can be added together to obtain a global set of equations,

$$\{q\} = [K_L + K_{NL}] \{a\} \quad (3.72)$$

SOLUTION PROCEDURE

The next step in the analysis is to solve the set of nonlinear equations presented by equation (3.72). The Newton-Raphson method will be used. Although derivations of this method are available, it is presented here for clarity.

To solve equation (3.72) an initial estimate of the vector $\{a\}$ is required. Switching to tensor notation, let this initial estimate be a_j^o. Further let

$$K_L = \bar{K}_{ij} \qquad \text{and}$$
$$K_{NL} = \bar{\bar{K}}_{ij} \tag{3.73}$$

then the residual force $\Psi^o i$, representing the degree to which body force equilibrium is not satisfied, is given by:

$$\Psi_i^o = (\bar{K}_{ij} + \bar{\bar{K}}_{ij}) a_j^o - q_i \tag{3.74}$$

To obtain a better estimate of a_j, say a_j^1, the residual force vector is expressed in a truncated Taylor series expanded about the estimate a_j^o. The Taylor series is truncated after the linear term. The expression is:

$$\Psi_i' = \Psi_i^\circ + (a_j^1 - a_j^o)\, \Psi_{i,j}^o \tag{3.75}$$

Now it is assumed that the new residual force vector will be the null vector. Then equation (3.75) becomes

$$a_j^1 = a_j^o - (\bar{\Psi}^o)_{i,j}\, \Psi_i^o \tag{3.76}$$

where $(\bar{\Psi}^o)_{i,j}\, \Psi_{j,k}^o = \delta_{ik}$

Using equation (3.74), an expression for $\Psi_{i,j}^o$ is obtained

$$\Psi_{i,j}^o = \bar{K}_{ik,j}\, a_k^o + \bar{K}_{ij} + \bar{\bar{K}}_{ij}^o\, a_k^o + \bar{\bar{K}}_{ij}^o \tag{3.77}$$

Or gathering terms

$$\Psi_{i,j}^o = (\bar{K}_{ij} + \bar{\bar{K}}_{ij}^o) + \bar{K}_{ik,j} + \bar{\bar{K}}_{ik,j}^o)\, a_k^o \tag{3.78}$$

Since $\bar{K}_{ik}$ is independent of the a_j's, $\bar{K}_{ik,j} = 0$. Equation (3.78) becomes

$$\Psi^{o}_{ij} = (\bar{K}_{ij} + \bar{\bar{K}}_{ij}) + \bar{\bar{K}}_{ik,j} a^{o}_{k} \tag{3.79}$$

All terms on the right hand side of this equation are known except for the third order tensor $K_{ik,j}$.

This tensor is evaluated in one of two basic ways. First, the third order tensor can be evaluated and the indicated tensor multiplication carried out. A second alternative is explained by Zienkiewicz (33). He condenses $K_{ik,j} a^{o}_{k}$ into a second order tensor called the initial stress or geometric matrix. Both of these methods require additional, extensive calculations on the elemental level for a classical three dimensional analysis. For an element such as described here, the calculations would be even more extensive due to the coupling between the translational degrees of freedom and the larger number of rotational degrees of freedom.

To avoid these additional calculations, equation (3.79) is replaced by the approximation

$$\Psi^{o}_{ij} \approx \bar{K}_{ij} + \bar{\bar{K}}^{o}_{ij} \tag{3.80}$$

The inversion process is then carried out as shown in equation (3.76). The approximation given by equation (3.80) will reduce the rate of convergence (63), but this should be offset by fewer calculations required at each iteration.

This process is continued until either the error as indicated by the size of the residual force vector or the difference between successive approximations to the degree of freedom vector is small. There are various measures that can be used to define the size of these vectors and hence convergence (83).

The method which is used in this study varies per degree of freedom. If the degree of freedom is one at which an external force is applied, convergence occurs if the size of the residual force is some set proportion less than the applied external force. If the degree of freedom does not have an externally applied force, the size of the residual force is compared to an absolute value. Convergence occurs if the absolute value of the residual force is less than the set value. Global convergence occurs if the residual forces for all degrees of freedom are within their respective convergence criteria.

After convergence occurs at one load level, the load is proportionally increased, and the basic solution process is repeated until a convergent solution is reached. In previous nonlinear analyses, load incrementation is continued until the collapse load is reached, that is until the stiffness matrix becomes singular. The methods which analyze behavior in the post collapse phase normally switch to displacement incrementation.

The current stiffness parameter has been used previously but a detailed derivation is not available in the literature. Such a derivation is presented in Appendix 3.

The basic formulas for the current stiffness parameter are as follows. The stiffness parameter, S_p, is used when the loading is proportional, that is when some load $\{q\}$ is defined by:

$$\{q\} = p\{q_r\} \tag{3.81}$$

where p is the proportionality factor and $\{q_r\}$ is a reference load, usually the initial load. The current stiffness parameter is defined by,

$$S_p = \frac{\frac{\partial \{a_r\}^T}{\partial p}\{q_r\}}{\frac{\partial \{a\}^T}{\partial p}\{q_r\}} \tag{3.82}$$

where $\{a_r\}$ is the degree of freedom vector at the reference load and $\{a\}$ is the degree of freedom vector at the corresponding load $\{q\}$. The partial derivatives are then approximated using finite differences. Equation (3.82) becomes,

$$S_p = \frac{\Delta p \, \Delta \{a_r\}^T \{q_r\}}{\Delta p_r \, \Delta \{a\}^T \{q_r\}} \tag{3.83}$$

If the load steps, p, are all equal then

$$S_p \approx \frac{\Delta \{a_r\}^T \{q_r\}}{\Delta \{a\}^T \{q_r\}} \tag{3.84}$$

The sign of S_p indicates the stability condition of the structure according to the following relations.

$S_p > 0$ stable equilibrium

$S_p = 0$ neutral equilibrium (3.85)

$S_p < 0$ unstable equilibrium

To apply equations (3.85), it is necessary to project the value of S_p. This is done with a two term Taylor Series in which the first derivative is approximated by a first order finite difference formula

$$(S_p)_{i+1} = (S_p)_i + \{[(S_p)_i - (S_p)_{i-1}]/\Delta p\} \Delta p \tag{3.86}$$

If the projected value of S_p is negative and the solution does not converge, the point of collapse has been reached.

The overall solution procedure for a nonlinear problem is then:

1. Solve the linear problem and use the linear solution as a first approximation to the solution of the nonlinear problem.
2. Solve the nonlinear problem.
3. If convergence occurs, continue; if non-convergence occurs, stop the solution.
4. Calculate the current stiffness parameter and use eqn. (3.85) to determine the current state. Stop at neutral equilibrium.

5. Increment the load by the set proportion and recalculate the load vector.

6. Return to step 2 and repeat.

4. RESULTS

In this chapter, three areas will be covered which demonstrate the convergence characteristics of the element, the accuracy of the element, and the applicability of the element to nonlinear laminated plate problems.

The effects on convergence of different conditions will be investigated. The number of elements in the reference surface will be varied to examine the influence of element size. Since this element includes transverse effects, the number of layers in the thickness direction of the plate will also be varied. Last, the effect of different materials and plate geometries will be investigated. Five specific linear cases are inspected to cover a range of different materials and geometries.

The accuracy of the element is determined by comparing computer results against other solution results. The displacement accuracy of the element for linear problems can be inferred from the convergence study. Stress accuracy for linear problems is examined by comparing with results obtained for three semi-infinite, laminated, composite plates. The accuracy of the nonlinear solution is studied by comparing with the previously calculated results for a square orthotropic plate.

To demonstrate the range and applicability of the element, two additional nonlinear problems will be studied. First the change in stresses for an orthotropic semi-infinite plate undergoing large displacements will be studied. Second, the method will be used to determine the collapse load for a square orthotropic plate with a centrally located hole.

CONVERGENCE

The first case that will be examined for convergence is a semi-infinite isotropic plate under uniform loading. The ratio of the thickness to the width for this plate is .02; therefore it can be classified as a thin plate. An illustration of the structure and a typical finite-element mesh are in figure 4.1. The graph showing the effects of increasing the number of elements or the number of layers is figure 4.2. Represented on the vertical axis is the ratio of the displacement in the z direction, w (at the midpoint), found using this element and the classic value of w (84). Plotted along the horizontal axis are the divisions along the side of the plate.

Increasing the number of divisions in a consistent manner causes the results to approach the classic result. Also increasing the number of layers improves the accuracy of the solution. For the plate with 50 side divisions and 100 elements, increasing the layers from one to two improves the accuracy by 12%; increasing from two to four layers improves accuracy by 2%, and increasing from four to six layers improves accuracy by .2%. Any larger number of divisions does not noticeably improve accuracy. The highest accuracy achieved was 86% of the classical result for a plate with 50 side divisions and 8 layers. If the finite element solution continued to approach the classical solution at the same rate, 220 elements would be required to achieve 100% accuracy. The loading for all cases is found using eqn. (3.62)

The second case to be investigated is a square, clamped, isotropic plate under uniform loading. A drawing of the plate and a typical element mesh are shown in figure 4.3. The graph of the results is figure 4.4. The axes on the graph are the same as those in figure 4.2. The convergence rate relative to

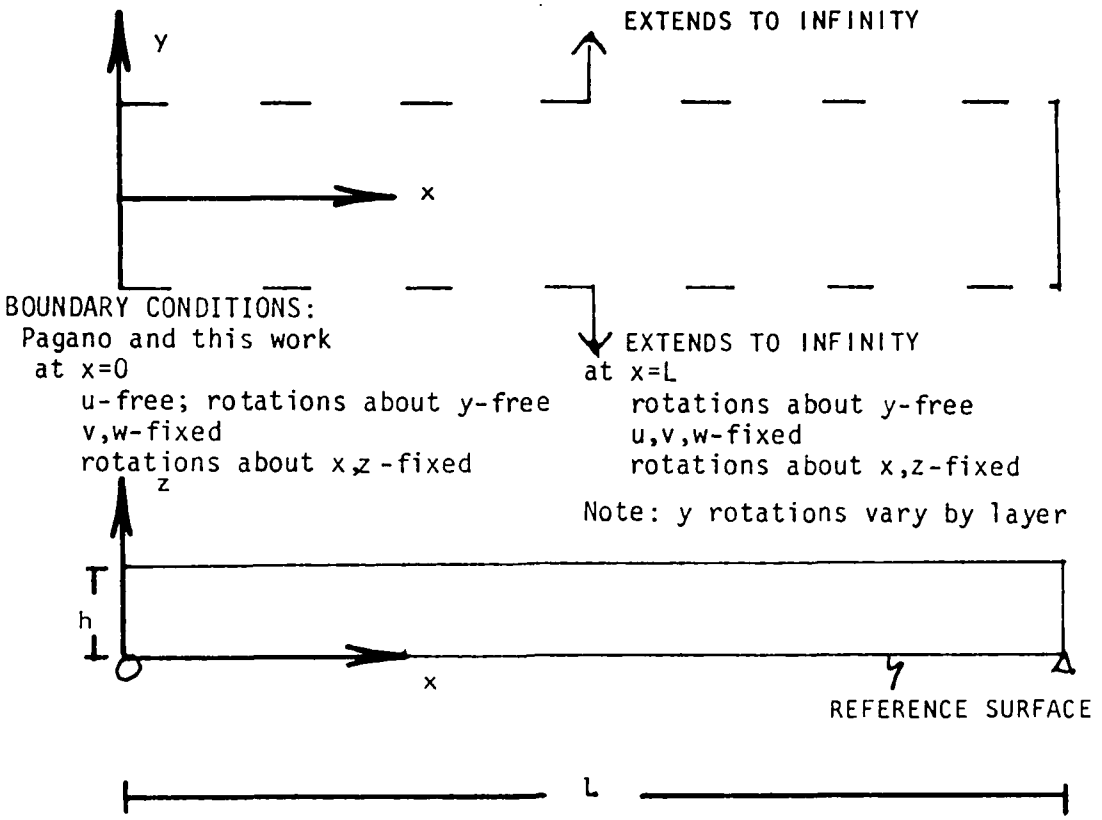

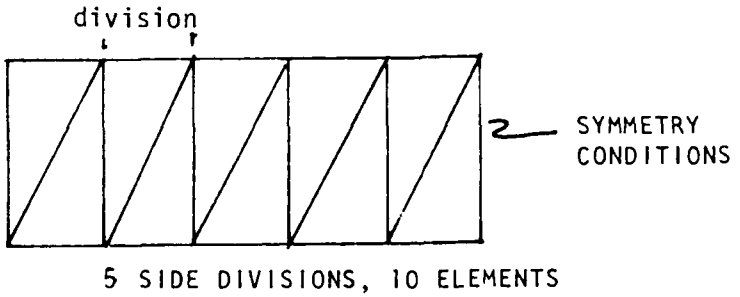

Figure 4.1: Semi-infinite Plate Geometry and Finite Element Model

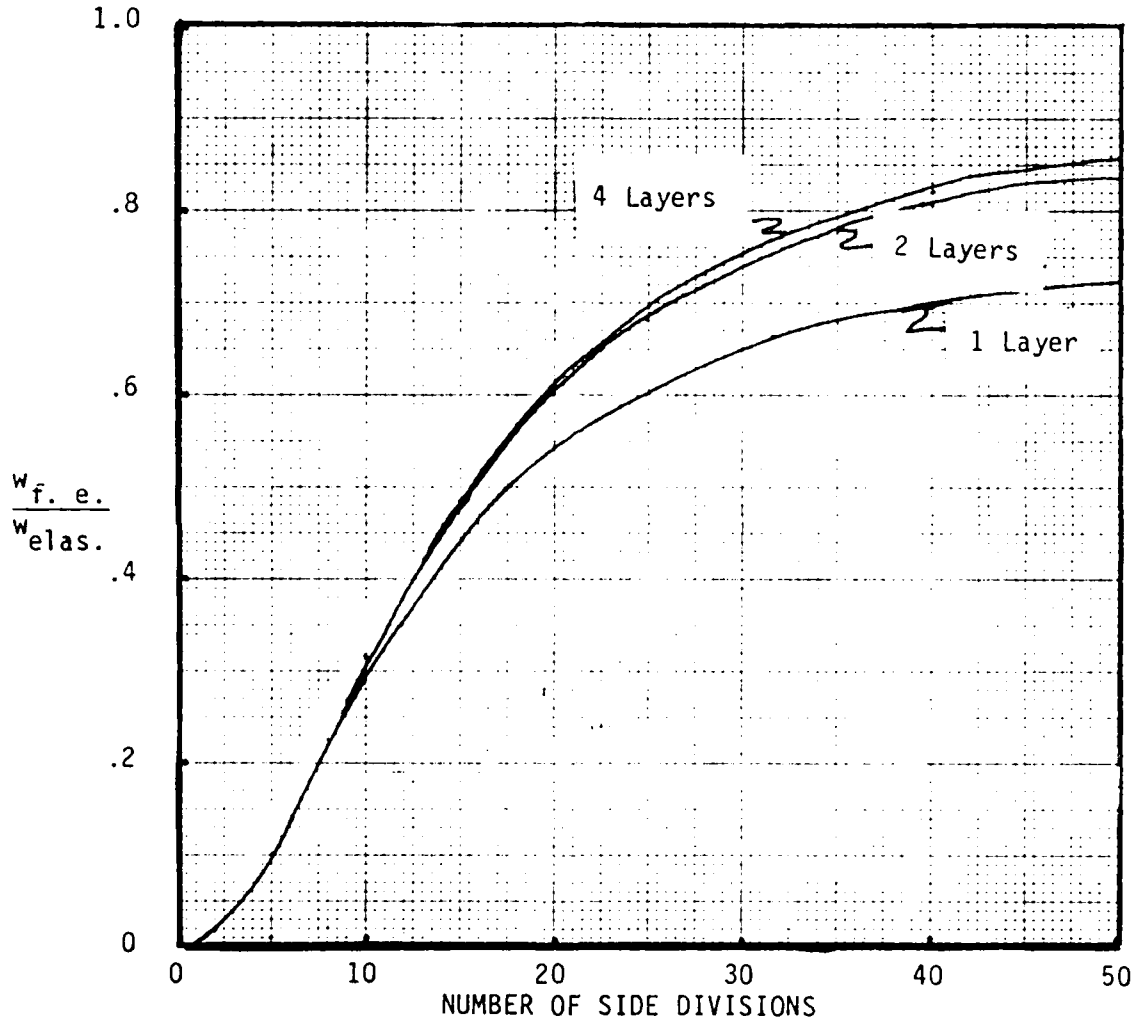

FIGURE 4.2: Convergence Graph for Semi-infinite Plate.

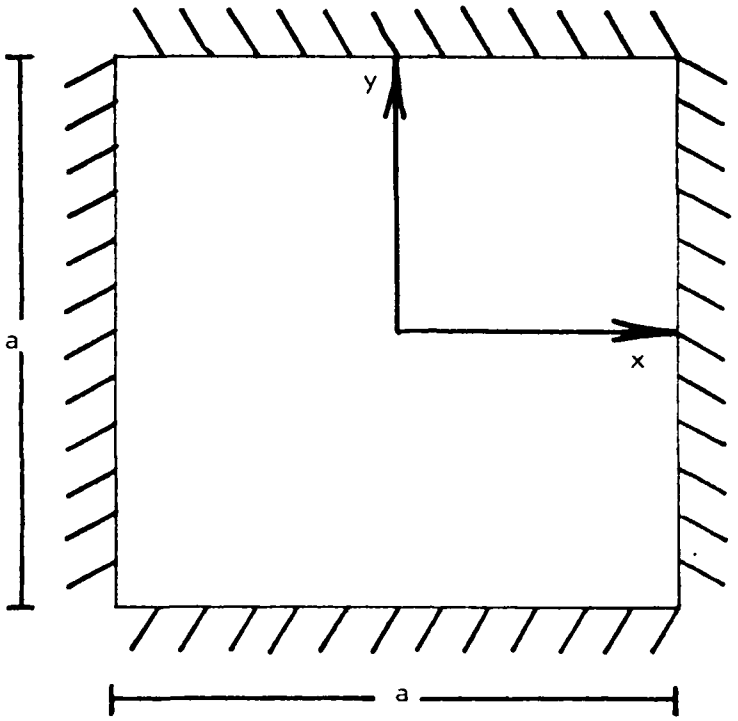

Clamped Boundary Conditions

@ $x = i$
$w = o$
$u = o$
$\frac{\partial u}{\partial z} = o$

@ $y = \pm a/2$
$w = o$
$v = o$
$\frac{\partial v}{\partial z} = o$

FINITE ELEMENT MODEL

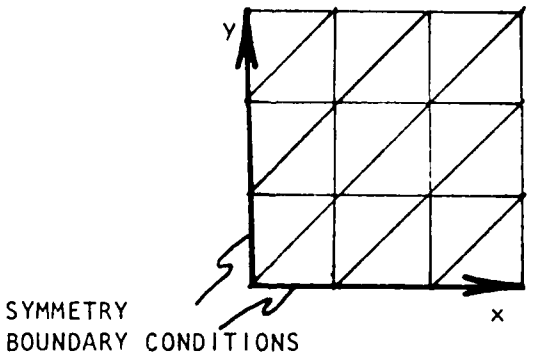

FIGURE 4.3: Square Plate Geometry and Finite Element Model

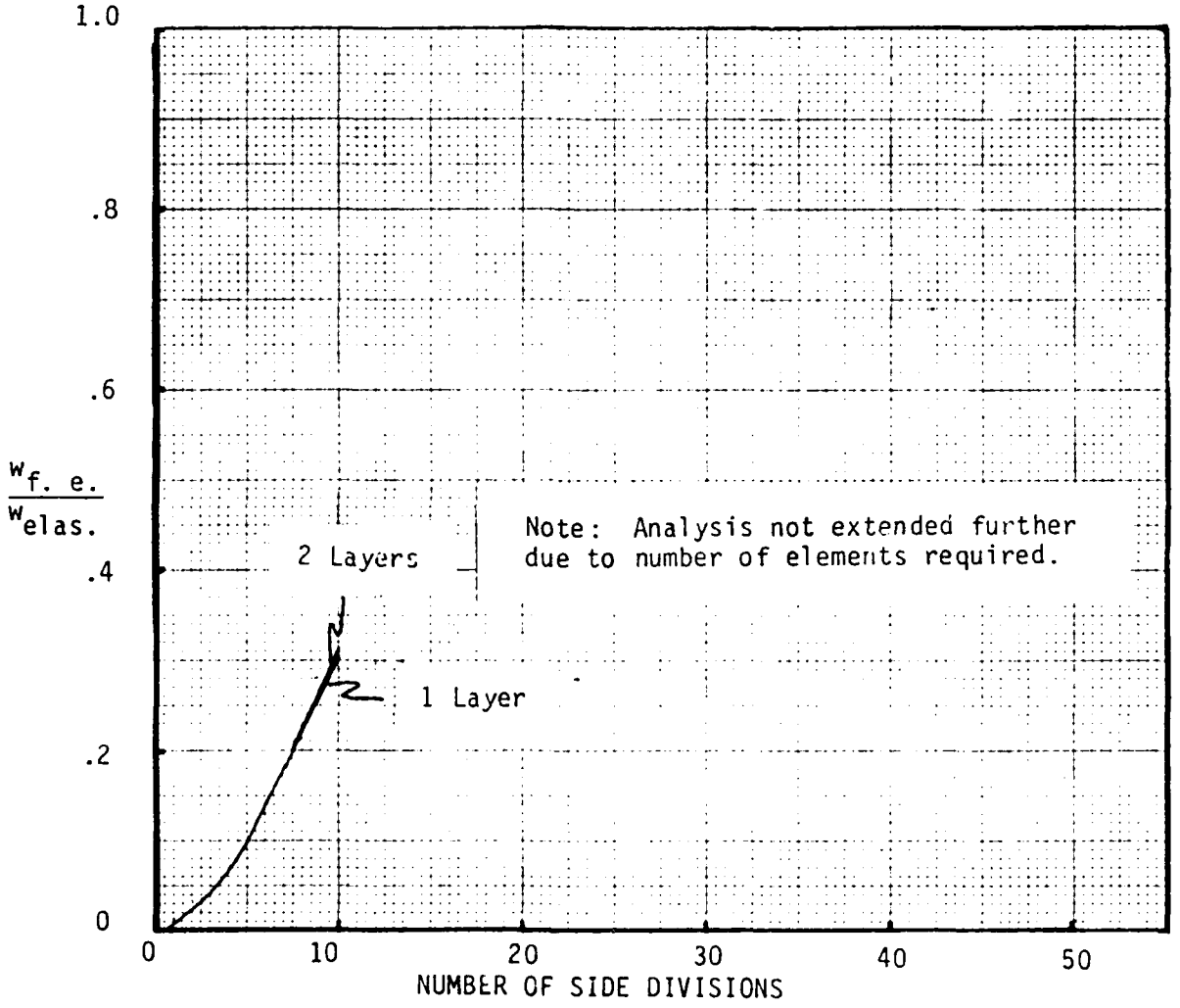

FIGURE 4.4: Convergence Graph for Square Isotropic Plate.

the number of side divisions is the same for the semi-infinite and the square plate as the number of divisions is increased. However the two dimensional nature of the square plate may lead to a requirement for more elements. In order to obtain the classical results(85), 110 side divisions and approximately 24,000 elements would be required. Increasing the number of layers for the square plate did not have a large effect because the mesh was large.

The third case is a semi-infinite orthotropic plate under transverse sinusoidal loading, q, where

$$q = q_o \sin \frac{\pi x}{a} \qquad (4.1)$$

The plate set-up and the mesh arrangement are the same as shown in Figure 4.1. The fibers run in the x-direction. The layers are all of the same thickness and the ratio of plate thickness to width is .02. The material properties are given in Table 4.1.

TABLE 4.1 COMPOSITE MATERIAL PROPERTIES

$E_L / E_T = 25$	$G_{LT} / E_T = .5$
$G_{TT} / E_T = .2$	$V_{LT} = V_{TT} = .25$

L signifies the direction parallel to the fibers.

T signifies the direction perpendicular to the fibers.

The axes for the results graph, Figure 4.5, are labeled the same as they were in the previous two examples. The results are compared with the analytical

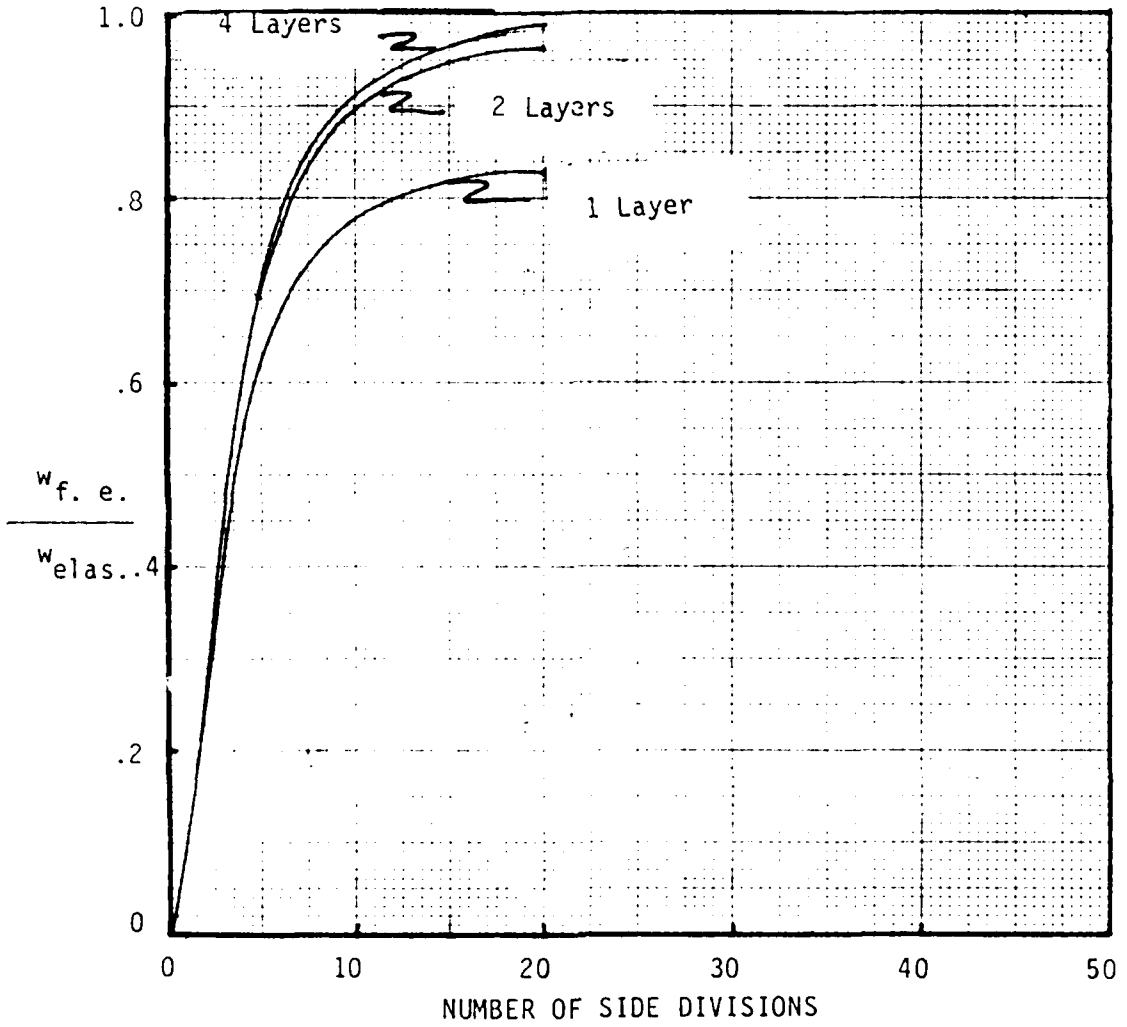

FIGURE 4.5: Convergence Graph for Thin Semi-infinite Orthotropic Plate

results obtained by Pagano (3).

The finite element solution for the orthotropic plate converges twice as fast as the solution for the isotropic plate. For the plate with 20 side divisions, going from one layer to two layers, increases accuracy by 14.1%, going from two layers to four layers increases accuracy by 1.4%, going from four to six layers increases accuracy by .1%, and going from six to eight layers increases accuracy .01%. The most accurate solution is obtained with 20 side divisions and eight layers when the finite element result is 99% of the analytical result.

The fourth problem that is examined for convergence is a thick semi-infinite orthotropic plate. This problem is similar to the previous one except that the ratio of thickness to width is .25. As can be seen from Figure 4.6, the finite element results converge quickly to the classical results (3). With four layers and four side divisions, the finite element solution is equal to the classical result for the w displacement. Increasing the number of side divisions past four does not affect the accuracy. With four side divisions, going from one layer to two layers improves accuracy by 13.9% and going from two layers to four layers improves accuracy by .5%.

The last convergence example is for a square, laminated composite plate under transverse sinusoidal loading, q, where

$$q = q_o \sin \frac{\pi x}{a} \quad \sin \frac{\pi y}{a} \qquad (4.2)$$

The basic set-up of the plate and the finite element mesh are similar to that shown in Figure 4.3. The boundary conditions for this plate are simple supports.

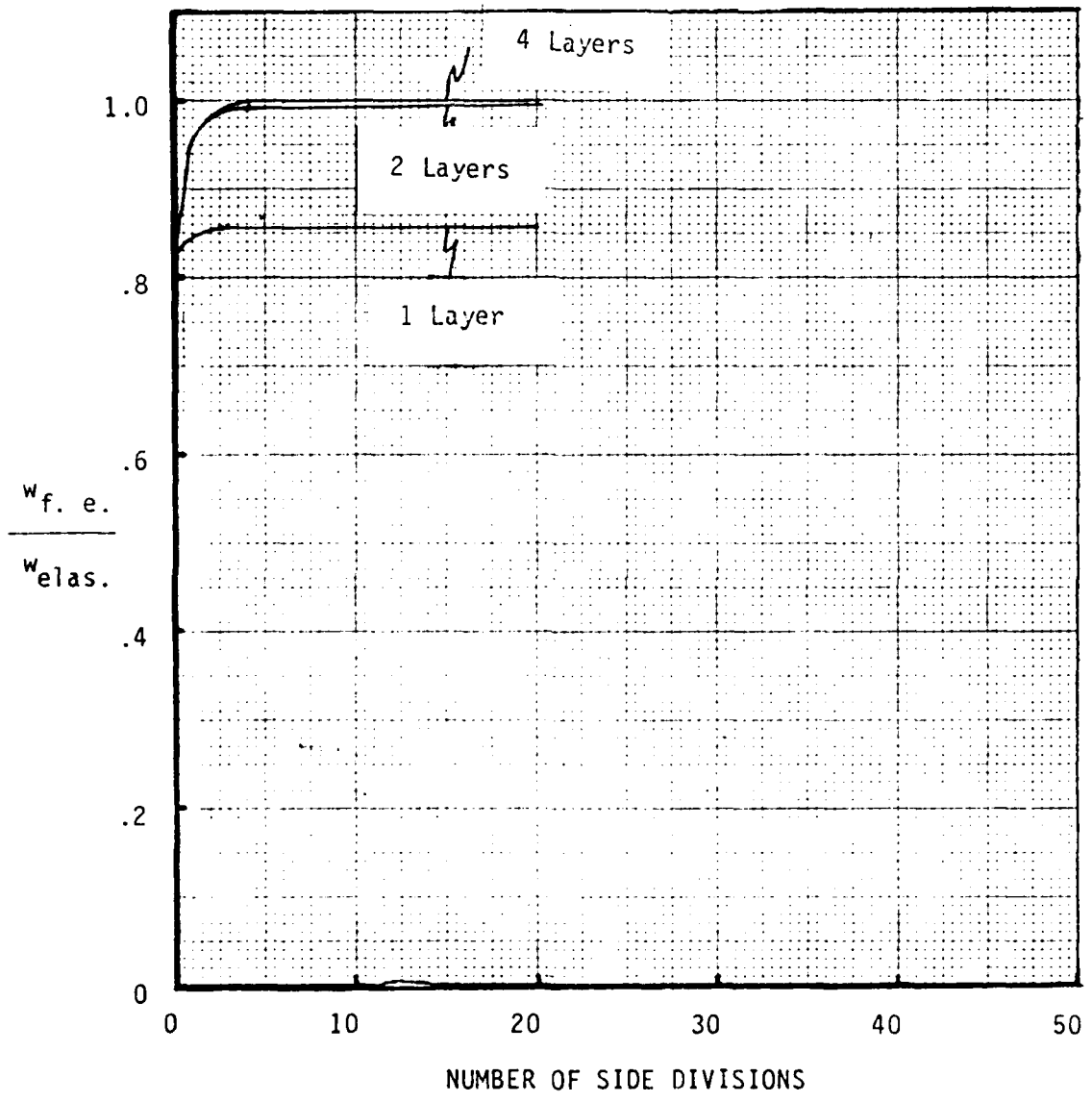

FIGURE 4.6: Convergence Graph for Thick Semi-infinite Orthotropic Plate

Along the edges the transverse displacement, s, is fixed and the normal to the reference surface at the edges is not allowed to rotate perpendicular to the edge. The plate is a symmetric (0,90) laminate of graphite epoxy; the material properties are shown in Table 4.2. The thickness ratios vary from .02 to .2.

TABLE 4.2	COMPOSITE MATERIAL PROPERTIES
$E_L / E_T = 40$	$G_{LT}/E_T = .6$
$G_{TT}/E_T = .5$	$V_{LT} = V_{TT} = .25$

As can be seen in Figure 4.7, the finite element solution for the thick plates, where the ratio of thickness to width is .2 and .15, approaches the shear deformation theory (SDT) solution (23) quickly. With five side divisions the finite element solution is 99% of the SDT solution. As the plate becomes thinner, the rate of convergence decreases. For a plate with a thickness ratio of .02, a convergent solution is not obtained. Although the rate of convergence does appear to be steady.

Through these five examples, convergence has been studied. The examples have indicated the effect of the number of elements and the number of layers on convergence. Plates with simple and clamped supports have been studied. The materials have ranged from isotropic to laminated orthotropic. Now that convergence has been studied, the accuracy of the element for linear and nonlinear problems must be examined, although the validity of the method can no longer be questioned. With this method it is possible to include transverse shear effects and obtain usable results.

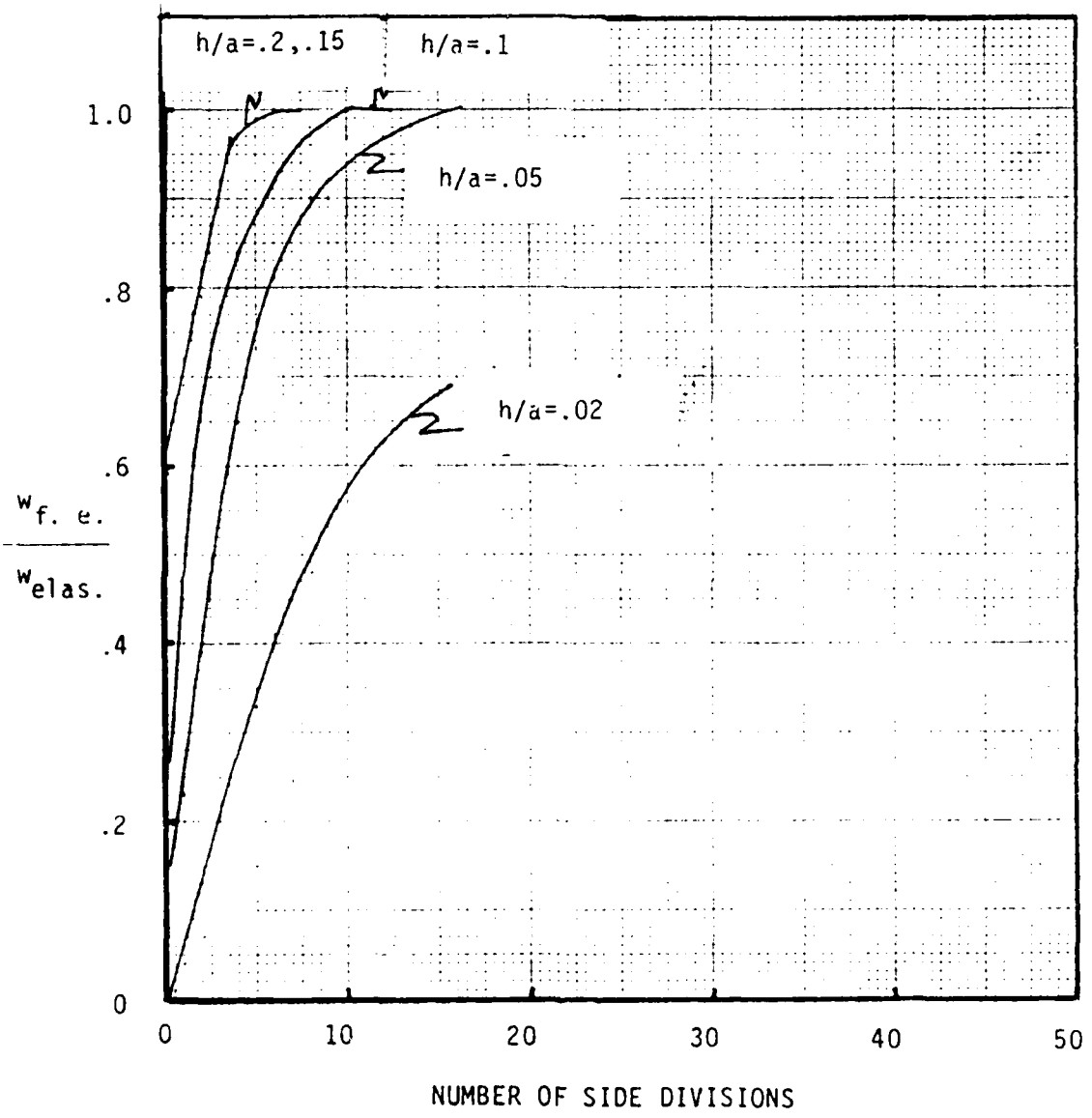

FIGURE 4.7: Convergence Graph for $(0,90)_s$ Square Plate

ACCURACY

Although the transverse displacement accuracy for some linear cases was examined in the convergence section, the in-plane displacement and stress accuracy for linear problems was not investigated. Three further linear cases will be studied. All three cases are semi-infinite, anisotropic plates under sinusoidal transverse loading, equation 4.1. The geometry of the problems are shown in Figure 4.1. All cases have the edges with simple supports. The material properties are given in Table 4.1. Case 1 is an orthotropic plate with the fibers aligned in the x direction. Case 2 is a two layer, unsymmetric composite plate with the fibers in the bottom layer parallel to the x axis and the fibers in the top layer parallel to the y axis. Case 3 is a three layer symmetrically laminated composite plate. In the upper and lower layers, the fibers are aligned in the x direction. In the middle layer, the fibers are aligned with the y axis. The results of this analysis are compared against those of Pagano obtained using elasticity (3). For all of these cases, the following normalized quantities will be used

$$\bar{\sigma}_x = \frac{\sigma_x(\frac{\ell}{2}, z)}{q_o} \tag{4.3}$$

$$\bar{\tau}_{xz} = \frac{\tau_{xz}(0, z)}{q_o} \tag{4.4}$$

$$\bar{u} = \frac{E_T u(0, z)}{h\, q_o} \tag{4.5}$$

$$\bar{w} = \frac{100\, E_T h^3 w(\frac{\ell}{2}, 0)}{q_o \ell^4} \tag{4.6}$$

$$S = \frac{\ell}{h} \tag{4.7}$$

$$\bar{z} = \frac{z}{h}$$

For case 1, the accuracy of the w prediction over a range of thickness ratios is examined. As can be seen in Figure 4.8, the predictions are accurate over a wide range of S values. The largest error is 3% for S=50. As can be seen in Figure 4.9, the stresses are also predicted accurately for a thick plate with S=4. The largest errors occur at the top and bottom of the plate. In Figure 4.10, the results for a slightly thinner plate are shown. The finite element results match the elasticity results extremely well. The last graph for case 1 is shown in Figure 4.11. In this graph the values of $\bar{\tau}_{xz}$ for the elasticity solution and the finite element solution are shown. The results using this finite element almost exactly match the elasticity results.

Since case 2 represents an unsymmetrical laminate, it represents a critical test for a proposed finite element. Comparing values for w in Figure 4.12, the finite element and elasticity results are the same over a range of thickness ratios. In Figure 4.13, the values for $\bar{\sigma}_x$ are compared. Again, the two results are essentially the same. The next area examined is the transverse shear stress, τ_{xz}. Looking at Figure 4.14, again the two methods give the same results. The largest difference occurs at the bottom of the plate. The last parameter that is investigated is $\bar{u}$ for S=4. Once again looking at Figure 4.15, finite element and elasticity results are the same.

The last linear case for the semi-infinite laminated plate is case 3. As can be seen from Figure 4.16, the finite element prediction for $\bar{w}$ loses accuracy as the plate becomes thinner. This lack of accuracy is caused by the same phenomena that caused slow convergence for a thin isotropic plate. For the thin isotropic plate and the thin, laminated, symmetric plate the transverse shear strain should go to zero, whereas

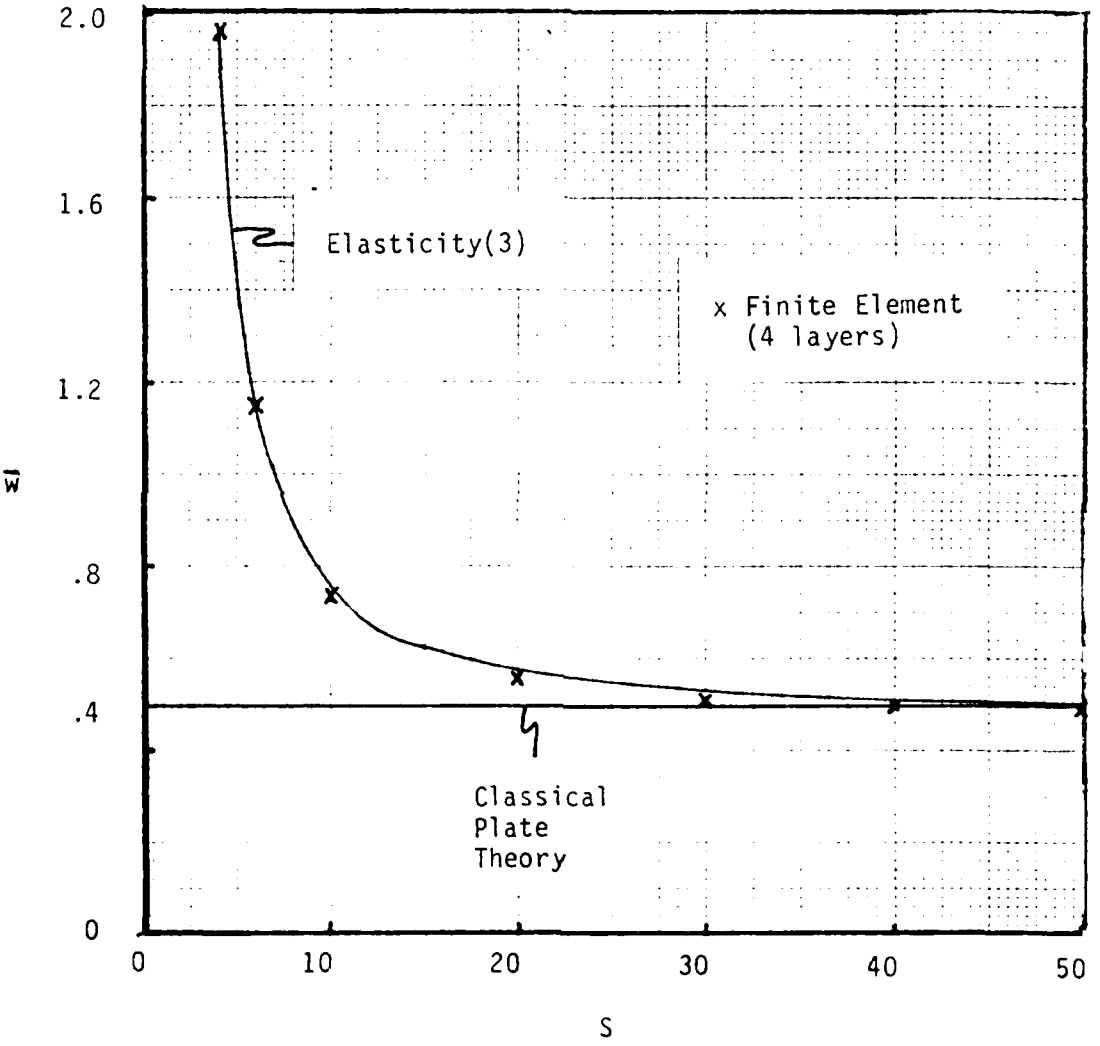

FIGURE4.8: Semi-infinite plate Case 1: $\bar{w}$ vs S Graph

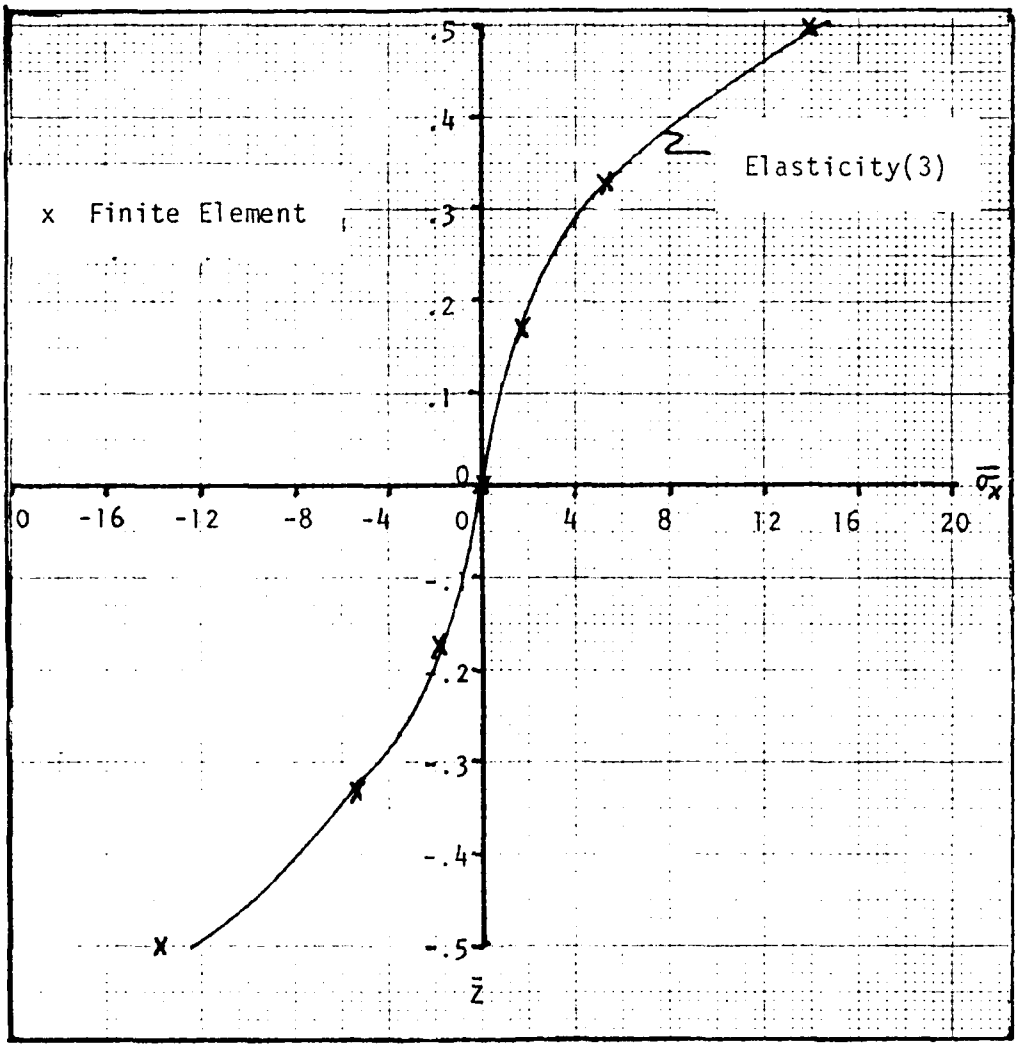

FIGURE 4.9: Semi-infinite Plate Case 1: $\bar{\sigma}_x$ vs. $\bar{z}$, S=4.

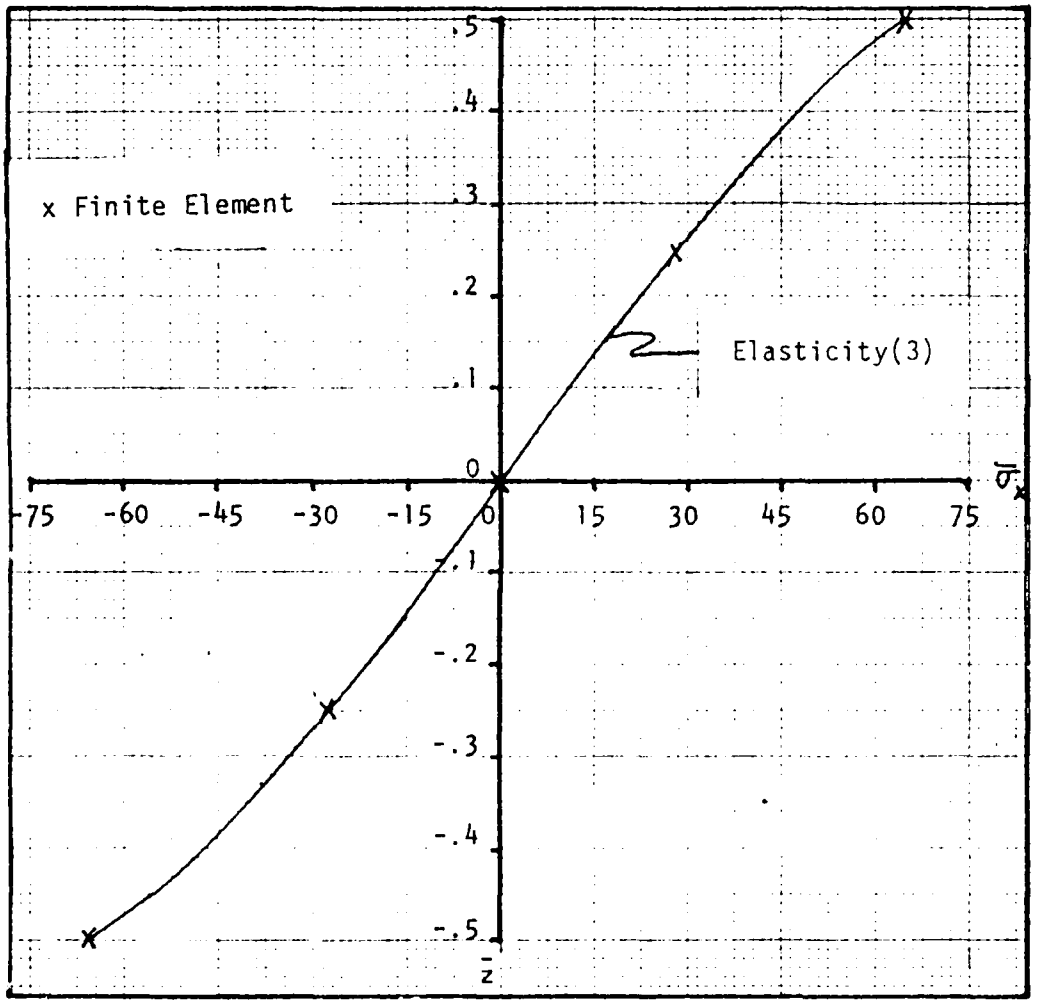

FIGURE 4.10: Semi-infinite Plate Case 1: $\bar{\sigma}_x$ vs. $\bar{z}$, S=10.

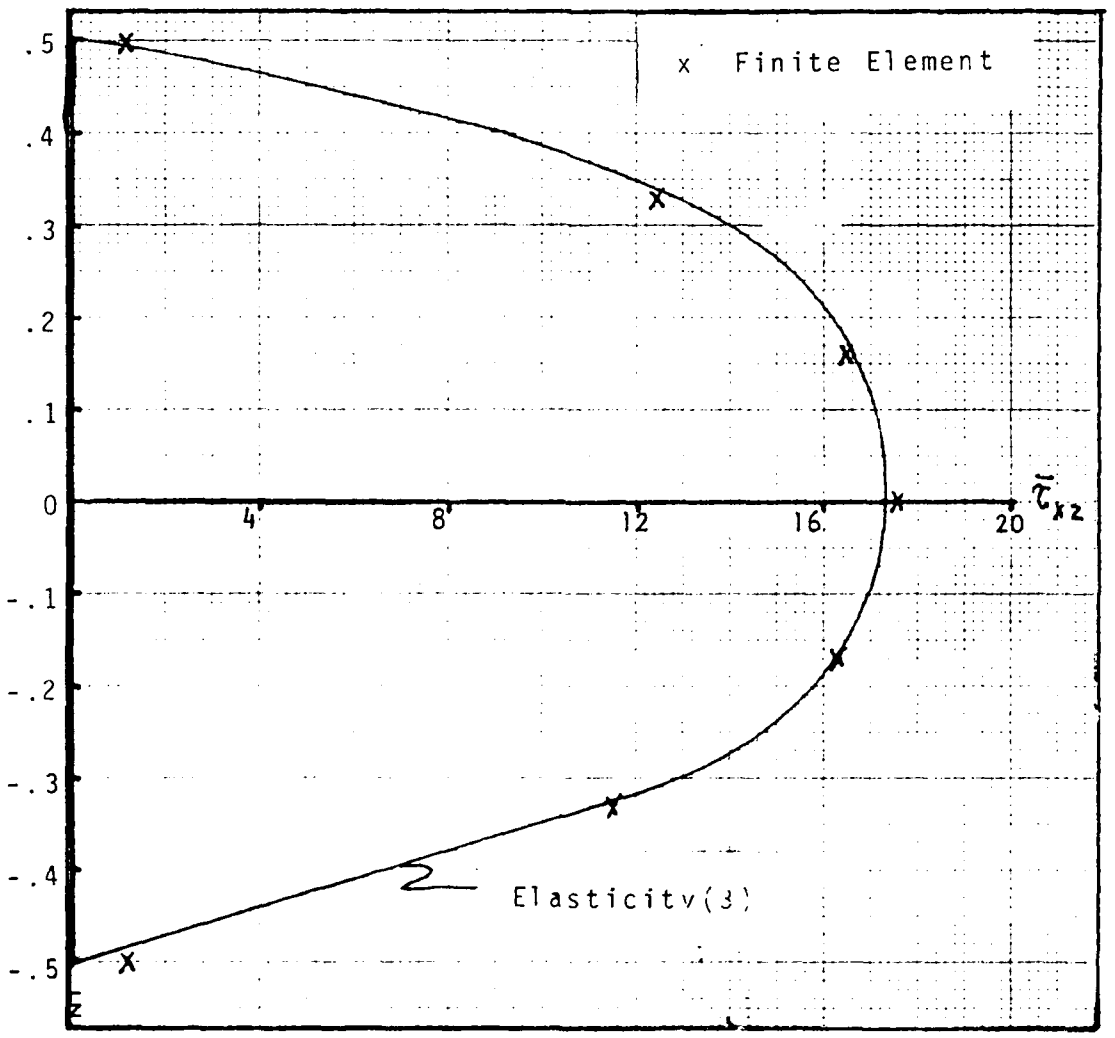

FIGURE 4.11: Semi-infinite Plate Case 1: $\bar{\tau}_{xz}$ vs. $\bar{z}$, S=4.

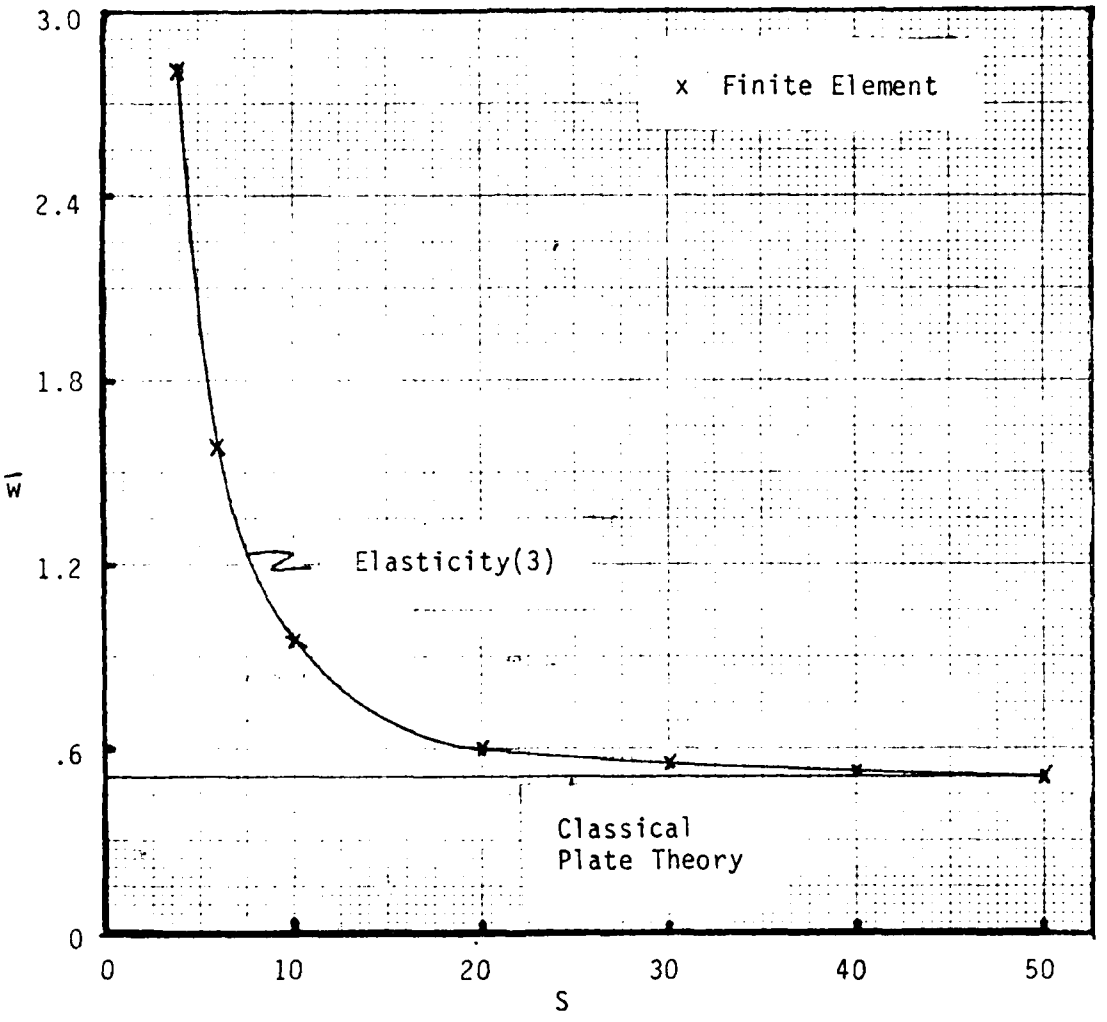

FIGURE 4.12: Semi-infinite Case 2: $\bar{w}$ vs. S Graph.

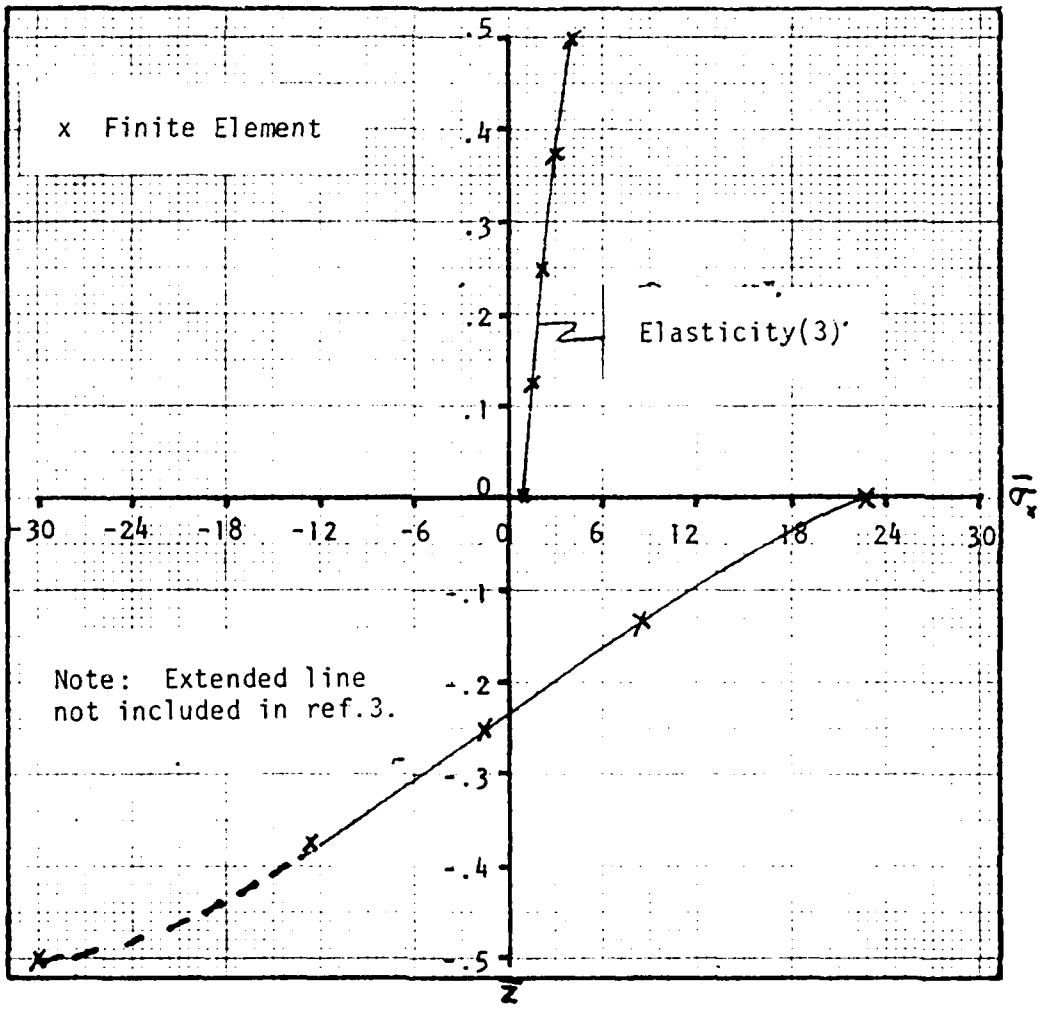

FIGURE 4.13: Semi-infinite Plate Case 2; $\bar{\sigma}_x$ vs $\bar{z}$ Graph, S=4.

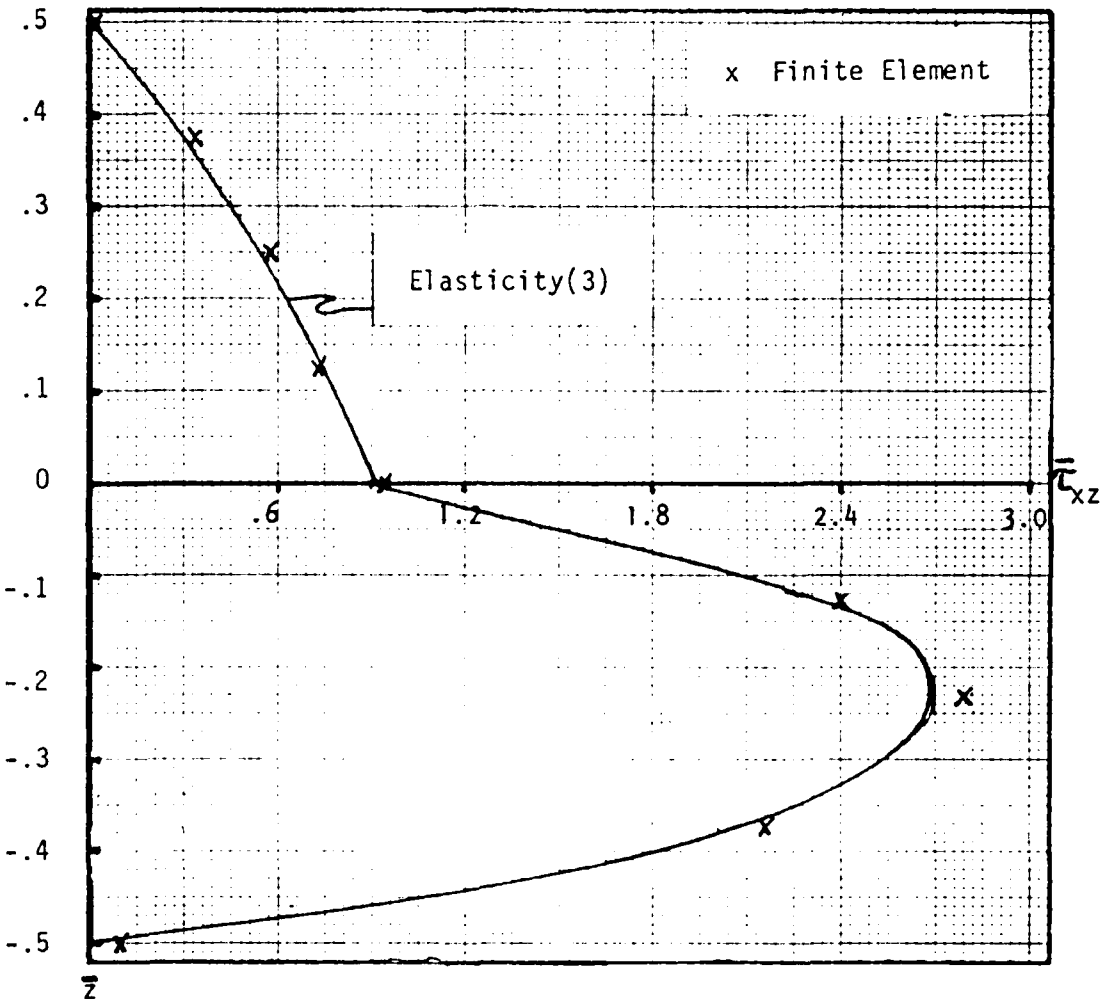

FIGURE4.14: Semi-infinite Plate Case 2; $\bar{\tau}_{xz}$ vs $\bar{z}$ Graph, S=4.

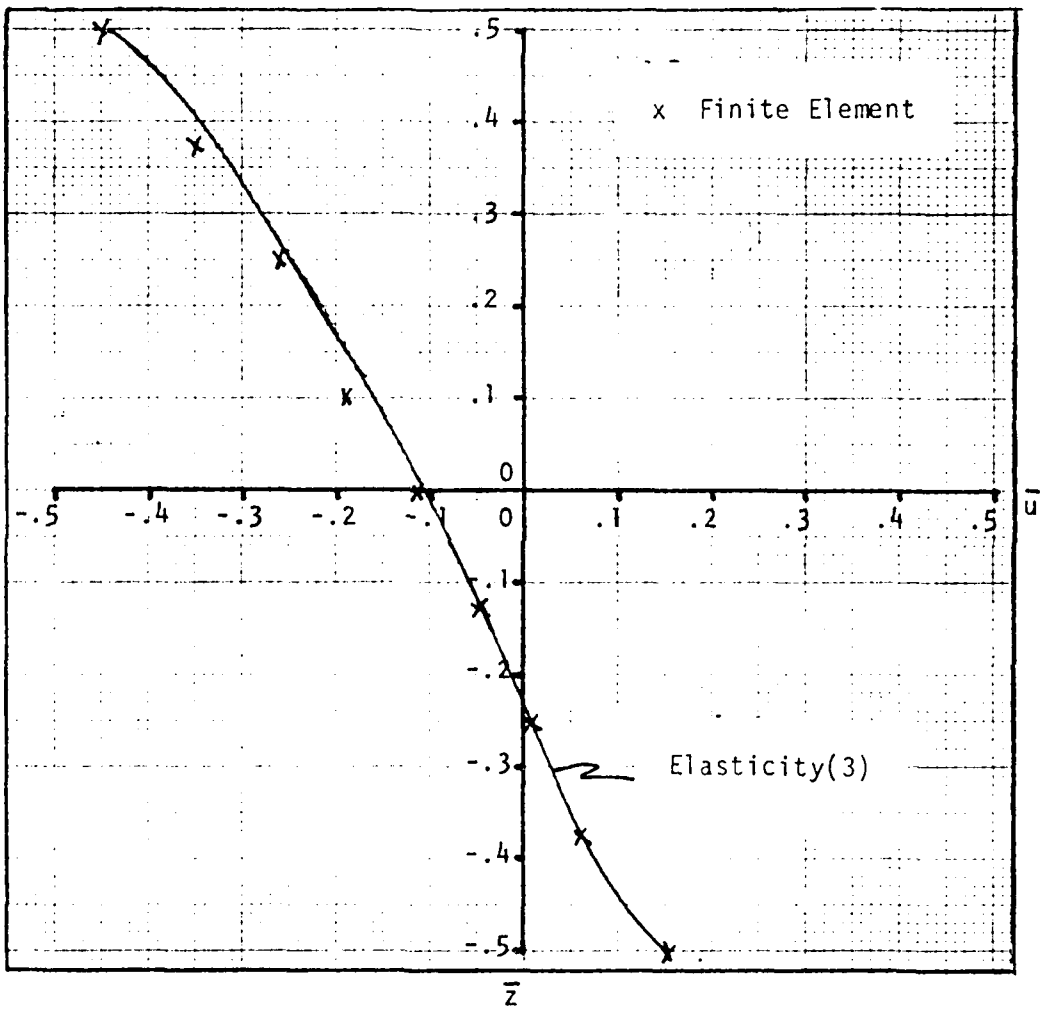

FIGURE 4.15: Semi-infinite Plate Case 2; $\bar{u}$ vs $\bar{z}$ Graph, S=4.

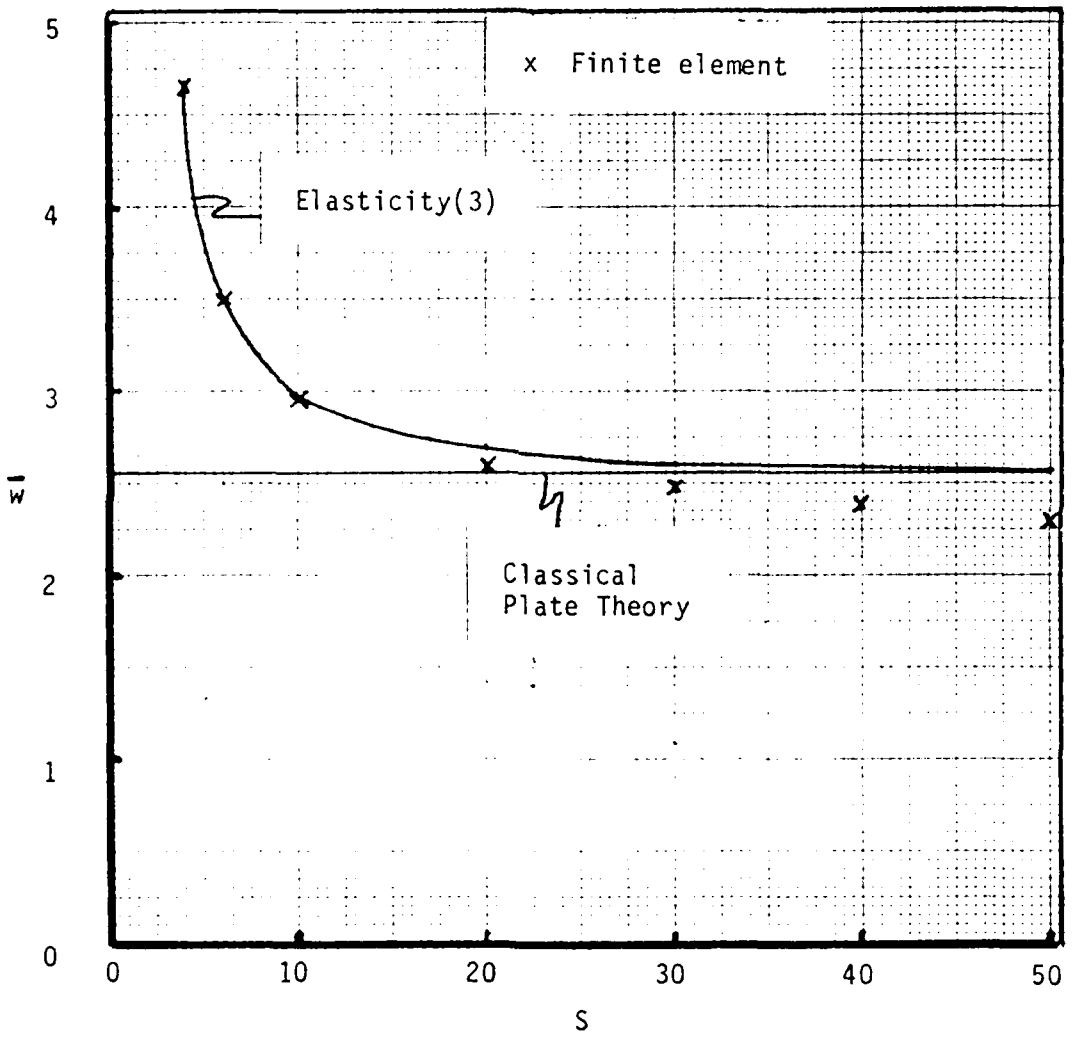

FIGURE 4.16: Semi-infinite Plate Case 3; $\bar{w}$ vs S Graph.

for thick plates and laminated unsymmetric plates, the shear strain is non-zero. The lack of accuracy results from the choice of the shape functions. From equations (I.57,58) the shear strain depends on the planar derivative of w and the z derivative of u and v. Since w varies linearly with respect to x and y, equation (3.29), the w derivative is a constant within the element. Since u and v vary quadratically with z, equations (3.42,43), the derivative is linear. Therefore, no matter how small the element is made the transverse strains will never go to zero within the element, and this element as derived will never be able to accurately handle these cases. To resolve this problem, more bending could be introduced in the element; that is, if the w shape function is made to be quadratic, the planar derivatives would be linear, and the element could resolve itself to zero shear strain.

For case 3, the results for $\bar{\sigma}_x$ are nearly identical for S=4 and S=10, Figures 4.17 and 4.18. The results for the shear stress, $\bar{\tau}_{xz}$, are also nearly identical. The small variation is caused by the difference in the conditions which are satisfied at the layer interfaces. In Pagano's solution, σ_z, τ_{xz}, u, and w must be equal at layer interfaces. In this finite element solution, the compatibility conditions, u and $u_{,z}$, are made equal at the interfaces. Since w is constant through the thickness, the conditions which Pagano satisfied are met by the compatibility conditions, but the compatibility conditions are not satisfied by making stresses equal at interfaces.

To investigate the effect of geometry on accuracy, a square orthotropic plate is examined. The present element results are compared with an elasticity solution (23) and another finite element solution (45). The loading is given by equation 4.2; the boundary conditions are

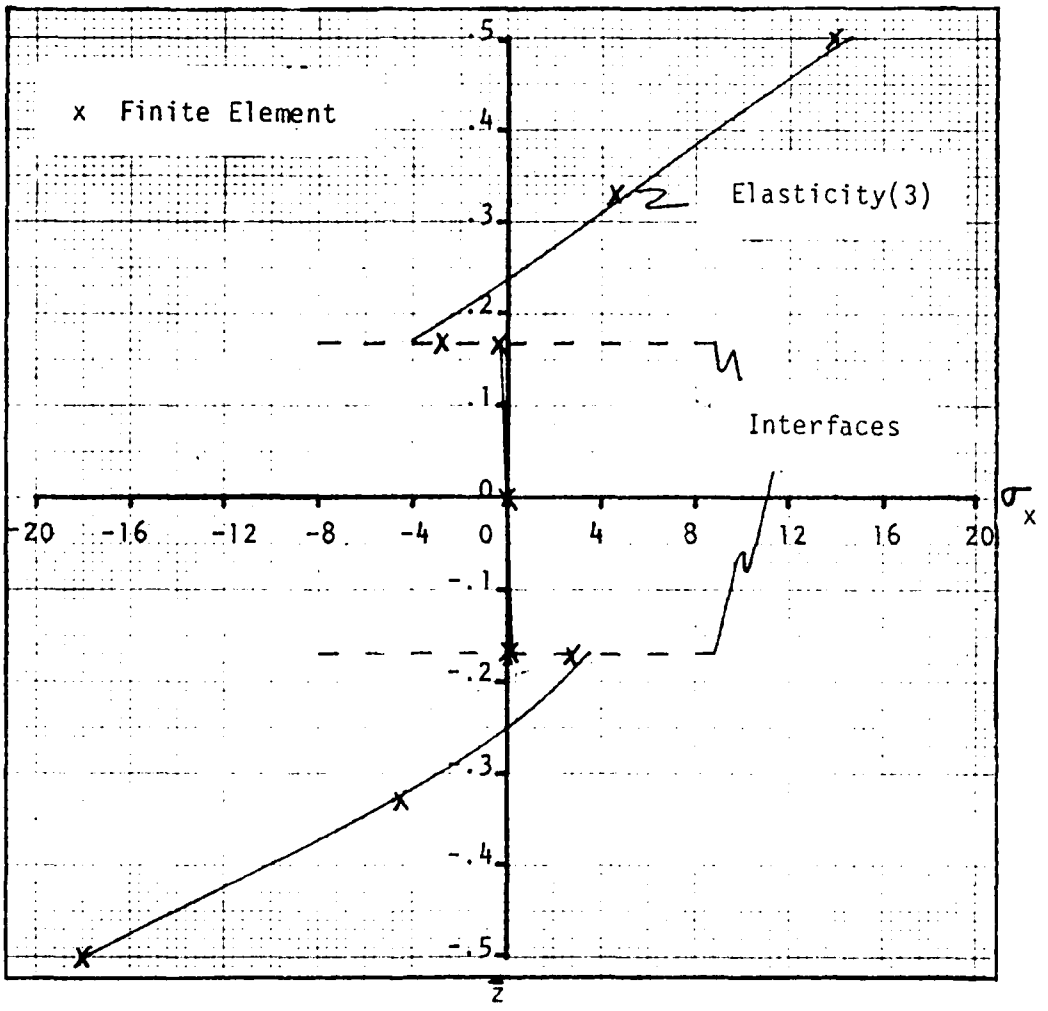

FIGURE 4.17: Semi-infinite Plate Case 3; $\bar{\sigma}_x$ vs $\bar{z}$ Graph, S=4.

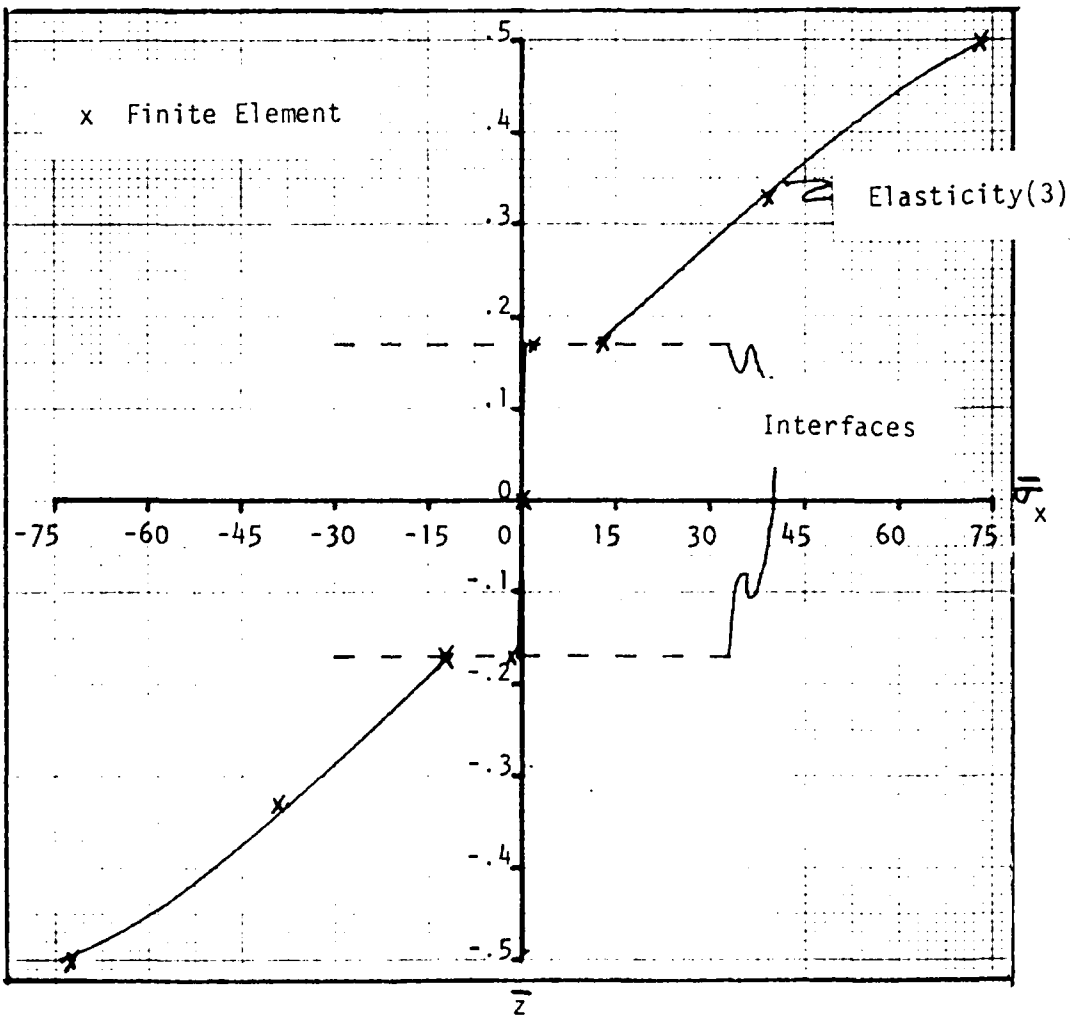

FIGURE 4.18: Semi-infinite Plate Case 3; $\bar{\sigma}_x$ vs z Graph, S=10.

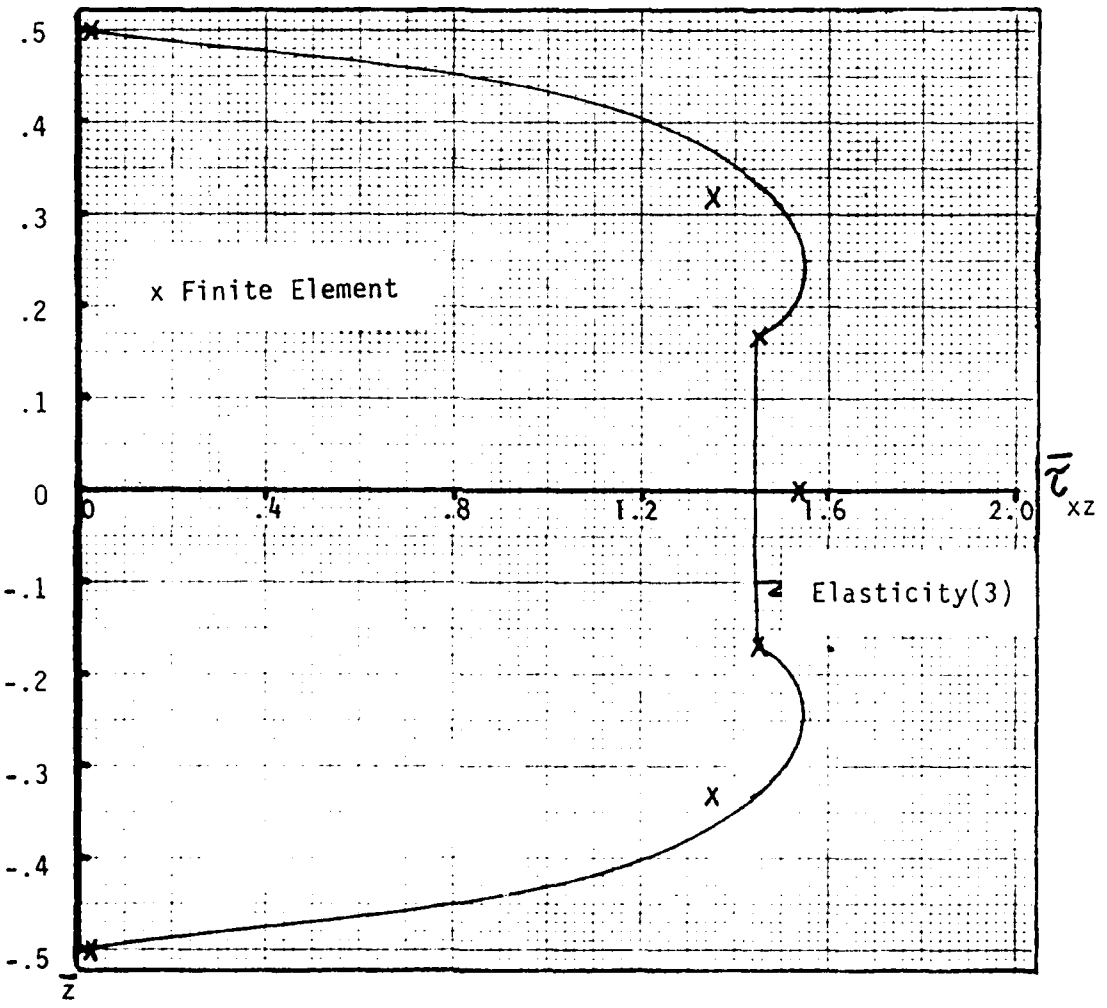

FIGURE 4.19: Semi-infinite Plate Case 3; $\bar{\tau}_{xz}$ vs $\bar{z}$ Graph, S=4.

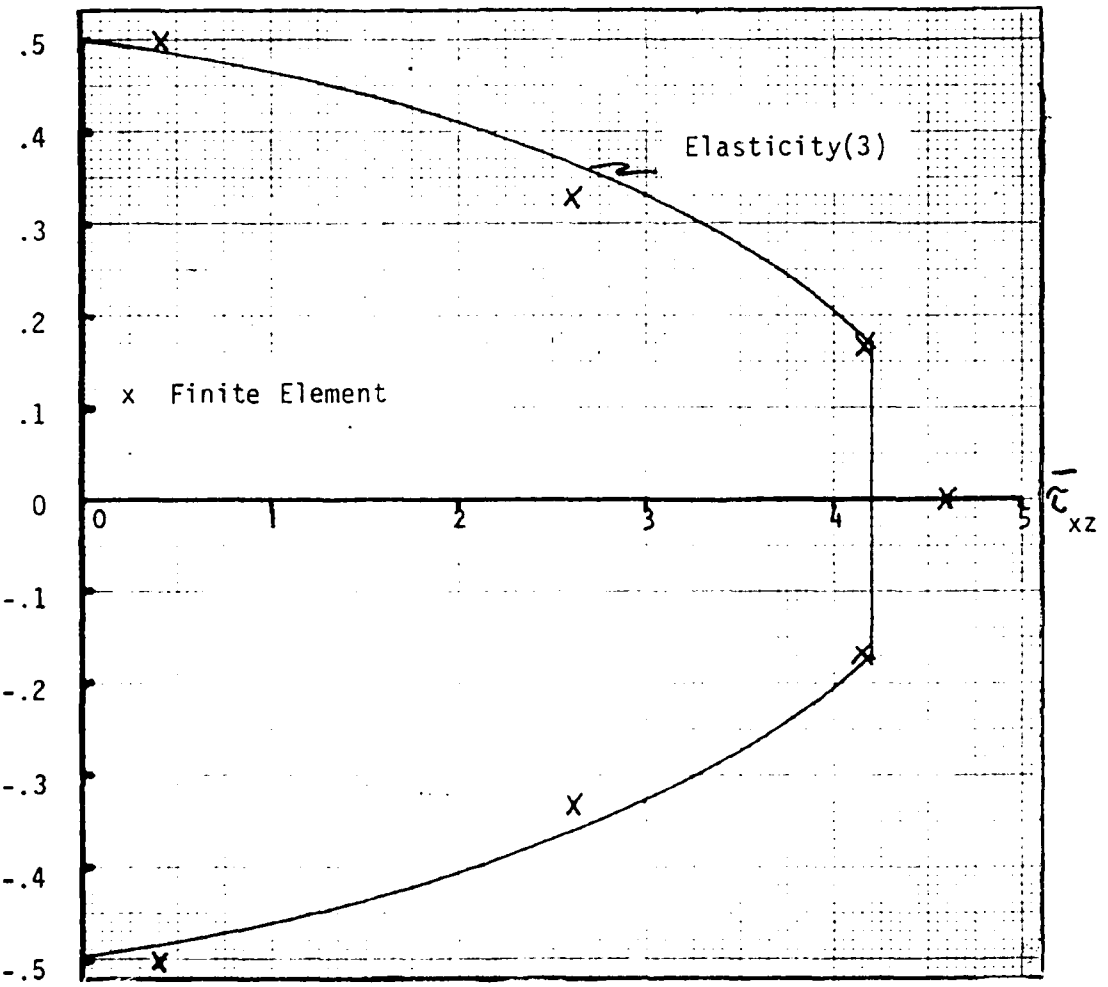

FIGURE 4.20: Semi-infinite Plate Case 3; $\bar{\tau}_{xz}$ vs z Graph, S=10.

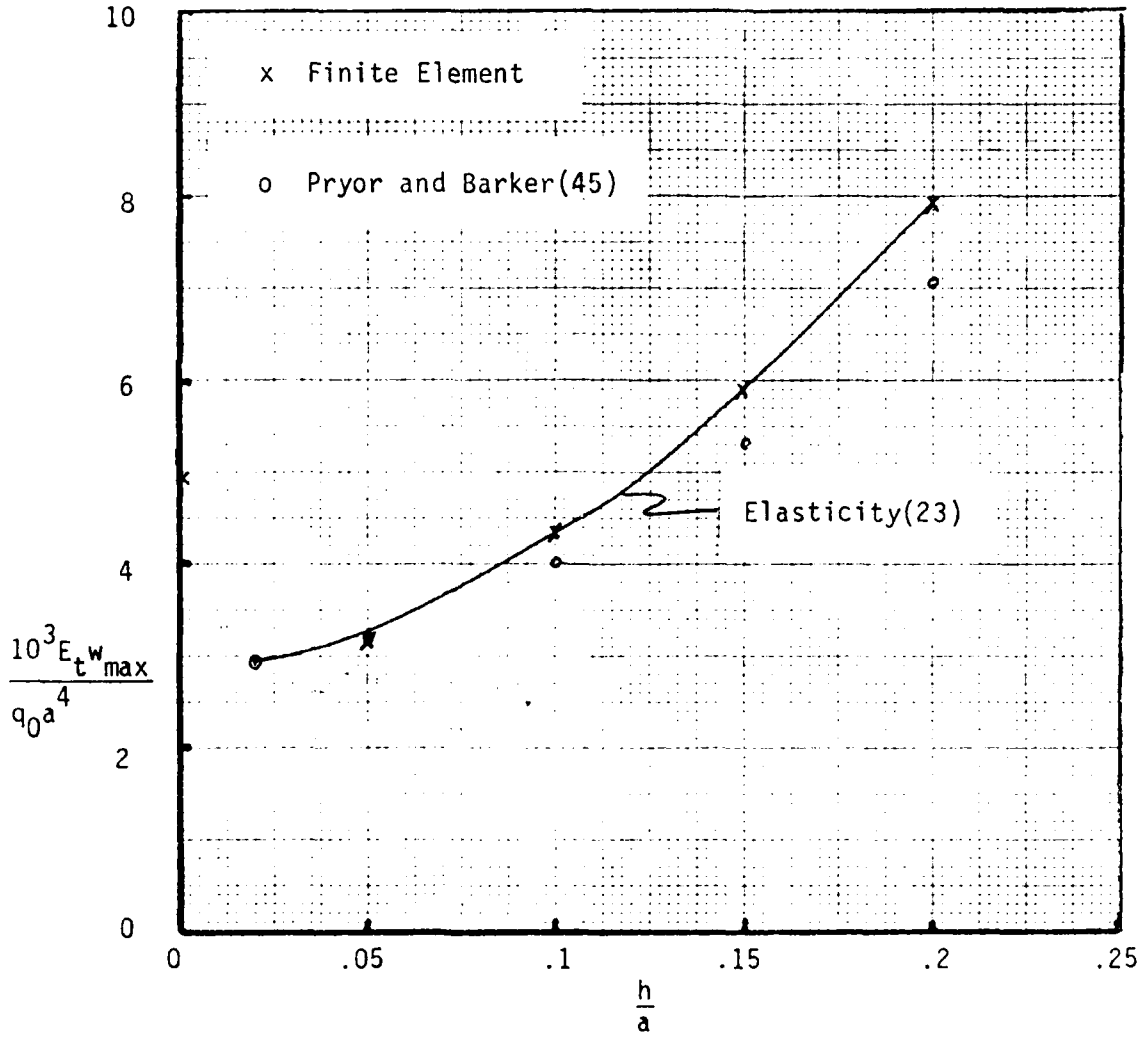

FIGURE 4.21: Square $(0,90)_s$ Plate; $\bar{w}$ vs h/a.

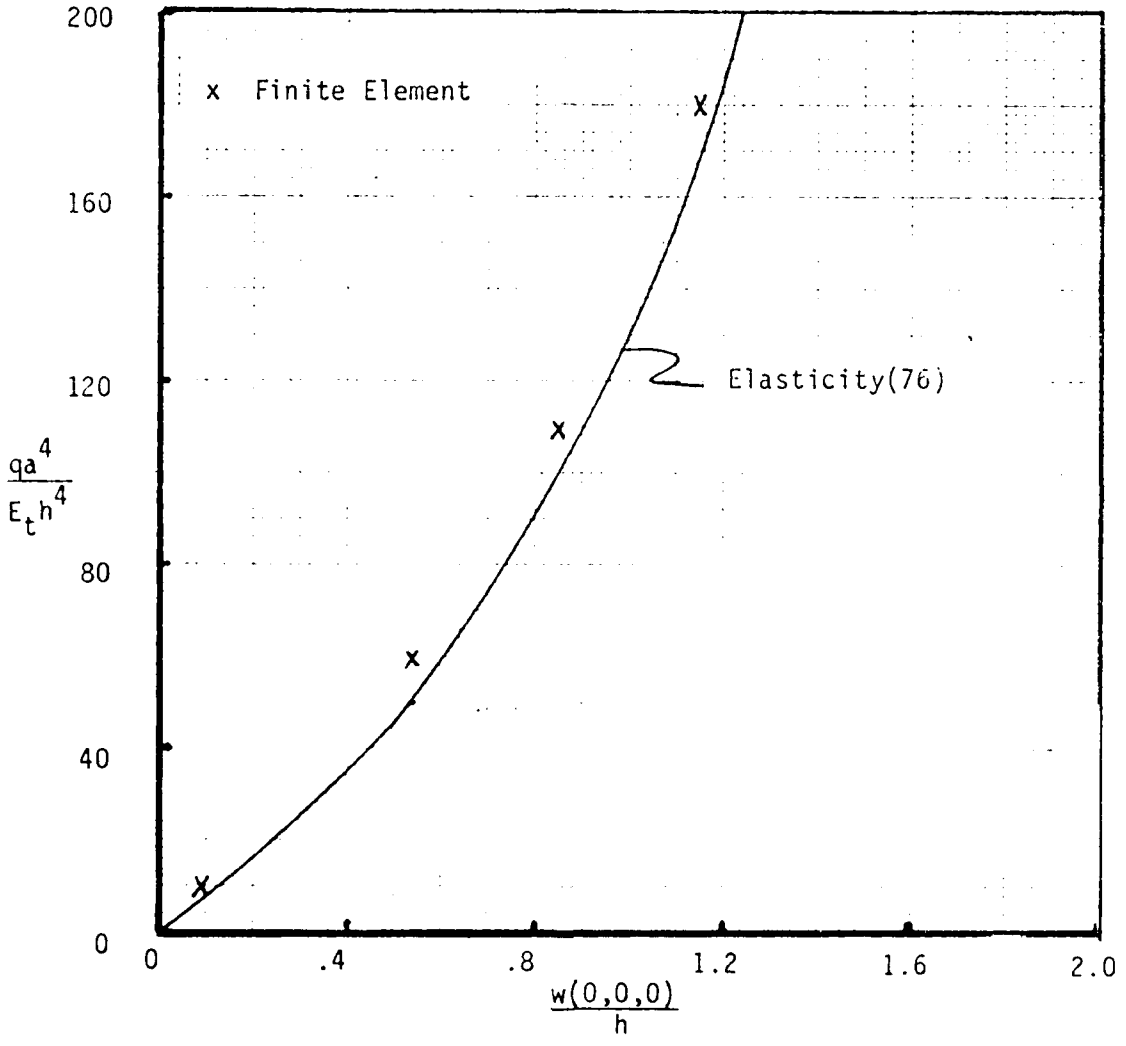

FIGURE 4.22: Nonlinear Load-deflection Graph for Square Orthotropic Plate.

described in the fifth convergence example, and the material properties are given in Table 4.2. As can be seen in Figure 4.21, the finite element results with the present element are better than those obtained by Pryor and Barker. The primary difference between the elements is that the normal remained straight in the element used by Pryor and Barker. By allowing the normal to both rotate and deform, the elasticity results can be duplicated.

The last example that will be investigated in this section is the nonlinear deformation of a square orthotropic plate. Since few nonlinear analyses of orthotropic plates have been done, it is difficult to find examples by which accuracy can be judged. The finite element results will be compared against some approximate elasticity results obtained by Chia (77). The plate is clamped on all edges and under a uniformly distributed transverse load. The material properties are given in Table 4.2. The comparison is presented in Figure 4.22. The finite element results and elasticity results are very close for this example.

RANGE AND APPLICABILITY

Two examples will be used to illustrate the applicability to nonlinear problems. First, the stresses in a semi-infinite unsymmetric, laminated plate will be examined. Second the collapse load for a square orthotropic plate with a central hole will be determined.

The semi-infinite orthotropic plate used in this analysis is the one described in case 2 in the accuracy portion of this chapter. The loading and boundary conditions are also the same.

The plot of normalized transverse displacement versus the normalized load is shown in Figure 4.23. As can be seen, nonlinear behavior is obtained. The load at point one corresponds to a linear load. While

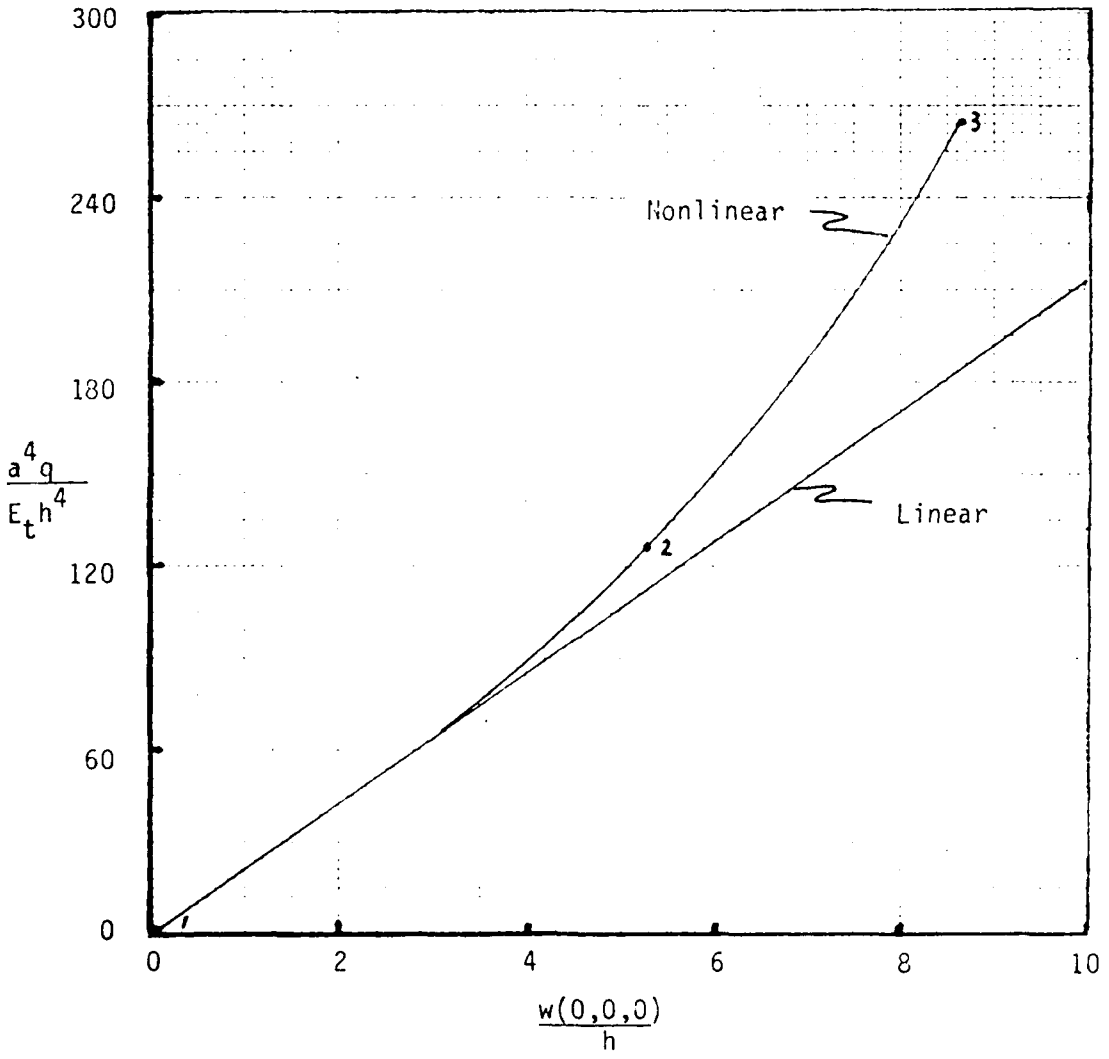

FIGURE 4.23: Finite Element Load-deflection Graph for Unsymmetric, Semi-infinite, Laminated Plate, S=40.

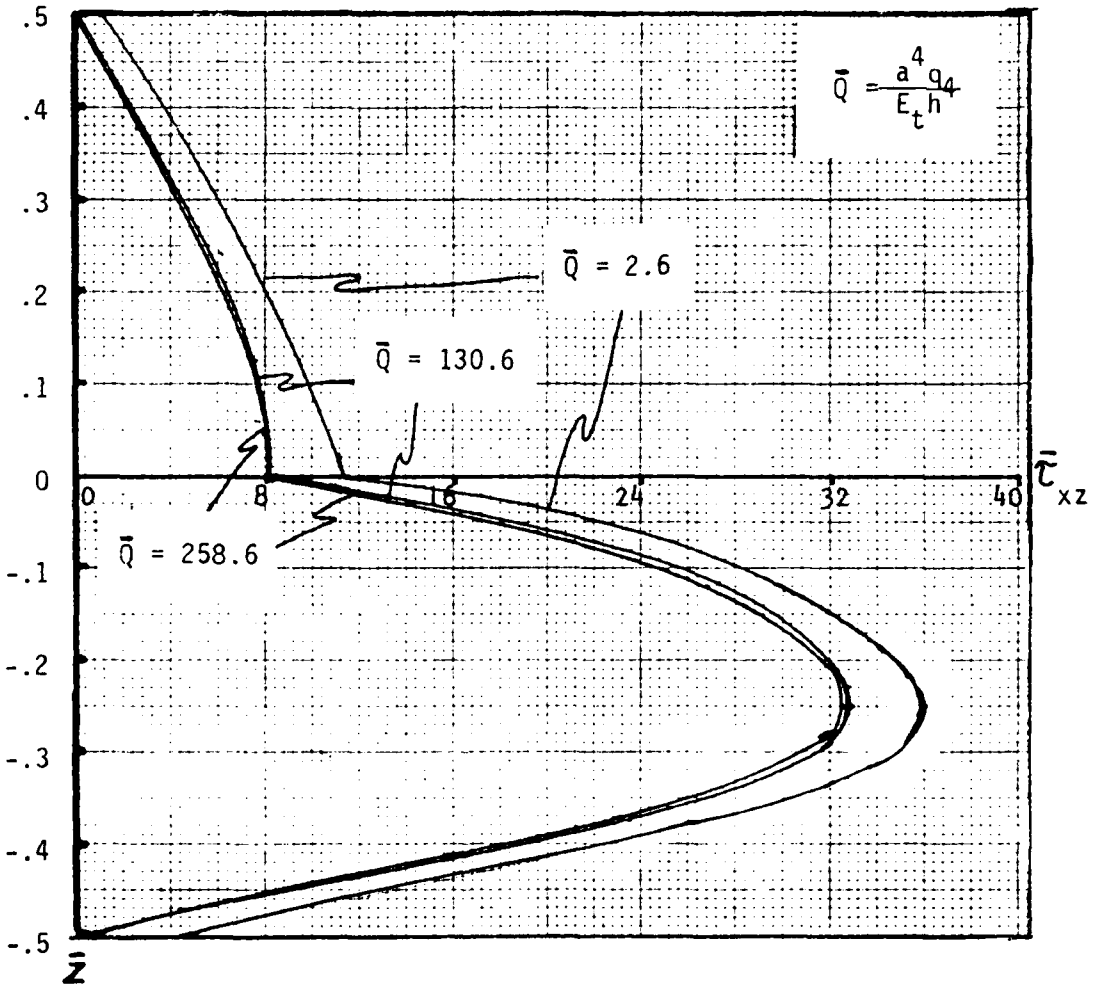

FIGURE 4.24: Finite Element $\bar{\tau}_{xz}$ Plot for Unsymmetric, Semi-infinite, Laminated Plate, S=40.

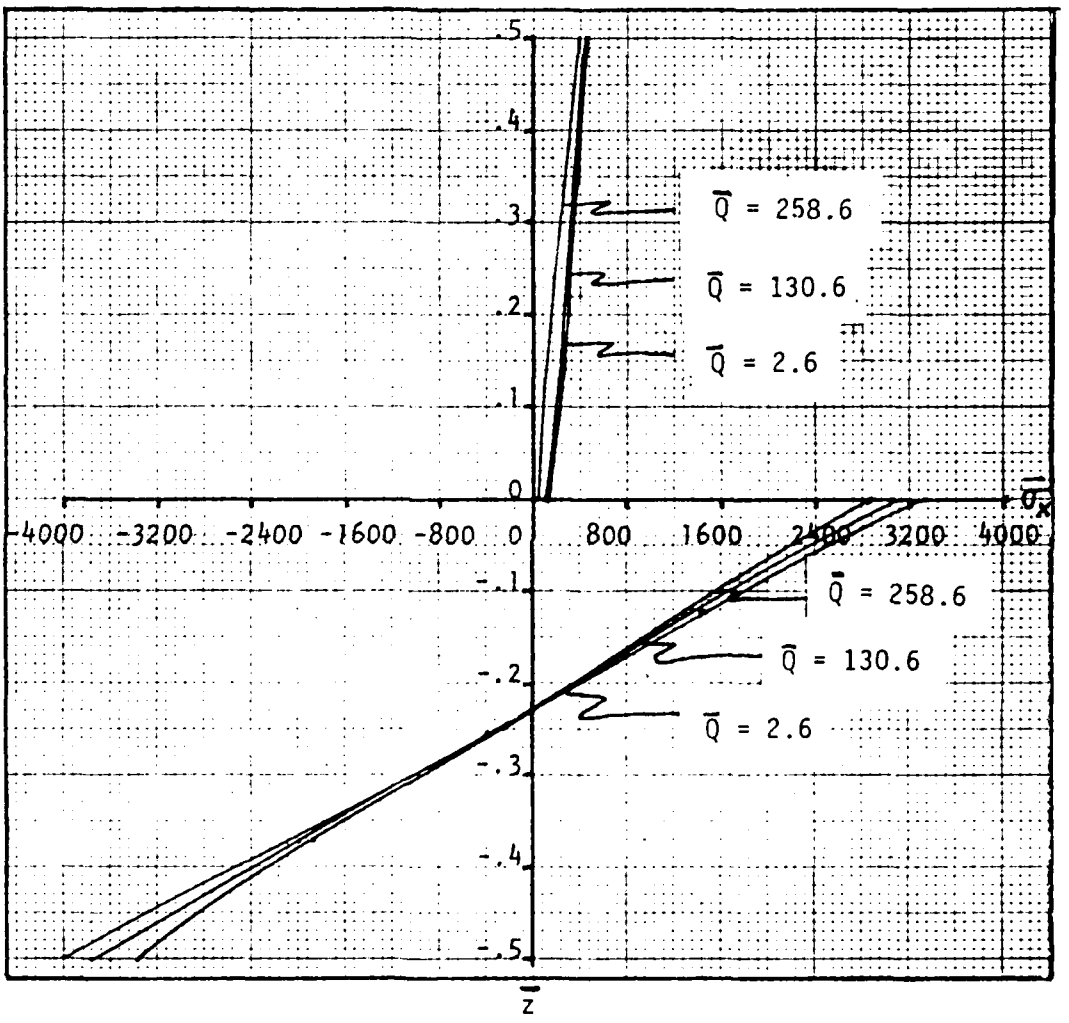

FIGURE 4.25: Finite Element $\bar{\sigma}_x$ Plot for Unsymmetric, Semi-infinite, Laminated Plate, S=40.

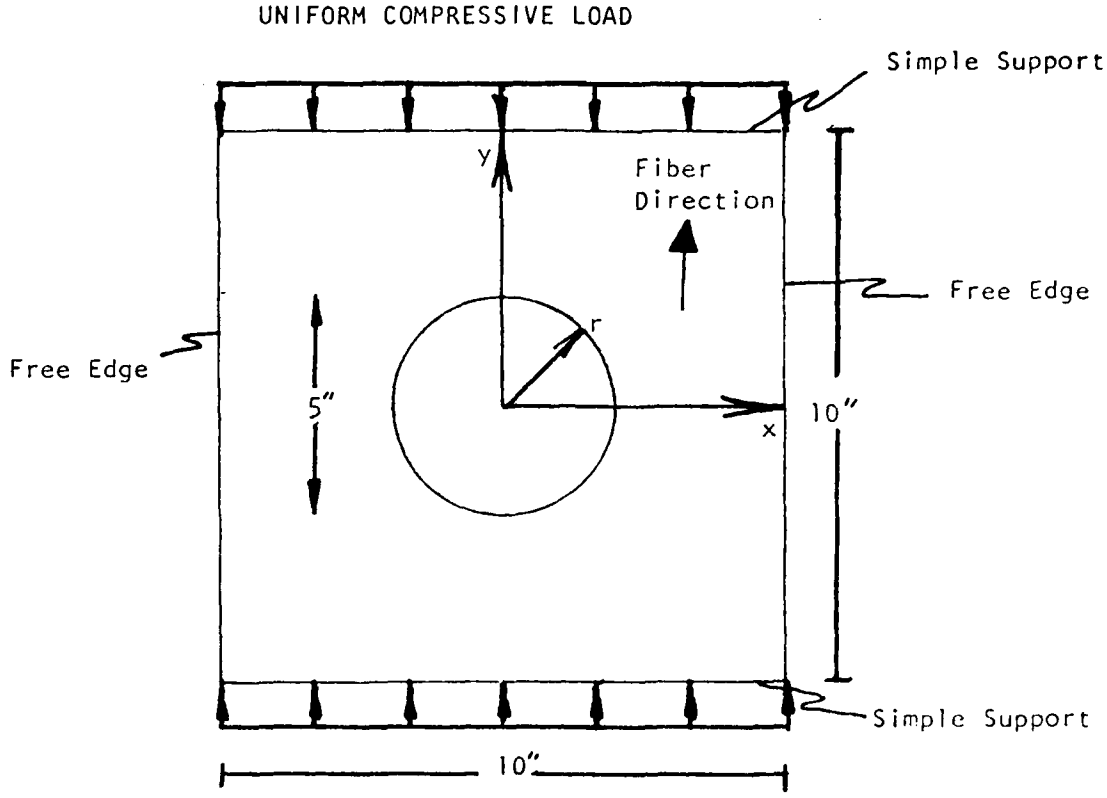

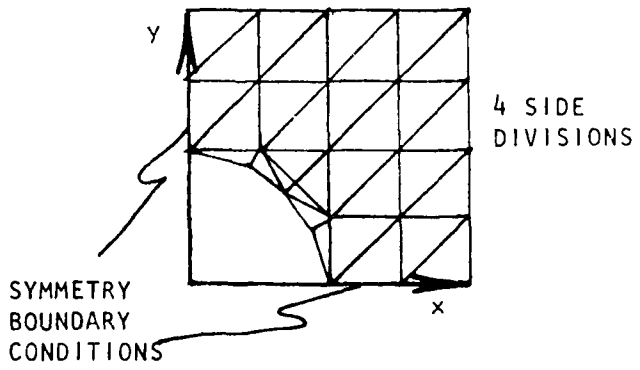

FIGURE 4.26: Square Plate With Hole, Geometry and Finite Element Model

loads two and three are nonlinear loads.

Shown in Figure 4.24 are plots of the normalized transverse shear stress, $\bar{\tau}_{xz}$. The distribution shape of $\bar{\tau}_{xz}$ does not change as the load becomes larger but the magnitudes do appear to move in the negative direction. The plots of the normal stress, $\bar{\sigma}_x$, are shown in Figure 4.25. The same behavior as is observed for $\bar{\tau}_{xz}$ is seen in $\bar{\sigma}_x$.

The last example ir this chapter is an orthotropic plate with a central hole under compressive load. The geometry of the plate and the finite element mesh use are shown in Figure 4.26.

The plot of load versus displacement for a plate with an S=50 thickness ratio is shown in Figure 4.27. The load is normalized by dividing it by the buckling load, $\bar{P}$, for an equivalent orthotropic plate with no hole. The transverse displacement is normalized by dividing by the displacement that would be experienced if the plate behavior were linear to the buckling load. The use of the current stiffness parameter allows the program to follow the behavior of the plate up to the collapse load. According to this analysis, the plate collapses when the compressive load is 76% of the classical buckling load for a perfect square plate.

In the Results chapter, the capabilities of this new element have been demonstrated. With this element, it is now possible to obtain accurate, convergent results for the linear and non-linear analysis of plates. The boundary conditions can vary in the transverse direction. The more specific accomplishments of this dissertation are contained in the Conclusions chapter.

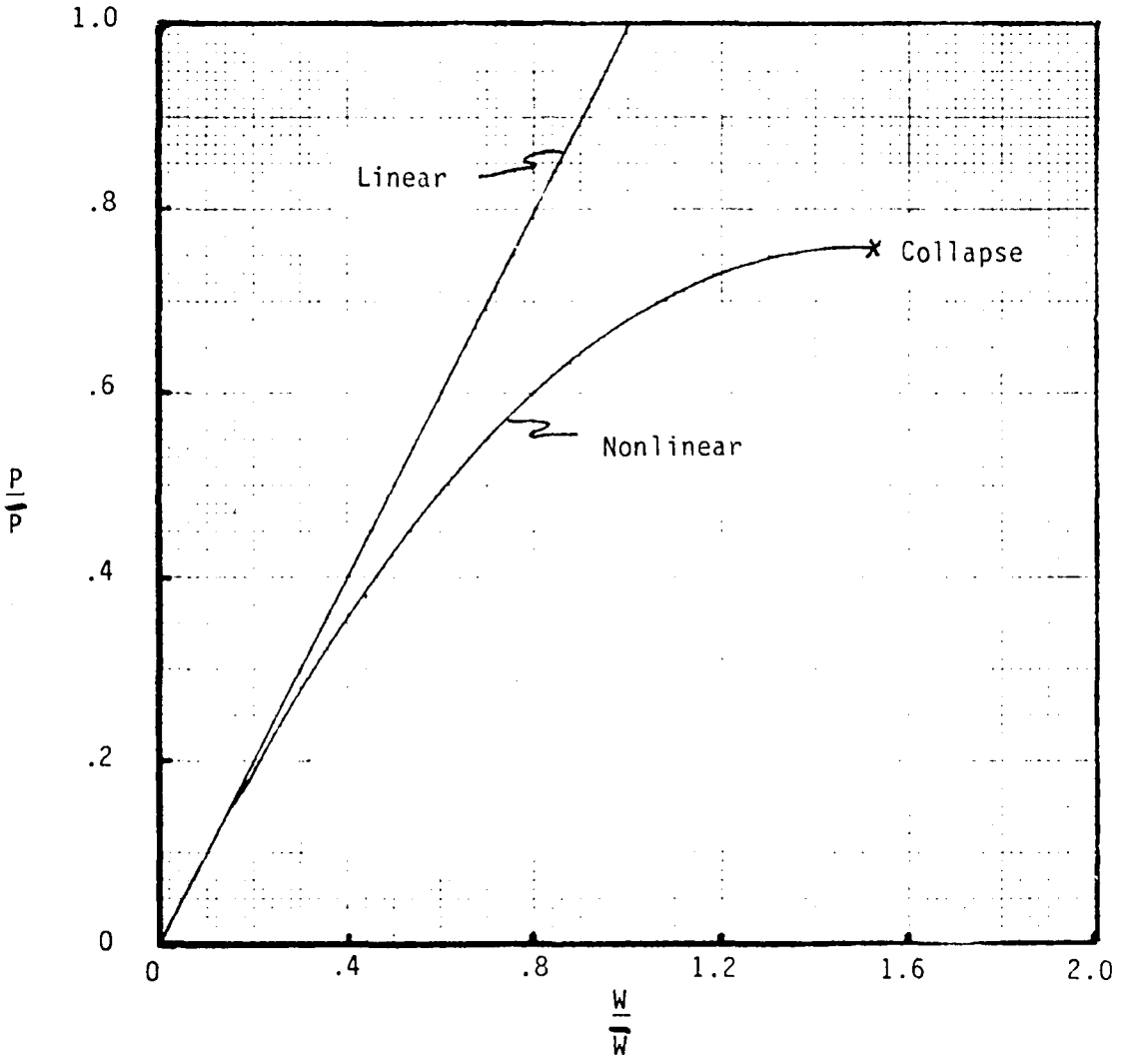

FIGURE 4.27: Load-deflection Curve for Square Orthotropic Plate with Central Hole.

5. Conclusions

The success of this dissertation must be measured against satisfying the original objective. The stated objective of this work is to formulate a numerical procedure for the large-displacement analysis of laminated composite structures with general loading and boundary conditions. In the "Introduction" chapter, it was also concluded that to accomplish this objective, nonlinear geometrical effects and normal shear effects must be accounted for.

To guage the success of this research, the development of the theory and the comparisons with other results are examined. After these two areas are examined, it is then possible to make conclusions as to how completely the objective has been met. Last, in this chapter, I will delineate the advantage of using this method.

The "Background" chapter and the "Theory" chapter outline the development of the method used in this dissertation. The first choice that was made was between finite differences and finite elements for the numerical procedure. The finite element method was chosen because of its greater flexibility in handling boundary conditions. This flexibility was demonstrated by solving problems with classical clamped simple support, and free edge boundary conditions. In addition, a mixed type of boundary condition was used where a displacement normal to the edge but in the plane of the plate was free, but the normal at the edge did not deform. The finite difference method would not have handled this variety of boundary conditions well.

The primary unique characteristic of this work was the way in which normal shear effects were handled. Previous methods have allowed the normal to rotate but not deform within each layer of a laminate. This approach resulted in discontinuities in shear strain at lamina interfaces. The finite element presented here overcomes these discontinuities by guaranteeing not only displacement but also shear strain continuity in the thickness direction. The original intent of this approach was to better model shear stresses without the complexity of a hybrid finite element. As can be seen in the results section, shear stress calculations using this finite element are almost the same as those obtained by classical elasticity methods.

Another unique characteristic of the development presented in this dissertation is the way in which nonlinear effects are included. The nonlinear effects are included at the basic elastic equation level rather than by extending a generalized theory. This minimizes the assumptions that are made and increases flexibility in the application of the element.

The specialization of the element now occurs through the geometrical definition of the structure. Using this approach, it is easy to specialize the element to plates or shells.

To illustrate how the element is used to analyze a specific structure, plate problems were chosen. Plate problems were chosen because there were many examples of laminated plate analysis to use in comparison and because applying the element to plates was a logical first step as opposed to jumping into the analysis of shells.

After the element was developed the next area that was approached was the solution procedure. A classical nonlinear equation solution procedure was used. There was no analysis done on how different solution procedures

affect solution efficiency; therefore, there is no efficiency analysis accomplished.

The one area af the solution process that includes unique information is the use of the current stiffness parameter. This parameter is used to determine when the nonlinear stiffness matrix becomes singular or otherwise when structural collapse occurs. The parameter has been presented before, but a derivation of the parameter has not been published to the best of my knowledge.

Now that the development process has been summarized and the reasoning behind the process presented, it is necessary to examine how solutions obtained using this element compare with other numerical and analytical results. The areas examined for comparison are convergence, accuracy, and applicability.

As is shown and explained in the "Results" chapter, the element did not converge well and was not accurate for thin, isotropic plates and thin, laminated, symmetric plates. The cause of this was that the shear strain would not go to zero as is physically expected(42). Since this element was meant to handle cases where the transverse shear is an important factor this shortcoming was somewhat expected, but was not resolved in this work other than to suggest a possible solution.

The element converged well for anisotropic materials. The element converged well for the range of thicknesses studied, but it converged faster for thicker plates. From examining the semi-infinite plate problem, it can be seen that the element converged faster for the unsymmetric laminate.

Increasing the number of modelling layers in a lamina does increase the convergence rate. Using more than two layers to model a lamina did not greatly increase the convergence rate. More layers can be used to obtain more intermediate values of transverse shear stresses in the lamina.

Turning to accuracy, again the solution obtained for isotropic materials was not good. When the finite element solution was compared with other solutions for orthotropic materials though, the accuracy obtained was excellent. The element predicted the displacements well, as would be expected with a displacement finite element. It also did a good job of predicting normal and shear stresses indicating the success of this approach.

Little material is available on the nonlinear behavior of laminated plates. The one comparison that was done showed that the method does give accurate results in situations where the displacements are large. In addition, it was also possible to keep track of stresses when the plate was undergoing large displacements.

The other problem that was handled under the applicability section of the "Theory" chapter was the collapse of a square plate with a centrally located hole. By using this finite element and the current stiffness parameter, it was possible to follow this structure to collapse. Since this plate was thin, it appears that the collapse load value was slightly higher than would be expected.

From examining the development and results, some strengths of this element are apparent. From the development, it is apparent that this element is perfectly suited for shear loading. In addition, by examining the loads that were applied to specific problems, it can be seen that distributed normal loads and compressive loads are also handled well. As previously stated the element can also be adapted to handle a variety of boundary conditions. Since the structure can be dividied into layers and the functional character of the director deformation is not predetermined for the entire thickness, great accuracy in predicting shear patterns is obtained. The use of the current

stiffness parameter facilitates easier nonlinear analysis. Even though these observations are made for plate analysis, the general character of the development makes it possible to adapt this element to other structural shapes.

As a final statement, I would conclude that the objective of this dissertation has been accomplished. Even though the element does not handle isotropic cases well, it can be used for the nonlinear analysis of laminated composites under a variety of loading and boundary conditions.

BIBLIOGRAPHY

1. Hadcock, R. N., "The Cautious Course to Introducing New SDM Technology into Production Systems," Astronautics and Aeronautics, 18; March 1980, pp. 31-33.

2. Card M. F., "Highlights 1979: Structures," Astronautics and Aeronautics 17; December 1979, pp. 98-100.

3. Pagano, N. J., "Exact Solutions for Composite Laminates in Cylindrical Bending," Journal of Composite Materials, 3; July 1969, pp. 398-411.

4. Gould, P. L., Static Analysis of Shells. Lexington, Massachusetts: D.C. Heath and Co., 1977.

5. Hildebrand, F. B., Reissner, E. and Thomas, G. B. Notes on the Foundation of the Theory of Small Displacements of Orthotropic Shells, NACA TN-1833. Washington D.C.: National Advisory Committee for Aeronautics, March 1949.

6. Ambartsumyan, S. A., Theory of Anisotropic Shells. NASA TFF-118, Washington D.C.: National Aeronautics and Space Administration, May 1964.

7. Ambartsumyan, S. A., Theory of Anisotropic Plates. Stamford, Conn.: Technomic Publishing Co., 1970.

8. Calcote, L. R. The Analysis of Laminated Composite Structures. New York: Van Nostrand Reinhold, Co., 1969.

9. Jones, R. M. Mechanics of Composite Materials. Washington, D.C.: Scripto Book Co., 1975.

10. Reissner, E. Small Bending and Stretching of Sandwich-Type Shells. NACA TN-1832, Washington D.C.; National Advisory Committee for Aeronautics, March 1949.

11. Reissner, E. "The Effect of Transverse Shear Deformation on the Bending of Elastic Plates," Journal of Applied Mechanics, 12; pp. 69-77, (1945).

12. Mindlin, R. D. "Influence of Rotatory Inertia and Shear on Flexural Motions of Isotropic, Elastic Plates," Journal of Applied Mechanics, 18; pp. 31-38 (1951).

13. Ericksen, J. L. and Truesdell, C. "Exact Theory of Stress and Strain in Rods and Shells," Archive of Rational Mechanics, 1; pp. 295-323 (1957).

14. Green, A. E., Naghdi, P. M. and Wainwright, W. L., "A General Theory of a Cosserat Surface," Archive of Rational Mechanics, 20; pp. 287-308 (1965).

15. Cohen, H. "A Nonlinear Theory of Elastic Directed Curves," International Journal of Engineering Science, 4; pp. 511-524 (1966).

16. Bercha, F. D. and Glockner, P. G. "Thick Shell and Oriented Surface Theories," Journal of the Engineering Mechanics Division, Proc. of ASCE, 98; pp. 823-833 (August, 1972).

17. Eringen, A. C. "Mechanics of Micromorphic Continua," Mechanics of Generalized Continua. ed. by E. Kroner, New York. Springer-Verlag, New York, Inc. (1968).

18. Eringen, A. C. "Nonlocal Polar Elastic Continua," International Journal of Engineering Science, 10; pp. 1-6, (1972).

19. Mindlin, R. D. "Microstructure in Linear Elasticity," Archive for Rational Mechanics, 16; pp. 51-78 (1964).

20. Perkins, R. W. Jr. and Thompson, D. "Experimental Evidence of a Couple-stress Effect," AIAA Journal, 11; pp. 1053-1055 (1973).

21. Yang, P. C., Norris, C. H. and Stavsky, Y. "Elastic Wave Propagation in Heterogeneous Plates," International Journal of Solids and Structures, 2; pp. 665-684 (1966).

22. Whitney, J. M. and Leissa, D. "Analysis of Heterogeneous Anisotropic Plates," Journal of Applied Mechanics, 36; pp. 261-266 (1969).

23. Whitney, J. M. "The Effect of Transverse Shear Deformation on the Bending of Laminated Plates," Journal of Composite Materials, 3; pp. 534-537 (1969)

24. Whitney, J. M. and Pagano, N.J. "Shear Deformation in Heterogeneous Anisotropic Plates," Journal of Applied Mechanics, 37; pp. 1031-1036 (1970).

25. Whitney, J. M. "The Effect of Boundary Conditions on the Response of Laminated Composites," Journal of Composite Materials, 4; pp. 192-203 (1970).

26. Whitney, J. M. "Stress Analysis of Thick Laminated Composite and Sandwich Plates," Journal of Composite Materials, 6· pp. 426-441 (1972).

27. Whitney, J. M. "Analysis of Anisotropic Rectangular Plates," AIAA Journal, 10; pp. 1344-1345 (1972).

28. Whitney, J. M. and Sun, E. T. "A Higher Order Theory for Extensional Motion of Laminated Composites," Journal of Sound and Vibrations, 30, pp. 85-98 (1973).

29. Grot, R. A. "A Continuum Model for Curvilinear Laminated Composites," International Journal of Solids and Structures, 8; pp. 439-462 (1972).

AD-A135 997 FORMULATION OF A NONLINEAR COMPATIBLE FINITE ELEMENT FOR THE ANALYSIS OF..(U) AIR FORCE INST OF TECH WRIGHT-PATTERSON AFB OH SCHOOL OF ENGI.. W P WITT

2/2

UNCLASSIFIED DEC 82 AFIT/DS/AA/83-1 F/G 12/1 NL

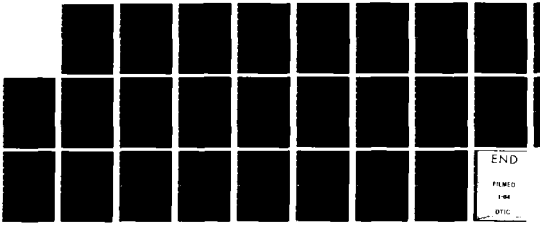

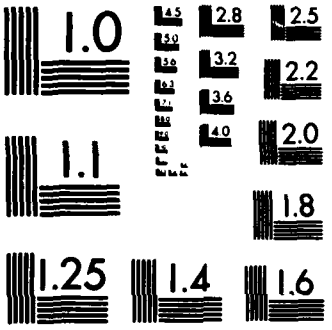

MICROCOPY RESOLUTION TEST CHART
NATIONAL BUREAU OF STANDARDS-1963-A

30. Srinivas, S. "A Refined Analysis of Composite Laminates," Journal of Sound and Vibrations, 30; pp. 495-507 (1973).

31. Epstein, M. and Glockner, P. G. "Nonlinear Analysis of Multilayered Shells," International Journal of Solids and Structures, 13; pp. 1081-1089 (1977).

32. Pagano, N. J. "Stress Fields in Composite Laminates," International Journal of Solids and Structures, 14; pp. 385-400 (1978).

33. Zienkiewicz, O. C. "The Finite Element Method, 3rd Edition. London: McGraw-Hill Book Company, LTD., 1977.

34. Tong, P. and Rosettos, J. N. Finite Element Method. Cambridge, Massachusetts: The MIT Press, LTD., 1979.

35. Hinton, E. and Owen, D. R. J. An Introduction to Finite Element Methods. Sweansea, United Kingdom: Pineridge Press, LTD., 1979.

36. Abel, J. F. and Popov, E. P. "Static and Dynamic Analysis of Sandwich Structures," Proceedings of the 2nd Conference on Matrix Methods in Structural Mechanics, AFFDL TR-68-150, Wright-Paterson AFB, Ohio; pp. 950-969 (1968).

37. Melosh, R. J. "Structural Analysis of Solids," Proceedings of ASCE, 89; pp. 205-223 (1963).

38. Clough, R. W. and Fellipa, C. A. "A Refined Quadrilateral Element for Analysis of Plate Bending," Proceedings of 2nd Conference on Matrix Methods in Structural Mechanics, AFFDL TR-68-150, Wright-Patterson AFB, Ohio, pp. 399-440 (1968).

39. Zienkiewicz, O. C. and Hinton, E. "Reduced Integration, Function Smoothing, and Nonconformity in Finite Element Analysis," Journal of the Franklin Institute, 302; pp. 443-459 (1976).

40. Pugh, E. D. L., Hinton, E. and Zienkiewicz, O. C. "A Study of Quadrilateral Plate Bending Elements with Reduced Integration," International Journal for Numerical Methods in Engineering, 12; pp. 1059-1079 (1978).

41. Reddy, J. N. "A Comparison of Closed-Form and Finite Element Solutions of Thick, Laminated, Anisotropic Rectangular Plates," Report OU-AMNE-79-19; University of Oklahoma, Norman, Oklahoma (1979).

42. Blockner, R. A. "A Penalty Function Approach for the Nonlinear Finite Element Analysis of Thin Shells," PhD Dissertation, University of Dayton, Dayton, Ohio (1979).

43. Hinton, E., Razzuque, A., and Zienkiewicz, O. C. "A Simple Finite Element Solution for Plates of Homogeneous, Sandwish, and Cellular Construction," Proceedings of the Institution of Civil Engineering, 59; pp. 43-65 (1978).

44. Bert, C. W. et.al. "Analysis of Thick Rectangular Plates Laminated of Bimodular Material," Report OU-AMNE-80-2, University of Oklahoma, Norman, Oklahoma (1980)

45. Pryor, C. W. and Barker, R. M. "A Finite Element Including Transverse Shear Effects for Application to Laminated Plates," AIAA Journal, 9; pp. 912-917 (1971).

46. Mau, S. T., Tong, P. and Pian, T. H. H. "Finite Element Solutions for Laminated Thick Plates," Journal of Composite Materials, 6; pp. 304-311 (1972).

47. Mathers, M. D. "Finite Element Analysis of Laminated Composite Plates and Shells," ScD Dissertation, George Washington University, Washington D.C. (1976).

48. Eldridge, C. "Nonlinear Analysis of Orthotropic, Laminated Shells of Revolution by the Finite Element Method," PhD Dissertation, Tennessee Technological University, Tennessee (1977).

49. Chang, P. N. "Finite Element Analysis of Laminated Plates and Shells," PhD Dissertation, University of Southern California, Los Anglees, CA. (1978).

50. Lo, K. H., Christensen, R. M. and Wu, E. M. "A Higher Order Theory of Plate Deformation," Journal of Applied Mechanics, 44; pp. 663-669 (1977).

51. Spilker, R. L., Chou, S. C. and Orringer, O. "Alternate Hybrid-Stress Elements for Analysis of Multilayer Composite Plates," Journal of Composite Materials, 11; pp. 51-70 (1970).

52. Deak, A. L. and Alturi, S. "Nonlinear Hybrid Stress Finite Element Analysis of Laminated Shells," Computational Methods in Nonlinear Mechanics, pp. 79-88 (1977).

53. Koiter, W. T. "Elastic Stability and Postbuckling Behavior," in Nonlinear Problems, ed. by R. E. Langer. Madison, Wisconsin; The University of Wisconsin Press; 1963.

54. Brebbia, C. A. and Connor, J. J. Fundamentals of Finite Element Techniques for Structural Engineers. New York: John Wiley and Sons, 1974.

55. Wood, R. D. and Zienziewicz, O. C. "Geometrically Nonlinear Finite Element Analysis of Beams, Frames, Arches and Axisymmetric Shells," Computers and Structures, 7; pp. 725-736 (1977).

56. Dodds, R. H.; Lopez, L. A. and Pecknold, D. A. Numerical and Software Requirements for General Nonlinear Finite Element Analysis, UILU-ENG-78-2020. Urbana, Illinois University of Illinois at Urbana-Champaign, September, 1978.

57. Green, A. E. and Zerna, W. Theoretical Elasticity. London: Oxford University Press, 1954.

58. Malvern, L. E. Introduction to the Mechanics of a Continuous Medium. Englewood Cliffs, New Jersey: Prentice-Hall, Inc., 1969.

59. Saada, A. S. Elasticity: Theory and Applications. New York: Pergamon Press, Inc., 1974.

60. Oliveira, U. R. E. "A Method of Fictitious Forces for the Geometrically Nonlinear Analysis of Structures," Computational Methods in Nonlinear Mechanics, pp. 383-392 (1974).

61. Kao, R. "A Comparison of Newton-Rhapson and Incremental Procedures for Geometrically Nonlinear Analysis," International Journal of Composites and Structures, 4; pp. 1091-1097 (1974).

62. Stricklin, J. A. and Haisler, W. E. "Formulation and Solution Procedures for Nonlinear Structural Analysis, 1"; pp. 125-136 (1977).

63. Bergan, P. G. et.al. "Solution Techniques for Nonlinear Finite Element Problems," International Journal for Numerical Methods in Engineering 12; pp. 1677-1696 (1978).

64. Noor, A. K. and Peters, J. M. "Reduced Basis Techniques for Nonlinear Analysis of Structures," AIAA Journal, 18; pp. 455-462 (1980).

65. Haisler, W. E. and Stricklin, J. A. "Displacement Incrementation in Nonlinear Structural Analysis by the Self-Correcting Method," International Journal for Numerical Methods in Engineering, 11; pp. 3-10 (1977).

66. Haisler, W. E. and Stricklin, J. A. "Computational Methods for Solving Nonlinear Structural Mechanics Problems," Computational Methods in Nonlinear Mechanics; pp. 393-404 (1974).

67. Oden, J. T. et. al., editors. Computational Methods in Nonlinear Mechanics. Austin, Texas. The Texas Institute for Computational Mechanics, 1974.

68. Langer, R. E., editor. Nonlinear Problems. Madison, Wisconsin: The University of Wisconsin Press, 1963

69. Brush, D. O. and Almroth, B. O. Buckling of Bars, Plates, and Shells. New York: McGraw-Hill Book Company, 1975.

70. Khot, N. S. On the Effects of Fiber Orientation and Nonhomogeneity or Buckling and Postbuckling Behavior of Fiber-reinforced Cylindrical Shells under Uniform Avial Compression, AFFDL-TR-68-19. Wright-Patterson AFB, Ohio: Air Force Flight Dynamics Laboratory, May 1968.

71. Khot, N. S. On the Influence of Initial Geometric Imperfections on the Buckling and Postbuckling Behavior of Fiber-reinforced Cylindrical Shells Under Uniform Axial Compression, AFFDL-TR-68-136. Wright-Patterson AFB, Ohio: Air Force Flight Dynamics Laboratory, October 1968.

72. Khot, N. S. and Venkayya, V. B. Effect on Fiber Orientation on Initial Postbuckling Behavior and Imperfection Sensitivity of Composite Cylindrical Shells, AFFDL-TR-70-125. Wright-Patterson AFB, Ohio: Air Force Flight Dynamics Laboratory, December 1970.

73. Tennyson, R. C. Muggeridge, D. B., Chain, K. H. and Khot, N. S. Buckling of Fiber-Reinforced Circular Cylinders Under Axial Compression, AFFDL-TR-72-102. Wright-Patterson AFB, Ohio: Air Force Flight Dynamics Laboratory, August 1972.

74. Bauld, N. R. and Satyamarthy, K. Collapse Load Analysis for Plates and Panels. Clemson University: Clemson, S. C., March 1978.

75. Booton, M. and Tennyson, R. C. "Buckling of Imperfect Anisotropic Circular Cylinders under Combined Loading," AIAA Journal, 17; pp. 278-287 (1980).

76. Chia, C. Y. "Large Deflections of Rectangular Orthotropic Plates," Journal of the Engineering Mechanics Division, AFCS, 98; pp. 1285-1299 (1972).

77. Noor, A. K. and Mathers, M. D. "Nonlinear Finite Element Analysis of Laminated Composite Shells," Computational Methods in Nonlinear Mechanics; pp. 999-1009 (1974).

78. Prabhakara, M. K. "Finite Deflections of Unsymmetric Angle Ply Anistropic Rectangular Plate Under Edge Moments," Journal of Applied Mechanics, 44; pp. 171-172 (1977).

79. Epstein, M. and Glockner, P. G. "Nonlinear Analysis of Multilayered Shells," International Journal of Solids and Structures, 13; pp. 1081-1089 (1977).

80. Reddy, J. N. and Chao, W. C. "Large Deflection and Large Amplitude Free Vibrations of Laminated Composite Material Plates," Report OU-AMNE-80-7, University of Oklahoma, Norman, Oklahoma (1980).

81. Ashwell, D. G. and Gallagher, R. H. Finite Element for Thin Shells and Curved Members. New York: John Wiley and Sons, 1976.

82. Bergan, P. G. and Clough, R. W. "Convergence Criteria for Interative Processes," AIAA Journal, 10; pp. 1107-1108 (1977).

83. Timoshenko, S. and Woinowsky-Kreiger, S. Theory of Plates and Shells. New York: McGraw-Hill Book Co., 1959.

84. Levy, S. "Square Plate with Clamped Edges Under Normal Pressure Producing Large Deflections," NACA CR 740, 1942.

APPENDIX I: Derivation of Strain-Displacement Relations

The objective of establishing these equations is to describe the relationship between the displacements of a point in a structure of arbitrary, curvature and thickness and the strain at the same point. To start, the location of the point must be established relative to a three-dimensional reference frame, Figure 3.1. The location is given by , where

$$\vec{R} = \vec{r}(\xi^\alpha) + \xi^3 \vec{d}(\xi^\alpha) \qquad \alpha = 1,2 \qquad \text{(I.1)}$$

In this relation, $\vec{d}$ is a director which is perpendicular to a reference surface and passes through the point located by $\vec{R}$, and $\vec{r}$ is the location of the intersection of the director with the reference surface. Both $\vec{r}$ and $\vec{d}$ are functions of only the two surface coordinates. The metric of the deformed surface, g_{ij} is then given by

$$g_{ij} = \vec{R}_{,i} \cdot \vec{R}_{,j} \qquad i = 1,2,3 \qquad \text{(I.2)}$$

where the comma indicates covariant differentiation.

If the point now undergoes a displacement $\vec{u}$, its new location is described by $\vec{R}^*$, where

$$\vec{R}^* = \vec{R} + \vec{u} \qquad \text{(I.3)}$$

The metric in the deformed configuration g^*_{ij} is

$$g^*_{ij} = \vec{R}^*_{,i} \cdot \vec{R}^*_{,j} \qquad \text{(I.4)}$$

Substituting I.3 into I.4 and differentiating,

$$g^*_{ij} = \vec{R}_{,i} \cdot \vec{R}_{,j} + \vec{R}_{,i} \cdot \vec{u}_{,j} + \vec{R}_{,j} \cdot \vec{u}_{,i} + \vec{u}_{,i} \cdot \vec{u}_{,j} \qquad \text{(I.5)}$$

The Lagrangian strain γ_{ij} is then defined using the metrics by

$$\gamma_{ij} = \tfrac{1}{2}(g^*_{ij} - g_{ij}) \qquad \text{(I.6)}$$

Using equations I.2 and I.5, equation I.6 becomes

$$\gamma_{ij} = \frac{1}{2}(\vec{R}_{,i}\cdot\vec{R}_{,j} + \vec{R}_{,i}\cdot\vec{u}_{,j} + \vec{R}_{,j}\cdot\vec{u}_{,i} + \vec{u}_{,i}\cdot\vec{u}_{,j} - \vec{R}_{,i}\cdot\vec{R}_{,j}) \tag{I.7}$$

Simplifying

$$\gamma_{ij} = \frac{1}{2}(\vec{R}_{,i}\cdot\vec{u}_{,j} + \vec{R}_{,j}\cdot\vec{R}_{,i} + \vec{u}_{,i}\cdot\vec{u}_{,j}) \tag{I.8}$$

Now let the displacement $\vec{u}$ be divided into two parts, Figure 3.1. One part, $\bar{\vec{u}}$, which is a function of only the surface coordinates ξ^1 and ξ^2 and is associated with the deformation of the reference surface. The other part, $\hat{\vec{u}}$, which is a function of all three coordinates and is associated with the deformation of the director. $\vec{u}$ is then given by

$$\vec{u} = \bar{\vec{u}}(\xi^\alpha) + \hat{\vec{u}}(\xi^\alpha, \xi^3) \qquad \alpha = 1,2 \tag{I.9}$$

The derivative of $\vec{u}$ can then be represented by,

$$\vec{u}_{,\alpha} = \bar{\vec{u}}_{,\alpha} + \hat{\vec{u}}_{,\alpha} \tag{I.10}$$

$$\vec{u}_{,3} = \hat{\vec{u}}_{,3} \tag{I.11}$$

The derivatives of $\vec{R}$ can then be obtained from equation I.1

$$\vec{R}_{,\alpha} = \vec{r}_{,\alpha} + \xi^3\vec{d}_{,\alpha} \tag{I.12}$$

$$\vec{R}_{,3} = \vec{d} \tag{I.13}$$

Now letting $\vec{r}_{,\alpha} = \vec{a}_\alpha$ where $|\vec{a}_\alpha| = a_\alpha$ are

the Lame' constants of the reference surface, the strain equations I.8 are:

$$\gamma_{\alpha\beta} = \tfrac{1}{2}\left[(\vec{a}_\alpha + \xi^3\vec{d}_{,\alpha})\cdot(\vec{\tilde{u}}_{,\beta} + \vec{\hat{u}}_{,\beta}) + (\vec{a}_\beta + \xi^3\vec{d}_{,\beta})\cdot(\vec{\tilde{u}}_{,\alpha} + \vec{\hat{u}}_{,\alpha}) + (\vec{\tilde{u}}_{,\alpha} + \vec{\hat{u}}_{,\alpha})\cdot(\vec{\tilde{u}}_{,\beta} + \vec{\hat{u}}_{,\beta})\right] \tag{I.14}$$

$$\gamma_{\alpha 3} = \tfrac{1}{2}\left[(\vec{a}_\alpha + \xi^3\vec{d}_{,\alpha})\cdot\vec{\hat{u}}_{,3} + \vec{d}\cdot(\vec{\tilde{u}}_{,\alpha} + \vec{\hat{u}}_{,\alpha}) + (\vec{\tilde{u}}_{,\alpha} + \vec{\hat{u}}_{,\alpha})\cdot\vec{\hat{u}}_{,3}\right] \tag{I.15}$$

$$\gamma_{33} = \vec{d}\cdot\vec{\hat{u}}_{,3} + \tfrac{1}{2}\vec{\hat{u}}_{,3}\cdot\vec{\hat{u}}_{,3} \tag{I.16}$$

Now let $\vec{e}_\alpha$ be unit vectors in the surface such that

$$\vec{e}_\alpha = \frac{\vec{a}_\alpha}{|\vec{a}_\alpha|} \quad \text{or} \quad \vec{a}_\alpha = a_\alpha\vec{e}_\alpha \tag{I.17}$$

Using I.17 in equations I.14, I.15, and I.16, the strains become

$$\gamma_{\alpha\beta} = \tfrac{1}{2}\left[(a_\alpha\vec{e}_\alpha + \xi^3\vec{d}_{,\alpha})\cdot(\vec{\tilde{u}}_{,\beta} + \vec{\hat{u}}_{,\beta}) + (a_\beta\vec{e}_\beta + \xi^3\vec{d}_{,\beta})\cdot(\vec{\tilde{u}}_{,\alpha} + \vec{\hat{u}}_{,\alpha}) + (\vec{\tilde{u}}_{,\alpha} + \vec{\hat{u}}_{,\alpha})\cdot(\vec{\tilde{u}}_{,\beta} + \vec{\hat{u}}_{,\beta})\right] \tag{I.18}$$

$$\gamma_{\alpha 3} = \tfrac{1}{2}\left[(a_\alpha\vec{e}_\alpha + \xi^3\vec{d}_{,\alpha})\cdot\vec{\hat{u}}_{,3} + \vec{d}\cdot(\vec{\tilde{u}}_{,\alpha} + \vec{\hat{u}}_{,\alpha}) + (\vec{\tilde{u}}_{,\alpha} + \vec{\hat{u}}_{,\alpha})\cdot\vec{\hat{u}}_{,3}\right] \tag{I.19}$$

$$\gamma_{33} = \vec{d}\cdot\vec{\hat{u}}_{,3} + \tfrac{1}{2}\vec{\hat{u}}_{,3}\cdot\vec{\hat{u}}_{,3} \tag{I.20}$$

Now it is assumed that the reference surface coordinates are measured in the principal directions. This assumption leads to two identities

$$\vec{e}_\alpha\cdot\vec{e}_\beta = 0 \tag{I.21}$$

$$\vec{e}_\alpha \cdot \vec{d} = 0 \tag{I.22}$$

Further, the assumption is also made that the director only deforms and does not change length. Using this assumption, it is possible to represent the displacements as follow:

$$\tilde{\vec{u}} = \tilde{u}\vec{e}_1 + \tilde{v}\vec{e}_2 + w\vec{d} \tag{I.23}$$

$$\hat{\vec{u}} = \hat{u}\vec{e}_1 + \hat{v}\vec{e}_2 \tag{I.24}$$

Then the derivatives of these displacements seen in equation I.10 can be written

$$\tilde{\vec{u}}_{,\alpha} = \tilde{u}_{,\alpha}\vec{e}_1 + \tilde{u}\vec{e}_{1,\alpha} + \tilde{v}_{,\alpha}\vec{e}_2 + \tilde{v}\vec{e}_{2,\alpha} + w_{,\alpha}\vec{d} + w\vec{d}_{,\alpha} \tag{I.25}$$

$$\hat{\vec{u}}_{,\alpha} = \hat{u}_{,\alpha}\vec{e}_1 + \hat{u}\vec{e}_{1,\alpha} + \hat{v}_{,\alpha}\vec{e}_2 + \hat{v}\vec{e}_{2,\alpha} \tag{I.26}$$

$$\hat{\vec{u}}_{,3} = \hat{u}_{,3}\vec{e}_1 + \hat{v}_{,3}\vec{e}_2 \tag{I.27}$$

Since the basic vector and the reference surface displacements depend only on the surface coordinate

$$\tilde{u}_{,3} = \tilde{v}_{,3} = w_{,3} = \vec{e}_{1,3} = \vec{e}_{\alpha,3} = \vec{d}_{,3} = 0 \tag{I.28}$$

and

$\vec{d}$ is a unit vector which only depends on surface coordinates,

$$\vec{d} \cdot \vec{d}_{,\alpha} = 0 \tag{I.29}$$

Now the Lagrangian strains are expressed as:

$$\gamma_{11} = \xi a_1(\tilde{u}_{,1} + \hat{u}_{,1}) + \tfrac{1}{2}\left[(\tilde{u}_{,1} + \hat{u}_{,1})^2 + (\tilde{v}_{,1} + \hat{v}_{,1})^2 + w_{,1}^2\right]$$
$$+ \vec{e}_1 \cdot \vec{e}_{2,1}(a_1 + \tilde{u}_{,1} + \hat{u}_{,1})(\tilde{v} + \hat{v}) + \vec{e}_1 \cdot \vec{d}_{,1}\left[a_1 w + (\tilde{u}_{,1} + \hat{u})(\xi^3 + w)\right]$$

$$+\vec{e}_{1,1}\cdot\vec{e}_{1,1}\left[\tfrac{1}{2}(\tilde{u}+\hat{u})^2\right]+\vec{e}_{1,1}\cdot\vec{e}_2(\tilde{u}+\hat{u})(\tilde{v}_{,1}+\hat{v}_{,1})+\vec{e}_{1,1}\cdot\vec{e}_{2,1}(\tilde{u}+\hat{u})(\tilde{v}+\hat{v})$$
$$+\vec{e}_{1,1}\cdot\vec{d}\,(\tilde{u}+\hat{u})w_{,1}+\vec{e}_{1,1}\cdot\vec{d}_{,1}(\tilde{u}+\hat{u})(\xi^3+w)+\vec{e}_2\cdot\vec{e}_{2,1}(\tilde{v}+\hat{v})(\tilde{v}_{,1}+\hat{v}_{,1})$$
$$+\vec{e}_2\cdot\vec{d}_{,1}(\tilde{v}_{,1}+\hat{v}_{,1})(\xi^3+w)+\vec{e}_{2,1}\cdot\vec{e}_{2,1}\left[\tfrac{1}{2}(\tilde{v}+\hat{v})^2\right]+\vec{e}_{2,1}\cdot\vec{d}\,(\tilde{v}+\hat{v})w_{,1}$$
$$+\vec{e}_{2,1}\cdot\vec{d}_{,1}(\tilde{v}+\hat{v})(\xi^3+w)+\vec{d}_{,1}-\vec{d}_{,1}\left[\tfrac{1}{2}w(2\xi^3+w)\right]\Big\} \qquad (I.30)$$

$$\gamma_{22}=\Big\{a_2(\tilde{v}_{,2}+\hat{v}_{,2})+\tfrac{1}{2}\left[(\tilde{u}_{,2}+\hat{u}_{,2})^2+(\tilde{v}_{,2}+\hat{v}_{,2})^2+w_{,2}^2\right]+\vec{e}_1\cdot\vec{e}_{1,2}(\tilde{u}+\hat{u})(\tilde{u}_{,2}+\hat{u}_{,2})$$
$$+\vec{e}_1\cdot\vec{e}_{2,2}(\tilde{u}_{,2}+\hat{u}_{,2})(\tilde{v}+\hat{v})+\vec{e}_1\cdot\vec{d}_{,2}(\tilde{u}_{,2}+\hat{u}_{,2})(\xi^3+w)$$
$$+\vec{e}_{1,2}\cdot\vec{e}_{1,2}\left[\tfrac{1}{2}(\tilde{u}+\hat{u})^2\right]+\vec{e}_{1,2}\cdot\vec{e}_2(\tilde{u}+\hat{u})(a_2+\tilde{v}_{,2}+\hat{v}_{,2})$$

$$+\vec{e}_{1,2}\cdot\vec{e}_{2,2}(\tilde{u}+\hat{u})(\tilde{v}+\hat{v})+\vec{e}_{1,2}\cdot\vec{d}\,(\tilde{u}+\hat{u})w_{,2}+\vec{e}_{1,2}\cdot\vec{d}_{,2}$$
$$(\tilde{u}+\hat{u})(\xi^3+w)$$
$$+\vec{e}_2\cdot\vec{d}_{,2}\left[(\tilde{v}_{,2}+\hat{v}_{,2})(\xi^3+w)+a_2w\right]+\vec{e}_{2,2}\cdot\vec{e}_{2,2}\left[\tfrac{1}{2}(\tilde{v}+\hat{v})^2\right]$$
$$+\vec{e}_{2,2}\cdot\vec{d}\,(\tilde{v}+\hat{v})w_{,2}+\vec{e}_{2,2}\cdot\vec{d}_{,2}(\tilde{v}+\hat{v})(\xi^3+w)$$
$$+\vec{d}_{,2}\cdot\vec{d}_{,2}\left[\tfrac{1}{2}(2\xi^3+w)w\right]\Big\} \qquad (I.31)$$

$$\gamma_{12}=\tfrac{1}{2}\Big\{a_1(\tilde{u}_{,2}+\hat{u}_{,2})+a_2(\tilde{v}_{,1}+\hat{v}_{,1})+(\tilde{u}_{,1}+\hat{u}_{,1})(\tilde{u}_{,2}+\hat{u}_{,2})$$
$$+(\tilde{v}_{,1}+\hat{v}_{,1})(\tilde{v}_{,2}+\hat{v}_{,2})+w_{,1}w_{,2}+\vec{e}_1\cdot\vec{e}_{2,1}(\tilde{u}_{,1}+\hat{u}_{,1})(\tilde{v}+\hat{v})$$
$$+\vec{e}_1\cdot\vec{e}_{2,2}(a_1+\tilde{u}_{,1}+\hat{u}_{,1})(\tilde{v}+\hat{v})+\vec{e}_1\cdot\vec{d}_{,1}(\tilde{u}_{,2}+\hat{u}_{,2})(\xi^3+w)$$
$$+\vec{e}_{1,1}\cdot\vec{d}\,(\tilde{u}+\hat{u})w_{,2}+\vec{e}_{1,1}\cdot\vec{e}_{1,2}(\tilde{u}+\hat{u})^2+\vec{e}_{1,1}\cdot\vec{e}_{2,2}(\tilde{u}+\hat{u})(\tilde{v}+\hat{v})$$
$$+\vec{e}_{1,1}\cdot\vec{d}_{,2}(\tilde{u}+\hat{u})(\xi^3+w)+\vec{e}_{1,2}\cdot\vec{e}_2(\tilde{u}+\hat{u})(\tilde{v}_{,1}+\hat{v}_{,1})+\vec{e}_{1,2}\cdot\vec{d}\,(\tilde{u}+\hat{u})w_{,1}$$
$$+\vec{e}_{1,2}\cdot\vec{e}_{2,1}(\tilde{u}+\hat{u})(\tilde{v}+\hat{v})+\vec{e}_{1,2}\cdot\vec{d}_{,1}(\tilde{u}+\hat{u})(\xi^3+w)$$
$$+\vec{e}_2\cdot\vec{d}_{,1}\left[a_2w+(\tilde{v}_{,2}+\hat{v}_{,2})(\xi^3+w)\right]+\vec{e}_2\cdot\vec{d}_{,2}(\tilde{v}_{,1}+\hat{v}_{,1})(\xi^3+w)$$
$$+\vec{e}_{2,1}\cdot\vec{d}\,(\tilde{v}+\hat{v})w_{,2}+\vec{e}_{2,1}\cdot\vec{e}_{2,2}(\tilde{v}+\hat{v})^2+\vec{e}_{2,2}\cdot\vec{d}\,(\tilde{v}+\hat{v})w_{,1}$$
$$+\vec{e}_{2,2}\cdot\vec{d}_{,1}(\tilde{v}+\hat{v})(\xi^3+w)+\vec{d}_{,1}\cdot\vec{d}_{,2}w(2\xi^3+w)\Big\} \qquad (I.32)$$
$$+\vec{e}_1\cdot\vec{d}_{,2}\left[a_1w+(\tilde{u}_{,1}+\hat{u}_{,1})(\xi^3+w)\right]+\vec{e}_{1,1}\cdot\vec{e}_2(\tilde{u}+\hat{u})(a_2+\tilde{v}_{,2}+\hat{v}_{,2})$$

From Equation (I.16)

$$\gamma_{33} = \vec{d} \cdot \vec{\hat{u}}_{,3} + \frac{1}{2} \vec{\hat{u}}_{,3} \cdot \vec{\hat{u}}_{,3} \tag{I.16}$$

Expanding this and using equation (I.28)

$$\gamma_{33} = w_{,3} + \frac{1}{2} \left(\hat{u}_{,3}^2 + \hat{V}_{,3}^2 + w_{,3}^2 \right) \tag{I.33}$$

From equation (I.19)

$$\gamma_3 = \frac{1}{2} \left[a_1 \hat{u}_{,3} + w_{,1} + \left(\tilde{u}_{,1} + \hat{u}_{,1} \right) \hat{u}_{,3} + \left(\tilde{V}_{,1} + \hat{V}_{,1} \right) \hat{V}_{,3} + w_{,1} \right.$$
$$+ \vec{e}_1 \cdot \vec{a}_{,1} \hat{u}_{,3} \left(\xi_3^3 + w \right) + \vec{e}_1 \cdot \vec{e}_{2,1} \hat{u}_{,3} \left(\tilde{V} + \hat{V} \right) + \vec{e}_{1,1} \cdot \vec{e}_2 \left(\tilde{u} + \hat{u} \right) \hat{V}_{,3}$$
$$+ \vec{e}_{1,1} \cdot \vec{d} \left(\tilde{u} + \hat{u} \right) \left(1 + w_{,3} \right) + \vec{e}_2 \cdot \vec{a}_{,1} \hat{V}_{,3} \left(\xi_3^3 + w \right) + \vec{e}_{2,1} \cdot \vec{d} \cdot$$
$$\left. \left(\tilde{V} + \hat{V} \right) w_{,3} \right] \tag{I.34}$$

$$\gamma_{2,3} = \frac{1}{2} \left[a_2 \hat{V}_{,2} + w_{,2} + \left(\tilde{u}_{,2} + \hat{u}_{,2} \right) \hat{u}_{,3} + \left(\tilde{V}_{,1} + \hat{V}_{,1} \right) \hat{V}_{,3} + w_{,2} w_{,3} \right.$$
$$+ \vec{e}_1 \cdot \vec{e}_{2,2} \left(\tilde{V} + \hat{V} \right) \hat{u}_{,3} + \vec{e}_1 \cdot \vec{a}_{,2} \hat{V}_{,3} \left(\xi_3^3 + w \right) + \vec{e}_{1,2} \cdot \vec{e}_2 \left(\tilde{u} + \hat{u} \right) \hat{V}_{,3}$$
$$+ \vec{e}_{1,2} \cdot \vec{d} \left(\tilde{u} + \hat{u} \right) \left(1 + w_{,3} \right) + \vec{e}_2 \cdot \vec{a}_{,2} \hat{V}_{,3} \left(\xi_3^3 + w \right) + \vec{e}_{2,2} \cdot \vec{a}$$
$$\left. \left(\tilde{V} + \hat{V} \right) \left(1 + w_{,3} \right) \right] \tag{I.35}$$

From Gould (4) and Calcote (8) the derivatives of the basic vectors can be represented by

$$\vec{e}_{1,1} = \frac{a_{1,2}}{a_2}\vec{e}_2 - \frac{a_1}{R_1}\vec{d} \tag{I.36}$$

$$\vec{e}_{1,2} = \frac{a_{2,1}}{a_1}\vec{e}_2 \tag{I.37}$$

$$\vec{e}_{2,1} = \frac{a_{1,2}}{a_2}\vec{e}_1 \tag{I.38}$$

$$\vec{e}_{2,2} = -\frac{a_{2,1}}{a_1}\vec{e}_1 - \frac{a_2}{R_2}\vec{d} \tag{I.39}$$

$$\vec{d}_{,1} = \frac{a_1}{R_1}\vec{e}_1 \tag{I.40}$$

$$\vec{d}_{,2} = \frac{a_2}{R_2}\vec{e}_2 \tag{I.41}$$

where R_1 and R_2 are the principal radii of curvature for the reference surface. Substituting equations (I.36) through (I.41) into equations (I.30) through (I.35) a further expansion of the Lagrangian strain is obtained, where now $a_1 = A \quad a_2 = B \quad \xi^3 = z$

$$\begin{aligned}\gamma_{11} = {} & A\left(1+\frac{z}{R_1}\right)\left[\left(\tilde{u}_{,1}+\hat{u}_{,1}\right)+\frac{A_{,2}}{B}\left(\tilde{v}+\hat{v}\right)+\frac{A}{R_1}w\right] + \\ & \frac{1}{2}\left\{\left[\left(\tilde{u}_{,1}+\hat{u}_{,1}\right)+\frac{A_{,2}}{B}\left(\tilde{v}+\hat{v}\right)+\frac{A}{R}w\right]^2 + \right. \\ & \left[\left(\tilde{v}_{,1}+\hat{v}_{,1}\right)-\frac{A_{,2}}{B}\left(\tilde{u}+\hat{u}\right)\right]^2 \\ & \left. + \left[w_{,1}-\frac{A_1}{R_1}\left(\tilde{u}+\hat{u}\right)\right]^2\right\}\end{aligned} \tag{I.42}$$

$$\begin{aligned}\gamma_{22} = {} & B\left(1+\frac{z}{R_2}\right)\left[\frac{B_{,1}}{A}\left(\tilde{u}+\hat{u}\right)+\left(\tilde{v}_{,2}+\hat{v}_{,2}\right)+\frac{B}{R_2}w\right] + \\ & \frac{1}{2}\left\{\left[\frac{B_{,1}}{A}\left(\tilde{u}+\hat{u}\right)+\left(\tilde{v}_{,2}+\hat{v}_{,2}\right)+\frac{B}{R_2}w\right]^2+\left[\left(\hat{u}_{,2}+\hat{u}_{,2}\right)-\frac{B_{,1}}{A}\left(\tilde{v}+\hat{v}\right)\right]^2\right. \\ & \left. + \left[w_{,2}-\frac{B}{R_2}\left(\tilde{v}+\hat{v}\right)\right]^2\right\}\end{aligned} \tag{I.43}$$

$$\gamma_{12} = \frac{1}{2}\left\{\left(1+\frac{z}{R_1}\right)\left[A\left(\tilde{u}_{,2}+\hat{u}_{,2}\right) - B_{,1}\left(\tilde{v}+\hat{v}\right)\right] + \left(1+\frac{z}{R_2}\right)\left[B\left(\tilde{v}_{,1}+\hat{v}_{,1}\right)\right.\right.$$
$$\left. - A_{,2}\left(\tilde{u}+\hat{u}\right)\right] + \left[\left(\tilde{u}_{,2}+\hat{u}_{,2}\right) + \frac{A_{,2}}{B}\left(\tilde{v}+\hat{v}\right) + \frac{A}{R_1}W\right]\left[\left(\tilde{u}_{,2}+\hat{u}_{,2}\right) - \frac{B_{,1}}{A}\left(\tilde{v}+\hat{v}\right)\right]$$
$$+ \left[\left(\tilde{v}_{,1}+\hat{v}_{,1}\right) - \frac{A_{,2}}{B}\left(\tilde{u}+\hat{u}\right)\right]\left[\left(\tilde{v}_{,2}+\hat{v}_{,2}\right) + \frac{B_{,1}}{A}\left(\tilde{u}+\hat{u}\right) + \frac{B}{R_2}W\right]$$
$$\left. + \left[W_{,1} - \frac{A}{R_1}\left(\tilde{u}+\hat{u}\right)\right]\left[W_{,2} - \frac{B}{R_2}\left(\tilde{v}+\hat{v}\right)\right]\right\} \qquad \text{(I.44)}$$

$$\gamma_{33} = W_{,3} + \frac{1}{2}\left[\left(\tilde{u}_{,3}+\hat{u}_{,3}\right)^2 + \left(\tilde{v}_{,3}+\hat{v}_{,3}\right)^2 + W_{,3}^2\right] \qquad \text{(I.45)}$$

$$\gamma_{13} = \frac{1}{2}\left\{A\left(1+\frac{z}{R_1}\right)\hat{u}_{,3} + \left[W_{,1} - \frac{A}{R_1}\left(\tilde{u}+\hat{u}\right)\right] + \hat{u}_{,3}\left[\left(\tilde{u}_{,1}+\hat{u}_{,1}\right) + \frac{A_{,2}}{B}\left(\tilde{v}+\hat{v}\right)\right.\right.$$
$$\left. + \frac{A}{R}W\right] + W_{,3}\left[W_{,1} - \frac{A}{R_1}\left(\tilde{u}+\hat{u}\right)\right] + \hat{v}_{,3}\left[\left(\tilde{v}_{,1}+\hat{v}_{,1}\right) - \frac{A_{,2}}{B}\left(\tilde{u}+\hat{u}\right)\right]\right\} \qquad \text{(I.46)}$$

$$\gamma_{23} = \frac{1}{2}\left\{B\left(1+\frac{z}{R_2}\right)\hat{v}_{,3} + \left[W_{,2} - \frac{B}{R_2}\left(\tilde{v}+\hat{v}\right)\right] + \hat{u}_{,3}\left[\left(\tilde{u}_{,2}+\hat{u}_{,2}\right)\right.\right.$$
$$\left. - \frac{B_{,1}}{A}\left(\tilde{v}+\hat{v}\right)\right] + \hat{v}_{,3}\left[\left(\tilde{v}_{,2}+\hat{v}_{,2}\right) + \frac{B_{,1}}{A}\left(\tilde{u}+\hat{u}\right) + \frac{B}{R_2}W\right] + W_{,3}$$
$$\left.\left[W_{,2} - \frac{B}{R_2}\left(\tilde{v}+\hat{v}\right)\right]\right\} \qquad \text{(I.47)}$$

Equations (I.42) through (I.47) are the tensorial components of strain. To adjust them to the physical components of strain, so that the applicable physical constituitive equations can be used, they must be divided by the Lam'e constants. In anticipation of using these strains in matrix equations, I will also rename and reorder the strains such that

$$e_1 = \frac{\gamma_{11}}{A^2\left(1+z/R_1\right)^2} \qquad \text{(I.48)}$$

$$e_2 = \frac{\gamma_{22}}{B^2\left(1+z/R_2\right)^2} \qquad \text{(I.49)}$$

$$e_3 = \gamma_{33} \qquad \text{(I.50)}$$

$$e_4 = 2\,\frac{\gamma_{23}}{B(1+z/R_2)} \tag{I.51}$$

$$e_5 = 2\,\frac{\gamma_{13}}{A(1+z/R_1)} \tag{I.52}$$

$$e_6 = 2\,\frac{\gamma_{12}}{AB(1+z/R_1)(1+z/R_2)} \tag{I.53}$$

The physical strains are then given by

$$e_1 = \frac{1}{A(1+z/R_1)}\left[(\tilde{u}_{,1}+\hat{u}_{,1}) + \frac{A_{,2}}{B}(\tilde{v}+\hat{v}) + \frac{A}{R_1}w\right] + \frac{1}{2A^2(1+z/R_1)^2}\left\{\left[(\tilde{u}_{,1}+\hat{u}_{,1}) + \frac{A_{,2}}{B}(\tilde{v}+\hat{v}) + \frac{A}{R_1}w\right]^2 + \left[(\tilde{v}_{,1}+\hat{v}_{,1}) - \frac{A_{,2}}{B}(\tilde{u}+\hat{u})\right]^2 + \left[w_{,1} - \frac{A}{R_1}(\tilde{u}+\hat{u})\right]^2\right\} \tag{I.54}$$

$$e_2 = \frac{1}{B(1+z/R_2)}\left[(\tilde{v}_{,2}+\hat{v}_{,2}) + \frac{B_{,1}}{A}(\tilde{u}+\hat{u}) + \frac{B}{R_2}w\right] + \frac{1}{2B^2(1+z/R_2)^2}\left\{\left[(\tilde{v}_{,2}+\hat{v}_{,2}) + \frac{B_{,1}}{A}(\tilde{u}+\hat{u}) + \frac{B}{R_2}w\right]^2 + \left[(\tilde{u}_{,2}+\hat{u}_{,2}) + \frac{B_{,1}}{A}(\tilde{v}+\hat{v})\right]^2 + \left[w_{,2} - \frac{B}{R_2}(\tilde{v}+\hat{v})\right]^2\right\} \tag{I.55}$$

$$e_3 = w_{,3} + \frac{1}{2}\left[(\tilde{u}_{,3}+\hat{u}_{,3})^2 + (\tilde{v}_{,3}+\hat{v}_{,3})^2 + w_{,3}^2\right] \tag{I.56}$$

$$e_4 = \hat{v}_{,3} + \frac{1}{B(1+z/R_2)}\left[w_{,2} - \frac{B}{R_2}(\tilde{v}+\hat{v})\right] + \frac{1}{B(1+z/R_2)}\left\{\hat{u}_{,3}\left[(\tilde{u}_{,2}+\hat{u}_{,2}) - \frac{B_{,1}}{A}(\tilde{v}+\hat{v})\right] + \hat{v}_{,3}\left[(\tilde{v}_{,2}+\hat{v}_{,2}) + \frac{B_{,1}}{A}(\tilde{u}+\hat{u}) + \frac{B}{R_2}w\right] + w_{,3}\left[w_{,2} - \frac{B}{R_2}(\tilde{v}+\hat{v})\right]\right\} \tag{I.57}$$

$$e_5 = \hat{u}_{,3} + \frac{1}{A(1+z/R_1)}\left[w_{,1} - \frac{A}{R_1}(\tilde{u}+\hat{u})\right] + \frac{1}{A(1+z/R_1)}\left\{\hat{u}_{,3}\left[(\tilde{u}_{,1}+\hat{u}_{,1}) + \frac{A_{,2}}{B}(\tilde{v}+\hat{v}) + \frac{A}{R_1}w\right] + \hat{v}_{,3}\left[(\tilde{v}_{,1}+\hat{v}_{,1}) - \frac{A_{,2}}{B}(\tilde{u}+\hat{u})\right] + w_{,3}\left[w_{,1} - \frac{A}{R_1}(\tilde{u}+\hat{u})\right]\right\} \tag{I.58}$$

$$e_6 = \frac{1}{B(1+z/R_2)}\left[(\tilde{u}_{,2}+\hat{u}_{,2}) - \frac{B_{,1}}{A}(\tilde{v}+\hat{v})\right] + \frac{1}{A(1+z/R_1)}\left[(\tilde{v}_{,1}+\hat{v}_{,1}) - \frac{A_{,2}}{B}(\tilde{u}+\hat{u})\right] + \frac{1}{AB(1+z/R_1)(1+z/R_2)}\left\{\left[(\tilde{u}_{,1}+\hat{u}_{,1}) + \frac{A_{,2}}{B}(\tilde{v}+\hat{v}) + \frac{A}{R_1}w\right]\left[(\tilde{u}_{,1}+\hat{u}_{,1}) - \frac{B_{,1}}{A}(\tilde{v}+\hat{v})\right] + \left[(\tilde{v}_{,1}+\hat{v}_{,1}) - \frac{A_{,2}}{B}(\tilde{u}+\hat{u})\right]\left[(\tilde{v}_{,2}+\hat{v}_{,2}) + \frac{B_{,1}}{A}(\tilde{u}+\hat{u}) + \frac{B}{R_2}w\right] + \left[w_{,1} - \frac{A}{R_1}(\tilde{u}+\hat{u})\right]\left[w_{,2} - \frac{B}{R_2}(\tilde{v}+\hat{v})\right]\right\} \tag{I.59}$$

APPENDIX II - Derivation of Plate Finite Element

From equation 3.68, the linear part of the element stiffness matrix is

$$[K_L^E] = \int_V [\tilde{N} + \hat{N}]^T [L_o]^T [D] [L_o] [\tilde{N} + \hat{N}] \, dV \qquad \text{(II.1)}$$

Expanding this

$$\begin{aligned}[K_L^E] = & \int_V [\hat{N}]^T [L_o]^T [D] [L_o] [\tilde{N}] dV + \\ & \int_V [\tilde{N}]^T [L_o]^T [D] [L_o] [\hat{N}] dV + \\ & \int_V [\hat{N}]^T [L_o]^T [D] [L_o] [\tilde{N}] \, dV + \\ & \int_V [\hat{N}]^T [L_o]^T [D] [L_o] [\hat{N}] \, dV \end{aligned} \qquad \text{(II.2)}$$

Using linear algebra

$$[\hat{N}]^T [L_o]^T [D] [L_o] [\hat{N}] = \left([\hat{N}]^T [L_o]^T [D] [L_o] [\tilde{N}] \right)^T \qquad \text{(II.3)}$$

Then equation (II.2) becomes

$$\begin{aligned}[K_L^E] = & \int_V [\hat{N}]^T [L_o]^T [D] [L_o] [\tilde{N}] dV + \\ & \int_V [\tilde{N}]^T [L_o]^T [D] [L_o] [\hat{N}] dV + \\ & \left(\int_V [\tilde{N}]^T [L_o]^T [D] [L_o] [\hat{N}] dV \right)^T + \\ & \int_V [\hat{N}]^T [L_o]^T [D] [L_o] [\hat{N}] \, dV \end{aligned} \qquad \text{(II.4)}$$

The matrices, $[\tilde{N}]$ and $[\hat{N}]$, are given in equation (3.52) and (3.53). For a plate,

$$A = 1$$

$$B = 1 \qquad \text{(II.5)}$$

$$R_1 \to \infty$$

$$R_2 \to \infty$$

$$\xi_1 = X$$

$$\xi_2 = Y$$

Then

$$[L_o] = \begin{bmatrix} \frac{\partial}{\partial x} & 0 & 0 \\ 0 & \frac{\partial}{\partial y} & 0 \\ 0 & 0 & 0 \\ 0 & \frac{\partial}{\partial z} & \frac{\partial}{\partial y} \\ \frac{\partial}{\partial z} & 0 & \frac{\partial}{\partial x} \\ \frac{\partial}{\partial y} & \frac{\partial}{\partial x} & 0 \end{bmatrix} \qquad \text{(II.6)}$$

Looking first at the integral

$$\int_v \tilde{N}^T L_o^T D L_o \tilde{N} \, dV \qquad \text{(II.7)}$$

By examination $\tilde{N}^T L_o^T$ will have no dependence on X, Y, or Z with the given shape functions. The matrix, D, has no specific dependence on Z, but its values can change from layer to layer. Using these relations

$$\int_v \tilde{N}^T L_o^T D L_o \tilde{N} \, dV = \tilde{N}^T L_o \left(\int_z D \, dz \right) L_o \tilde{N} \int_x \int_y dy dx \qquad \text{(II.8)}$$

The integral $\int_x \int_y dy dx$ is the area of the element triangle at the reference surface which will be designated as Δ. The elements of the constituitive matrix in a layer k are D_{ij}^k.

The integration over z can be accounted for by defining

$$\mathcal{D}_{ij} = \sum_{k=1}^{n} D_{ij}^k t_k \qquad i,j = 1,2 \qquad \text{(II.9)}$$

n = number of layers

The integral then becomes

$$\int_V \tilde{N}^T L_o^T D L_o \tilde{N} dV = (\tilde{N}^T L_o^T \mathcal{D} L_o \tilde{N}) \frac{L}{2\Delta} = \frac{L}{2\Delta} {}'M \qquad \text{(II.10)}$$

The elements of ${}'M$ with dimensions $[9+2(n+1), 9+2(n+1)]$ are then

$${}'M_{i,j} = \frac{\partial L_i}{\partial x}\left(\mathcal{D}_{11}\frac{\partial L_j}{\partial x} + \mathcal{D}_{16}\frac{\partial L_j}{\partial y}\right) + \frac{\partial L_i}{\partial y}\left(\mathcal{D}_{16}\frac{\partial L_j}{\partial x} + \mathcal{D}_{66}\frac{\partial L_j}{\partial y}\right)$$

$${}'M_{i,j+3} = \frac{\partial L_i}{\partial x}\left(\mathcal{D}_{12}\frac{\partial L_k}{\partial y} + \mathcal{D}_{16}\frac{\partial L_j}{\partial x}\right) + \frac{\partial L_i}{\partial y}\left(\mathcal{D}_{26}\frac{\partial L_j}{\partial y} + \mathcal{D}_{66}\frac{\partial L_j}{\partial x}\right)$$

$${}'M_{i+3,j} = \frac{\partial L_i}{\partial y}\left(\mathcal{D}_{12}\frac{\partial L_j}{\partial x} + \mathcal{D}_{26}\frac{\partial L_j}{\partial y}\right) + \frac{\partial L_i}{\partial x}\left(\mathcal{D}_{16}\frac{\partial L_j}{\partial y} + \mathcal{D}_{66}\frac{\partial L_k}{\partial x}\right)$$

$${}'M_{i+3,j+3} = \frac{\partial L_i}{\partial y}\left(\mathcal{D}_{22}\frac{\partial L_j}{\partial y} + \mathcal{D}_{26}\frac{\partial L_j}{\partial x}\right) + \frac{\partial L_i}{\partial x}\left(\mathcal{D}_{26}\frac{\partial L_j}{\partial y} + \mathcal{D}_{66}\frac{\partial L_j}{\partial x}\right)$$

$${}'M_{i+6,j+6} = \frac{\partial L_i}{\partial y}\left(\mathcal{D}_{44}\frac{\partial L_k}{\partial y} + \mathcal{D}_{45}\frac{\partial L_j}{\partial x}\right) + \frac{\partial L_i}{\partial x}\left(\mathcal{D}_{45}\frac{\partial L_k}{\partial y} + \mathcal{D}_{55}\frac{\partial L_j}{\partial x}\right)$$

$${}'M_{i+6,j} = M_{i+6,j+3} \quad {}'M_{i,j+6} = M_{i+3,j+6} = 0 \quad i,j = 1,2,3 \qquad \text{(II.11)}$$

(where the L_i are the same as the shape functions N_i)

Looking now at the integrals

$$\int_V \tilde{N}^T L_o^T D L_o \hat{N} dV + \left(\int_V \tilde{N}^T L_o^T D L_o \hat{N} dV\right)^T \qquad \text{(II.12)}$$

The sum of these two integrals is a symmetric matrix. The matrices $\tilde{N}$ and L_o do not depend on Z, but the matrices D and $\hat{N}$ do have Z dependence. The integration can be accounted for by defining a new constituitive matrix $\mathcal{D}$

where

$$\mathcal{D}_{ij}^k = \frac{1}{6}\left(D_{ij}^k t_k^2 - D_{ij}^{k+1} t_{k+1}^2\right) + T_k \sum_{m=k+1}^{n} D_{ij}^m t_m$$

i,j = 1,2,3,6

k = interface numbers and layer number

n = number of layers

$$D^{k}_{ij} = \frac{1}{2} \sum_{m=k}^{k+1} D^{m}_{ij}\, t_m \qquad i,j = 4,5 \quad \text{(II.13)}$$

Using these definitions

$$\int_V \tilde{N}^T L_o^T D L_o \hat{N}\, dV = \frac{1}{2\Delta}\, {}^2M \qquad \text{(II.14)}$$

The elements of ${}^2M$ are

$${}^2M_{i,9+3k+j} = \frac{\partial L_i}{\partial x}\left(D^{k}_{11}\frac{\partial L_j}{\partial x} + D^{k}_{16}\frac{\partial L_j}{\partial y}\right) + \frac{\partial L_i}{\partial y}\left(D^{k}_{16}\frac{\partial L_j}{\partial x} + D^{k}_{66}\frac{\partial L_j}{\partial y}\right)$$

$${}^2M_{i,9+3(n+1+k)+j} = \frac{\partial L_i}{\partial x}\left(D^{k}_{12}\frac{\partial L_j}{\partial y} + D^{k}_{16}\frac{\partial L_j}{\partial x}\right) + \frac{\partial L_i}{\partial y}\left(D^{k}_{26}\frac{\partial L_j}{\partial y} + D^{k}_{66}\frac{\partial L_j}{\partial x}\right)$$

$${}^2M_{i+3,9+3k+j} = \frac{\partial L_i}{\partial y}\left(D^{k}_{12}\frac{\partial L_j}{\partial x} + D^{k}_{26}\frac{\partial L_j}{\partial y}\right) + \frac{\partial L_i}{\partial x}\left(D^{k}_{16}\frac{\partial L_j}{\partial x} + D^{k}_{66}\frac{\partial L_j}{\partial y}\right)$$

$${}^2M_{i+3,9+3(n+1+k)+j} = \frac{\partial L_i}{\partial y}\left(D^{k}_{22}\frac{\partial L_j}{\partial y} + D^{k}_{26}\frac{\partial L_j}{\partial x}\right) + \frac{\partial L_i}{\partial x}\left(D^{k}_{26}\frac{\partial L_j}{\partial y} + D^{k}_{66}\frac{\partial L_j}{\partial x}\right)$$

$${}^2M_{i+6,9+3k+j} = \frac{2\int L_i}{\Delta}\left(D^{k}_{45}\frac{\partial L_j}{\partial y} + D^{k}_{55}\frac{\partial L_j}{\partial x}\right)$$

$${}^2M_{i+6,9+3(n+1+k)+j} = \frac{2\int L_i}{\Delta}\left(D^{k}_{44}\frac{\partial L_j}{\partial y} + D^{k}_{45}\frac{\partial L_j}{\partial x}\right) \qquad \begin{matrix} i,j = 1,2,3 \\ k = 0,1,\cdots,n \end{matrix} \quad \text{(II.15)}$$

where

$$\int L_j = \int_x \int_y L_j\, dy\, dx$$

Using equation (II.3)

$${}^3M = {}^2M^T$$

Examining the last part of the linear stiffness matrix, we now integrate the expression

$$\int_V [\hat{N}]^T [L_o]^T [D] [L_o] [\hat{N}]\, dV \qquad \text{(II.16)}$$

The integration over z is accounted for by defining terms of the constituitive matrix by

$$D_{ij}^{kl} = \begin{cases} \frac{1}{20}\left(D_{ij}^{l} t_l^3 + D_{ij}^{l+1} t_{l+1}^3\right) - \frac{1}{6} D_{ij}^{l} t_{l+1}^2 \left(t_l + t_{l+1}\right) + T_l T_l \sum_{m=l+1}^{n} D_{ij}^{m} t_m & \text{for } K = l \\ \frac{1}{120} D_{ij}^{l} t_l^3 + \frac{1}{6} T_K \left(D_{ij}^{l} t_l^2 - D_{ij}^{l+1} t_{l+1}^2\right) + T_K T_l \sum_{m=l+1}^{n} D_{ij}^{m} t_m & \text{for } K = l-1 \\ \frac{1}{120} D_{ij}^{K} t_K^3 + \frac{1}{6} T_l \left(D_{ij}^{K} t_K^2 - D_{ij}^{K+1} t_{K+1}^2\right) + T_K T_l \sum_{m=K+1}^{n} D_{ij}^{m} t_m & \text{for } l = K-1 \\ \frac{1}{6} T_K \left(D_{ij}^{l} t_l^2 - D_{ij}^{l+1} t_{l+1}^2\right) + T_K T_l \sum_{m=l+1}^{n} D_{ij}^{m} t_m & \text{for } K < l-1 \\ \frac{1}{6} T_l \left(D_{ij}^{K} t_K^2 - D_{ij}^{K+1}\right. & \end{cases}$$

$$D_{ij}^{kl} = \begin{cases} \frac{1}{3}\left(D_{ij}^{l} t_l + D_{ij}^{l+1} t_{l+1}\right) & K = l \\ \frac{1}{6} D_{ij}^{l} t_l & K = l-1 \\ \frac{1}{6} D_{ij}^{K} t_K & K = l+1 \\ 0 & K < l-1,\ l < K-1 \end{cases} \qquad \begin{matrix} \text{(II.17)} \\ i,j = 4,5 \\ K,l = 0,\cdots,n \end{matrix}$$

Using these definitions and defining

$$\int_V \hat{N} L_o D L_o \hat{N} \, dV = \frac{1}{2\Delta} {}^{A}M \qquad \text{(II.18)}$$

the terms in this portion of the element stiffness matrix are given by

$$(4)M_{q+i+3R,\,9+j+3l} = \frac{dL_i}{dx}\left(D_{11}^{kl}\frac{dL_j}{dx} + D_{16}^{kl}\frac{dL_j}{dy} + \frac{2}{\Delta} D_{55}^{kl} \int L_i L_j + \right.$$
$$\left. \frac{dL_i}{dy}\left(D_{16}^{kl}\frac{dL_j}{dx} + D_{66}^{kl}\frac{dL_j}{dy}\right)\right.$$

$$(4)\ M_{9+i+3(n+1+k),\,9+j+3(n+1+\ell)} = \frac{\partial L_i}{\partial Y}\left(D_{22}^{k\ell}\frac{\partial L_j}{\partial Y} + D_{26}\frac{\partial L_j}{\partial x}\right) + \frac{2}{\Delta} D_{44}^{k\ell}\int L_i L_j + \frac{\partial L_i}{\partial x}\left(D_{26}^{k\ell}\frac{\partial L_j}{\partial x}\right)$$

$$(4)\ M_{9+i+3k,\,9+j+3(n+1+\ell)} = \frac{\partial L_i}{\partial x}\left(D_{12}^{k\ell}\frac{\partial L_j}{\partial Y} + D_{16}^{k\ell}\frac{\partial L_j}{\partial x}\right) + \frac{2}{\Delta} D_{45}^{k\ell}\int L_i L_j + \frac{\partial L_i}{\partial Y}\left(D_{26}^{k\ell}\frac{\partial L_j}{\partial Y} + D_{66}^{k\ell}\frac{\partial L_j}{\partial x}\right)$$

$$(4)\ M_{9+j+3(n+1+\ell),\,9+i+3k} = M_{9+i+3k,\,9+j+3(n+1+\ell)}$$

$$\text{WHERE } \int L_i L_j = \int_x \int_y L_i L_j \, dx\, dy \qquad (II.19)$$

$i, j = 1, 2, 3$

$k, \ell = 0, 1, \ldots n$

Then the total linear element stiffness matrix is

$$\left[K_L^E\right] = \frac{1}{2\Delta}\left[{}^1M + {}^2M + {}^3M + {}^4M\right] \qquad (II.20)$$

From equation (3.69) there are three parts to the nonlinear stiffness matrix.

$$\left[K_{NL}^E\right] = \int_V \left[\tilde{N}+\hat{N}\right]^T \left[L_0\right]^T \left[D\right]\left[\tilde{L}_1+\hat{L}_1\right]\left[\tilde{N}+\hat{N}\right] dV + \left(\int_V \left[\tilde{N}+\hat{N}\right]^T \left[L_0\right]^T \left[D\right]\left[\tilde{L}_1+\hat{L}_1\right]\left[\tilde{N}+\hat{N}\right] dV\right)^T + \int_V \left[\tilde{N}+\hat{N}\right]^T \left[\tilde{L}_1+\hat{L}_1\right]^T \left[D\right]\left[\tilde{L}_1+\hat{L}_1\right]\left[\tilde{N}+\hat{N}\right] dV \qquad (II.21)$$

Looking first at the portion composed of a matrix and its transpose and expanding.

$$\int_V [\tilde{N}+\hat{N}]^T [L_0]^T [D] [\tilde{L}_1+\hat{L}_1] [\tilde{N}+\hat{N}]\, dV + \left(\int_V [\tilde{N}+\hat{N}]^T [L_0]^T [D] [\tilde{L}_1+\hat{L}_1] [\tilde{N}+\hat{N}]\, dV\right)^T$$

$$= \int_V \{\tilde{N}^T L_0^T D \tilde{L}_1 \tilde{N} + \tilde{N}^T L_0^T D \tilde{L}_1 \hat{N} + \tilde{N}^T L_0^T D \hat{L}_1 \tilde{N} + \tilde{N}^T L_0^T D \hat{L}_1 \hat{N} +$$

$$\hat{N}^T L_0^T D \tilde{L}_1 \tilde{N} + \hat{N}^T L_0^T D \tilde{L}_1 \hat{N} + \hat{N}^T L_0^T D \hat{L}_1 \tilde{N} + \hat{N}^T L_0^T D \hat{L}_1 \hat{N}\} dV$$

$$+ \int_V \{\tilde{N}^T \tilde{L}_1^T D L_0 \tilde{N} + \tilde{N}^T \tilde{L}_1^T D L_0 \hat{N} + \tilde{N}^T \hat{L}_1^T D L_0 \tilde{N} + \tilde{N}^T \tilde{L}_1^T D L_0 \hat{N}$$

$$+ \hat{N}^T \tilde{L}_1^T D L_0 \tilde{N} + \hat{N}^T \tilde{L}_1^T D L_0 \hat{N} + \hat{N}^T \hat{L}_1 D L_0 \tilde{N} + \hat{N}^T \hat{L}_1^T D L_0 \hat{N}\} dV \qquad \text{(II.22)}$$

Since the second matrix integral is the transpose of the first, it will not be calculated, but the transpose of the first integral will be added to the nonlinear portion of the element stiffness matrix.

As stated in Chapter 3, I have assumed that the rotation will be small.

Using this assumption, any term containing $[\hat{L}_1]$ can be eliminated since this matrix contains the rotation terms and the derivatives of the rotation terms. Applying this assumption, Equation (II.22) becomes

$$\int_V [\tilde{N}+\hat{N}]^T [L_0]^T [D] [\tilde{L}_1+\hat{L}_1] [\tilde{N}+\hat{N}]\, dV \approx$$

$$\int_V \{\tilde{N}^T L_0^T D \tilde{L}_1 \tilde{N} + \tilde{N}^T L_0^T D \tilde{L}_1 \hat{N} + \hat{N}^T L_0^T D \tilde{L}_1 \tilde{N} + \hat{N} L_0^T D \tilde{L}_1 \tilde{N}\} \qquad \text{(II.23)}$$

Examining the first part of this integral, $\int_V \tilde{N}^T L_0^T D \tilde{L}_1 \tilde{N}\, dV$, the only matrix that varies with z is $[D]$; therefore

$$\int_V \tilde{N}^T L_0^T D \tilde{L}_1 \tilde{N}\, dV = \int_x \int_y \tilde{N}^T L_0^T \left(\int_z D\, dz\right) \tilde{L}_1 \tilde{N}\, dy\, dx \qquad \text{(II.24)}$$

Using equation (II.9)

$$\int_V \tilde{N}^T L_o^T D \tilde{L} \tilde{N} \, dV = \int_x \int_y \tilde{N}^T L_o^T D \tilde{L}_1 \tilde{N} \, dy \, dx$$

$$\int_x \int_y \tilde{N}^T L_o^T D \tilde{L}_1 \tilde{N} \, dy \, dx = \frac{1}{2\Delta} {}^5M \qquad \text{(II.25)}$$

where

$$ {}^5M_{i,j+3(k-1)} = \frac{1}{2} \frac{\partial \tilde{u}_k}{\partial x} \frac{\partial L_j}{\partial x} \left(D_{11} \frac{\partial L_i}{\partial x} + D_{16} \frac{\partial L_i}{\partial y} \right) + \frac{1}{2} \frac{\partial \tilde{u}_k}{\partial y} \frac{\partial L_j}{\partial y} \left(D_{12} \frac{\partial L_i}{\partial x} + D_{26} \frac{\partial L_i}{\partial y} \right) + \frac{\partial \tilde{u}_k}{\partial x} \frac{\partial L_j}{\partial y} \left(D_{16} \frac{\partial L_i}{\partial x} + D_{66} \frac{\partial L_i}{\partial y} \right)$$

$$ {}^5M_{i+3,j+3(k-1)} = \frac{1}{2} \frac{\partial \tilde{u}_k}{\partial x} \frac{\partial L_j}{\partial x} \left(D_{12} \frac{\partial L_i}{\partial x} \right) + \frac{1}{2} \frac{\partial \tilde{u}_k}{\partial y} \frac{\partial L_j}{\partial y} \left(D_{22} \frac{\partial L_i}{\partial y} + D_{26} \frac{\partial L_i}{\partial x} \right) + \frac{\partial \tilde{u}_k}{\partial x} \frac{\partial L_j}{\partial y} \left(D_{26} \frac{\partial L_i}{\partial y} + D_{66} \frac{\partial L_i}{\partial x} \right)$$

$$i, j, k = 1, 2, 3 \qquad \text{(II.26)}$$

where $\tilde{u}_1 = \tilde{u}$

$\tilde{u}_2 = \tilde{v}$

$\tilde{u}_3 = w$

Now let ${}^6M = {}^5M^T$

The next part of equation (II.23) to be examined is

$$\int_V \hat{N}^T L_o^T D \tilde{L}_1 \hat{N} \, dV \qquad \text{(II.27)}$$

The integration over Z can be accounted for by using the elastic constants defined by equation (II.17). Using these definitions, the integral becomes

$$\int_V \hat{N}^T L_o^T D \tilde{L}_1 \hat{N} \, dV = \frac{1}{2\Delta} {}^7M \qquad \text{(II.28)}$$

$$
{}^{(7)}M_{9+i+3k,9+j+3l} = \frac{\partial L_i}{\partial x}\left(\frac{1}{2}D_{11}^{kl}\frac{\partial \tilde{u}}{\partial x}\frac{\partial L_j}{\partial x} + \frac{1}{2}D_{12}^{kl}\frac{\partial \tilde{u}}{\partial y}\frac{\partial L_j}{\partial y} + D_{16}^{kl}\frac{\partial \tilde{u}}{\partial x}\frac{\partial L_j}{\partial y}\right) + \frac{2S_{L_i L_j}}{\Delta}\left(D_{45}^{kl}\frac{\partial \tilde{u}}{\partial y} + D_{55}^{kl}\frac{\partial \tilde{u}}{\partial x}\right) + \frac{\partial L_j}{\partial y}\left(\frac{1}{2}D_{16}^{kl}\frac{\partial \tilde{u}}{\partial x}\frac{\partial L_j}{\partial x} + \frac{1}{2}D_{26}^{kl}\frac{\partial \tilde{u}}{\partial y}\frac{\partial L_j}{\partial y} + D_{66}\frac{\partial \tilde{u}}{\partial x}\frac{\partial L_j}{\partial y}\right)
$$

$$
{}^{(8)}M_{9+i+3(n+1+k),9+j+3l} = \frac{\partial L_i}{\partial y}\left(\frac{1}{2}D_{12}^{kl}\frac{\partial \tilde{u}}{\partial x}\frac{\partial L_j}{\partial x} + \frac{1}{2}D_{22}^{kl}\frac{\partial \tilde{u}}{\partial y}\frac{\partial L_j}{\partial y} + D_{26}^{kl}\frac{\partial \tilde{u}}{\partial x}\frac{\partial L_j}{\partial y}\right) + \frac{2S_{L_i L_j}}{\Delta}\left(D_{44}^{kl}\frac{\partial \tilde{u}}{\partial y} + D_{45}^{kl}\frac{\partial \tilde{u}}{\partial x}\right) + \frac{\partial L_i}{\partial x}\left(\frac{1}{2}D_{16}^{kl}\frac{\partial \tilde{u}}{\partial x}\frac{\partial L_j}{\partial x} + \frac{1}{2}D_{26}^{kl}\frac{\partial \tilde{u}}{\partial y}\frac{\partial L_j}{\partial y} + D_{66}^{kl}\frac{\partial \tilde{u}}{\partial x}\frac{\partial L_j}{\partial x}\right)
$$

$$
{}^{(9)}M_{9+i+3k,9+j+3(n+1+l)} = \frac{\partial L_i}{\partial x}\left(\frac{1}{2}D_{11}^{kl}\frac{\partial \tilde{v}}{\partial x}\frac{\partial L_j}{\partial x} + \frac{1}{2}D_{12}^{kl}\frac{\partial \tilde{v}}{\partial y}\frac{\partial L_j}{\partial y} + D_{16}^{kl}\frac{\partial \tilde{v}}{\partial y}\frac{\partial L_j}{\partial x}\right) + \frac{2S_{L_i L_j}}{\Delta}\left(D_{45}^{kl}\frac{\partial \tilde{v}}{\partial y} + D_{55}^{kl}\frac{\partial \tilde{v}}{\partial x}\right) + \frac{\partial L_i}{\partial y}\left(\frac{1}{2}D_{16}^{kl}\frac{\partial \tilde{v}}{\partial x}\frac{\partial L_j}{\partial x} + \frac{1}{2}D_{26}^{kl}\frac{\partial \tilde{v}}{\partial y}\frac{\partial L_j}{\partial y} + D_{66}\frac{\partial \tilde{v}}{\partial y}\frac{\partial L_j}{\partial x}\right)
$$

$$
{}^{(10)}M_{9+i+3(n+1+k),9+j+3(n+1+l)} = \frac{\partial L_i}{\partial y}\left(\frac{1}{2}D_{12}^{kl}\frac{\partial \tilde{v}}{\partial x}\frac{\partial L_j}{\partial x} + \frac{1}{2}D_{22}^{kl}\frac{\partial \tilde{v}}{\partial y}\frac{\partial L_j}{\partial y} + D_{26}^{kl}\frac{\partial \tilde{v}}{\partial y}\frac{\partial L_j}{\partial x}\right) + \frac{2S_{L_i L_j}}{\Delta}\left(D_{44}^{kl}\frac{\partial \tilde{v}}{\partial y} + D_{45}^{kl}\frac{\partial \tilde{v}}{\partial x}\right) + \frac{\partial L_i}{\partial x}\left(\frac{1}{2}D_{16}^{kl}\frac{\partial \tilde{v}}{\partial x}\frac{\partial L_j}{\partial x} + \frac{1}{2}D_{26}^{kl}\frac{\partial \tilde{v}}{\partial y}\frac{\partial L_j}{\partial y} + D_{66}^{kl}\frac{\partial \tilde{v}}{\partial y}\frac{\partial L_j}{\partial x}\right) \tag{II.29}
$$

$$
i,j = 1,2,3
$$
$$
k,l = 0,1,\cdots,n
$$

Also let $$ {}^{8}M = {}^{7}M^{T} \tag{II.30}$$

Looking at the next integral

$$\int_V \tilde{N}^T L_0^T D \tilde{L}_i \hat{N}_j dV \tag{II.31}$$

The Z integration is accounted for by using the elastic constant definition, equation (II.13). Then

$$\int_V \tilde{N}^T L_0^T D \tilde{L}_i \hat{N}_j dV = \frac{1}{2\Delta}\,{}^{9}M \tag{II.32}$$

$$
{}^{9}M_{i,9+j+3K} = \frac{\partial L_i}{\partial x}\left(\frac{1}{2}D_{11}^{K}\frac{\partial \tilde{u}}{\partial x}\frac{\partial L_i}{\partial x} + \frac{1}{2}D_{12}^{K}\frac{\partial \tilde{u}}{\partial y}\frac{\partial L_i}{\partial y} + D_{16}^{K}\frac{\partial \tilde{u}}{\partial x}\frac{\partial L_i}{\partial y}\right) + \frac{\partial L_i}{\partial y}\left(\frac{1}{2}D_{16}^{K}\frac{\partial \tilde{u}}{\partial x}\frac{\partial L_i}{\partial x} + \frac{1}{2}D_{26}^{K}\frac{\partial \tilde{u}}{\partial y}\frac{\partial L_i}{\partial y} + D_{66}^{K}\frac{\partial \tilde{u}}{\partial x}\frac{\partial L_i}{\partial y}\right)
$$

$$
{}^{9}M_{i+3,9+j+3K} = \frac{\partial L_i}{\partial y}\left(\frac{1}{2}D_{12}^{K}\frac{\partial \tilde{u}}{\partial x}\frac{\partial L_i}{\partial x} + \frac{1}{2}D_{22}^{K}\frac{\partial \tilde{u}}{\partial y}\frac{\partial L_i}{\partial y} + D_{26}^{K}\frac{\partial \tilde{u}}{\partial x}\frac{\partial L_i}{\partial y}\right) + \frac{\partial L_i}{\partial x}\left(\frac{1}{2}D_{16}^{K}\frac{\partial \tilde{u}}{\partial x}\frac{\partial L_i}{\partial x} + \frac{1}{2}D_{26}^{K}\frac{\partial \tilde{u}}{\partial y}\frac{\partial L_i}{\partial y} + D_{66}^{K}\frac{\partial \tilde{u}}{\partial x}\frac{\partial L_i}{\partial y}\right)
$$

$$
{}^{9}M_{i+6,9+j+3K} = \frac{\partial L_i}{\partial y}\frac{2\int L_i}{\Delta}\left(D_{44}^{K}\frac{\partial \tilde{u}}{\partial y} + D_{45}^{K}\frac{\partial \tilde{u}}{\partial x}\right) + \frac{\partial L_i}{\partial x}\frac{2\int L_i}{\Delta}\left(D_{45}^{K}\frac{\partial \tilde{u}}{\partial y} + D_{55}^{K}\frac{\partial \tilde{u}}{\partial x}\right)
$$

$$
{}^{9}M_{i,9+j+3(n+1+K)} = \frac{\partial L_i}{\partial x}\left(\frac{1}{2}D_{11}^{K}\frac{\partial \tilde{v}}{\partial x}\frac{\partial L_i}{\partial x} + \frac{1}{2}D_{12}^{K}\frac{\partial \tilde{v}}{\partial y}\frac{\partial L_i}{\partial y} + D_{16}^{K}\frac{\partial \tilde{v}}{\partial y}\frac{\partial L_i}{\partial x}\right) + \frac{\partial L_i}{\partial y}\left(\frac{1}{2}D_{16}^{K}\frac{\partial \tilde{v}}{\partial x}\frac{\partial L_i}{\partial x} + \frac{1}{2}D_{26}^{K}\frac{\partial \tilde{v}}{\partial y}\frac{\partial L_i}{\partial y} + D_{66}^{K}\frac{\partial \tilde{v}}{\partial y}\frac{\partial L_i}{\partial x}\right)
$$

$$
{}^{9}M_{i+3,9+j+3(n+1+K)} = \frac{\partial L_i}{\partial y}\left(\frac{1}{2}D_{12}^{K}\frac{\partial \tilde{v}}{\partial x}\frac{\partial L_i}{\partial x} + \frac{1}{2}D_{22}^{K}\frac{\partial \tilde{v}}{\partial y}\frac{\partial L_i}{\partial y} + D_{26}^{K}\frac{\partial \tilde{v}}{\partial y}\frac{\partial L_i}{\partial x}\right) + \frac{\partial L_i}{\partial x}\left(\frac{1}{2}D_{16}^{K}\frac{\partial \tilde{v}}{\partial x}\frac{\partial L_i}{\partial x} + \frac{1}{2}D_{26}^{K}\frac{\partial \tilde{v}}{\partial y}\frac{\partial L_i}{\partial y} + D_{66}^{K}\frac{\partial \tilde{v}}{\partial y}\frac{\partial L_i}{\partial x}\right)
$$

$$
{}^{9}M_{i+6,9+j+3(n+1+K)} = \frac{\partial L_i}{\partial y}\frac{2\int L_i}{\Delta}\left(D_{44}^{K}\frac{\partial \tilde{v}}{\partial y} + D_{45}^{K}\frac{\partial \tilde{v}}{\partial x}\right) + \frac{\partial L_i}{\partial x}\frac{2\int L_i}{\Delta}\left(D_{45}^{K}\frac{\partial \tilde{v}}{\partial y} + D_{55}^{K}\frac{\partial \tilde{v}}{\partial x}\right)
$$

$$
i,j = 1,2,3
$$

$$
K = 0,1,\cdots,n \qquad \text{(II.33)}
$$

Also,

$$
{}^{10}M = {}^{9}M^{T} \qquad \text{(II.34)}
$$

The last integral in this series is

$$\int_V \hat{N}^T L_o^T D \tilde{L}_1 \tilde{N} \, dV \tag{II.35}$$

Using (II.13), accounts for the $\bar{z}$ integration.

Then

$$\int_V \hat{N}^T L_o^T D \tilde{L}_1 \tilde{N} \, dV = \frac{1}{2\Delta} \, {}''M \tag{II.36}$$

The terms of ${}''M$ are given by

$$
\begin{aligned}
{}''M_{9i+3k,\, j+3(\ell-1)} &= \frac{1}{2} \frac{\partial \tilde{u}_\ell}{\partial x} \frac{\partial L_i}{\partial x} \left(D_{11}^k \frac{\partial L_i}{\partial x} + D_{16}^k \frac{\partial L_i}{\partial y} \right) + \frac{1}{2} \frac{\partial \tilde{u}_\ell}{\partial y} \frac{\partial L_i}{\partial y} \\
&\left(D_{12}^k \frac{\partial L_i}{\partial x} + D_{26}^k \frac{\partial L_i}{\partial y} \right) + \frac{\partial \tilde{u}_\ell}{\partial x} \frac{\partial L_i}{\partial y} \left(D_{16}^k \frac{\partial L_i}{\partial x} + D_{66}^k \frac{\partial L_i}{\partial y} \right)
\end{aligned}
$$

$$
\begin{aligned}
{}''M_{9i+3(n+1+k),\, j+3(\ell-1)} &= \frac{1}{2} \frac{\partial \tilde{u}_\ell}{\partial x} \frac{\partial L_i}{\partial x} \left(D_{12}^k \frac{\partial L_i}{\partial y} + D_{16}^k \frac{\partial L_i}{\partial x} \right) + \frac{1}{2} \frac{\partial \tilde{u}_\ell}{\partial y} \frac{\partial L_i}{\partial y} \\
&\left(D_{22}^k \frac{\partial L_i}{\partial y} + D_{26}^k \frac{\partial L_i}{\partial x} \right) + \frac{\partial \tilde{u}_\ell}{\partial x} \frac{\partial L_i}{\partial y} \left(D_{26}^k \frac{\partial L_i}{\partial y} + D_{66}^k \frac{\partial L_i}{\partial x} \right)
\end{aligned}
$$

(II.37)

$i, j, \ell = 1, 2, 3$

$k = 0, 1, \cdots, n$

where $\tilde{u}_1 = \tilde{u}$

$\tilde{u}_2 = \tilde{v}$

$\tilde{u}_3 = w$

Further, let

$${}^{12}M = {}''M^T \tag{II.38}$$

The last part of the nonlinear stiffness matrix is

$$\int_V [\tilde{N}+\hat{N}]^T [\tilde{L}_1+\hat{L}_1]^T [D][\tilde{L}_1+\hat{L}_1][\tilde{N}+\hat{N}]\,dV \tag{II.30}$$

Expanding this integral and eliminating $\hat{L}_1$ terms

$$\int_V [\tilde{N}+\hat{N}]^T [\tilde{L}_1+\hat{L}_1]^T [D][\tilde{L}_1+\hat{L}_1][\tilde{N}+\hat{N}]\,dV \approx \int_V \{\tilde{N}^T \tilde{L}_1^T D \tilde{L}_1 \tilde{N} +$$

$$\tilde{N}^T \tilde{L}_1^T D \tilde{L}_1 \hat{N} + \hat{N}^T \tilde{L}_1^T D \tilde{L}_1 \tilde{N} + \hat{N}^T \tilde{L}_1^T D \tilde{L}_1 \hat{N}\}\,dV \tag{II.40}$$

Since $\tilde{N}^T \tilde{L}_1^T D \tilde{L}_1 \hat{N} = (\hat{N}^T \tilde{L}_1^T D \tilde{L}_1 \tilde{N})^T$, equation (II.40) becomes

$$\int_V [\tilde{N}+\hat{N}]^T [\tilde{L}_1+\hat{L}_1]^T [D][\tilde{L}_1+\hat{L}_1][\tilde{N}+\hat{N}]\,dV \approx$$

$$\int_V \{\tilde{N}^T \tilde{L}_1^T D \tilde{L}_1 \hat{N} + \hat{N}^T \tilde{L}_1^T D \tilde{L}_1 \hat{N} + (\tilde{N}^T \tilde{L}_1^T D \tilde{L}_1 \hat{N})^T +$$

$$\hat{N} \tilde{L}_1^T D \tilde{L}_1 \hat{N}\}\,dV \tag{II.41}$$

Examining the first term of (II.41) and using (II.9) to defin elastic constants

$$\int_V \tilde{N}^T \tilde{L}_1^T D \tilde{L}_1 \hat{N}\,dV = \frac{1}{2\Delta}\,{}^{13}M \tag{II.42}$$

where the terms of ${}^{13}M$ are

$${}^{13}M_{i+3(k-1),j+3(\ell-1)} = \frac{1}{2}\frac{\partial \tilde{u}_k}{\partial x}\frac{\partial L_i}{\partial x}\left(\frac{1}{2}D_{11}\frac{\partial \tilde{u}_\ell}{\partial x}\frac{\partial L_j}{\partial x} + \frac{1}{2}D_{12}\frac{\partial \tilde{u}_\ell}{\partial y}\frac{\partial L_j}{\partial y} + D_{16}\frac{\partial \tilde{u}_\ell}{\partial x}\frac{\partial L_j}{\partial y}\right) +$$
$$\frac{1}{2}\frac{\partial \tilde{u}_k}{\partial y}\frac{\partial L_i}{\partial y}\left(\frac{1}{2}D_{12}\frac{\partial \tilde{u}_\ell}{\partial x}\frac{\partial L_j}{\partial x} + \frac{1}{2}D_{22}\frac{\partial \tilde{u}_\ell}{\partial y}\frac{\partial L_j}{\partial y} + D_{26}\frac{\partial \tilde{u}_\ell}{\partial x}\frac{\partial L_j}{\partial y}\right) +$$
$$\frac{\partial \tilde{u}_k}{\partial x}\frac{\partial L_i}{\partial y}\left(\frac{1}{2}D_{16}\frac{\partial \tilde{u}_\ell}{\partial x}\frac{\partial L_j}{\partial x} + \frac{1}{2}D_{26}\frac{\partial \tilde{u}_\ell}{\partial y}\frac{\partial L_j}{\partial y} + D_{66}\frac{\partial \tilde{u}_\ell}{\partial x}\frac{\partial L_j}{\partial y}\right)$$
$$i,j,k,\ell = 1,2,3 \tag{II.43}$$

The next term in (II.41) is

$$\int_V \tilde{N}^T \tilde{L}_1^T D \tilde{L}_1 \hat{N} \, dV \tag{II.44}$$

By using equation (II.13) and defining a new matrix ^{14}M, the result is

$$\int_V \tilde{N}^T \tilde{L}_1 D \tilde{L}_1 \hat{N} \, dV = \frac{1}{2\Delta} \, {}^{14}M \tag{II.45}$$

where

$$\begin{aligned} {}^{14}M_{9+i+3(k-1),\, j+3(\ell-1)(n+1)+3m} = {} & \frac{1}{2} \frac{\partial \tilde{u}_k}{\partial x} \frac{\partial L_i}{\partial x} \left(\frac{1}{2} D_{11}^m \frac{\partial \tilde{u}_\ell}{\partial x} \frac{\partial L_j}{\partial x} + \frac{1}{2} D_{12}^m \frac{\partial \tilde{u}_\ell}{\partial y} \frac{\partial L_j}{\partial y} + \right. \\ & \left. D_{16}^m \frac{\partial \tilde{u}_k}{\partial x} \frac{\partial L_j}{\partial y} \right) + \frac{1}{2} \frac{\partial \tilde{u}_k}{\partial y} \frac{\partial L_i}{\partial y} \left(\frac{1}{2} D_{12}^m \frac{\partial \tilde{u}_\ell}{\partial x} \frac{\partial L_j}{\partial x} + \right. \\ & \left. \frac{1}{2} D_{22}^m \frac{\partial \tilde{u}_\ell}{\partial y} \frac{\partial L_j}{\partial y} + D_{26}^m \frac{\partial \tilde{u}_\ell}{\partial x} \frac{\partial L_j}{\partial y} \right) + \frac{\partial \tilde{u}_k}{\partial x} \frac{\partial L_i}{\partial y} \\ & \left(\frac{1}{2} D_{16}^m \frac{\partial \tilde{u}_\ell}{\partial x} \frac{\partial L_j}{\partial x} + \frac{1}{2} D_{26}^m \frac{\partial \tilde{u}_\ell}{\partial y} \frac{\partial L_j}{\partial y} + D_{66}^m \frac{\partial \tilde{u}_\ell}{\partial x} \frac{\partial L_j}{\partial y} \right) \end{aligned}$$

$$\ell = 1, 2$$
$$i, j, k = 1, 2, 3 \tag{II.46}$$
$$m = 0, 1, \cdots, n$$

To account for the third term in the integral (II.41)

let

$$^{15}M = {}^{14}M^T$$

The last part of (II.41) to reduce is

$$\int_V \hat{N}^T \tilde{L}_1^T D \tilde{L}_1 \hat{N} \, dV \tag{II.47}$$

The $\tilde{z}$ integration in this integral is accounted for by using the constituitive matrix defined by (II.17). The integral is then represented by

$$\int_v \hat{N} \tilde{L}_i O \tilde{L}_j \hat{N} dV = \frac{1}{2\Delta} {}^{16}M \tag{II.48}$$

where

$$
\begin{aligned}
{}^{16}M_{9+i+3k+3(m-1)(n+1),\,9+j+3l+3(p-1)(n+1)} = {} & \frac{1}{2}\frac{\partial \tilde{u}_m}{\partial x}\frac{\partial L_i}{\partial x}\left(\frac{1}{2}D_{11}^{kl}\frac{\partial \tilde{u}_p}{\partial x}\frac{\partial L_j}{\partial x} + \right. \\
& \frac{1}{2}D_{12}^{kl}\frac{\partial \tilde{u}_p}{\partial y}\frac{\partial L_j}{\partial y} + D_{16}^{kl}\frac{\partial \tilde{u}_p}{\partial x}\frac{\partial L_j}{\partial y}\Big) + \frac{1}{2}\frac{\partial \tilde{u}_m}{\partial y}\frac{\partial L_i}{\partial y}\left(\frac{1}{2}D_{12}^{kl}\frac{\partial \tilde{u}_p}{\partial x}\frac{\partial L_j}{\partial x} + \right. \\
& \frac{1}{2}D_{22}^{kl}\frac{\partial \tilde{u}_p}{\partial y}\frac{\partial L_j}{\partial y} + D_{26}\frac{\partial \tilde{u}_p}{\partial x}\frac{\partial L_j}{\partial y}\Big) + \frac{2\int L_i L_j}{\Delta}\frac{\partial \tilde{u}_m}{\partial y}\left(D_{44}^{kl}\frac{\partial \tilde{u}_p}{\partial y} + \right. \\
& D_{45}^{kl}\frac{\partial \tilde{u}_p}{\partial x}\Big) + \frac{2\int L_i L_j}{\Delta}\left(D_{45}^{kl}\frac{\partial \tilde{u}_p}{\partial y} + D_{55}^{kl}\frac{\partial \tilde{u}_p}{\partial x}\right) + \\
& \frac{\partial \tilde{u}_m}{\partial x}\frac{\partial L_i}{\partial y}\left(\frac{1}{2}D_{16}^{kl}\frac{\partial \tilde{u}_p}{\partial x}\frac{\partial L_j}{\partial x} + \frac{1}{2}D_{26}^{kl}\frac{\partial \tilde{u}_p}{\partial y}\frac{\partial L_j}{\partial y} + \right. \\
& \left. D_{66}^{kl}\frac{\partial \tilde{u}_p}{\partial x}\frac{\partial L_j}{\partial y}\right)
\end{aligned}
$$

$$i,j = 1,2,3$$
$$k,l = 0,1,\cdots,n$$
$$m,p = 1,2$$

(II.49)

The element nonlinear stiffness matrix is

$$[K_{NL}^E] = \frac{1}{2\Delta}\left[{}^{5}M + {}^{6}M + {}^{7}M + {}^{8}M + {}^{9}M + {}^{10}M + {}^{11}M + {}^{12}M + {}^{13}M + {}^{14}M + {}^{15}M + {}^{16}M\right] \tag{II.50}$$

APPENDIX III: Derivation of Current Stiffness Parameter

The objective of deriving the current stiffness parameter is to clarify the conditions which govern its use. The current stiffness parameter is a scalar which can be used to predict collapse loads for continuous structures. By using this scalar, the problem of examining the singularity of a nonlinear stiffness matrix is avoided.

As a structure becomes unstable, there will start to be an unlimited displacement for a small increase in load. Representing the continuous structure as an infinite number of degrees of freedom, this instability is represented mathematically as,

$$\frac{\partial a_i}{\partial q_i} \longrightarrow \infty \qquad i=1,2 \ldots \tag{III.1}$$

where a_i is a generalized displacement and q_i is a generalized force.

For general loadings, the sign of $\frac{\partial a_i}{\partial q_i}$ cannot be determined prior to collapse. If proportional loading is used, some conclusions can be drawn. Proportional loading is defined by

$$q_i = p(q_r)_i \qquad i=1,2 \ldots \tag{III.2}$$

where q_i is the load on the structure, p is a proportionality factor, and $(q_r)_i$ is an initial load which is less than the collapse load.

Even with proportional loading, the sign of $\frac{\partial a_i}{\partial q_i}$ cannot be determined, but the sign of $\frac{\partial (a_r)_i}{\partial (q_r)_i}$ will be the same as the sign of $\frac{\partial a_i}{\partial q_i}$ prior to collapse. Since these terms are the same sign, the ratio of these two scalars will be positive prior to collapse. Since $\frac{\partial a_i}{\partial q_i}$ becomes infinite as collapse and $\frac{\partial (a_r)_i}{\partial (q_r)_i}$ is some finite number, collapse is defined by

$$\frac{\frac{\partial (a_r)_i}{\partial (q_r)_i}}{\frac{\partial a_j}{\partial q_j}} = 0 \tag{III.3}$$

The point of instability is either a local maximum, a local minimum, or an inflexion point for the total load-displacement curve. If the point of instability is a local maximum or minimum, the sign of the derivative ratio

will change. If the point of instability is an inflexion point, the sign of the derivative ratio will not change. Since the derivative ratio relates the way the structure is currently carrying a load to the way it originally carried a load, it can be called a current stiffness parameter. Since it is good only for proportional loading, this must be indicated in the symbol, S_p

$$S_p = \frac{\frac{d(a_r)_i}{d(q_r)_i}}{\frac{da_j}{dq_j}} \qquad \text{(III.4)}$$

With this scalar, the current stability status of a structure can be determined, that is

$S_p > 0$ structure stable or past inflection point headed for collapse.

$S_p = 0$ collapse point.

$S_p < 0$ post collapse.

Since this structure is undergoing proportional loading, S_p can be further simplified.

Using the chain rule

$$\frac{da_i}{dq_i} = \frac{da_i}{d\rho}\,\frac{d\rho}{dq_i} \qquad \text{(III.5)}$$

Then

$$S_p = \frac{\frac{d(a_r)_i}{d\rho}\,\frac{d\rho}{d(q_r)_i}}{\frac{da_j}{d\rho}\,\frac{d\rho}{dq_j}} \qquad \text{(III.6)}$$

Now multiplying numerator and denominator by the scalar $\frac{d\rho}{da_k}\,\frac{dq_k}{d\rho}$

$$S_p = \frac{\frac{\partial (a_r)_i}{\partial \rho} \frac{\partial \rho}{\partial (q_r)_i} \frac{\partial \rho}{\partial a_K} \frac{\partial q_K}{\partial \rho}}{\frac{\partial a_\ell}{\partial \rho} \frac{\partial \rho}{\partial q_\ell} \frac{\partial \rho}{\partial a_m} \frac{\partial q_m}{\partial \rho}}$$

$$= \frac{\frac{\partial (a_r)_i}{\partial \rho} \frac{\partial \rho}{\partial a_K} \frac{\partial \rho}{\partial (q_r)_i} \frac{\partial q_K}{\partial \rho}}{\frac{\partial a_\ell}{\partial \rho} \frac{\partial \rho}{\partial a_m} \frac{\partial q_m}{\partial \rho} \frac{\partial \rho}{\partial q_j}}$$

$$= \frac{\frac{\partial (a_r)_i}{\partial \rho} \frac{\partial \rho}{\partial a_K} \frac{\partial \rho}{\partial (q_r)_i} \frac{\partial q_K}{\partial \rho}}{\frac{\partial a_\ell}{\partial a_m} \frac{\partial q_m}{\partial q_\ell}}$$

$$S_p = \frac{\frac{\partial (a_r)_i}{\partial \rho} \frac{\partial \rho}{\partial a_K} \frac{\partial \rho}{\partial (q_r)_i} \frac{\partial q_K}{\partial \rho}}{\delta_{\ell m} \delta_{m j}} \qquad \text{(III.7)}$$

where $\delta_{\ell m}$ is the Kronecker delta.

From the definition of proportional loading,

$$\frac{\partial (q_r)_K}{\partial \rho} = \frac{\partial q_K}{\partial \rho} = (q_r)_K \qquad \text{(III.8)}$$

Using this relation,

equation (IV.7) becomes

$$S_p = \frac{\frac{\partial (a_r)_i}{\partial \rho} \frac{\partial \rho}{\partial a_K} \frac{\partial \rho}{\partial (q_r)_i} \frac{\partial (q_r)_K}{\partial \rho}}{\delta_{\ell m} \delta_{m j}}$$

$$S_p = \frac{\frac{\partial (a_r)_i}{\partial \rho} \frac{\partial \rho}{\partial a_K} \frac{\partial (q_r)_K}{\partial (q_r)_i}}{}$$

$$S_p = \frac{\frac{\partial (a_r)_i}{\partial \rho} \frac{\partial \rho}{\partial a_K} \delta_{Ki}}{\delta_{\ell m} \delta_{m j}} \qquad \text{(III.9)}$$

but also

$$\delta_{ki} = \frac{\partial q_i}{\partial q_n} = \frac{\partial q_i}{\partial p}\frac{\partial p}{\partial q_k} \tag{III.10}$$

$$S_p = \frac{\frac{\partial (a_r)_i}{\partial p}\frac{\partial p}{\partial a_k}\frac{\partial q_i}{\partial p}\frac{\partial p}{\partial q_k}}{\delta_{jm}\delta_{mj}} \tag{III.11}$$

Multiplying numerator and denominator by the scalar $\frac{\partial a_a}{\partial p}\frac{\partial q_a}{\partial p}$

$$S_p = \frac{\frac{\partial (a_r)_i}{\partial p}\frac{\partial q_i}{\partial p}\frac{\partial p}{\partial a_k}\frac{\partial p}{\partial q_k}\frac{\partial a_n}{\partial p}\frac{\partial q_n}{\partial p}}{\delta_{jm}\delta_{mj}\frac{\partial a_s}{\partial p}\frac{\partial q_s}{\partial p}}$$

$$= \frac{\frac{\partial (a_r)_i}{\partial p}\frac{\partial q_i}{\partial p}\frac{\partial q_n}{\partial p}\frac{\partial p}{\partial q_k}\frac{\partial a_n}{\partial p}\frac{\partial p}{\partial a_k}}{\frac{\partial a_s}{\partial p}\frac{\partial q_s}{\partial p}\delta_{jm}\delta_{mj}}$$

$$S_p = \frac{\frac{\partial (a_r)_i}{\partial p}\frac{\partial q_i}{\partial p}\delta_{nk}\delta_{nk}}{\frac{\partial a_s}{\partial p}\frac{\partial q_s}{\partial p}\delta_{jm}\delta_{mj}} \tag{III.12}$$

since $\delta_{nk} = \delta_{kn}$ and j, k, m, and n are dummy variables

$$S_p = \frac{\frac{\partial (a_r)_i}{\partial p}\frac{\partial q_i}{\partial p}}{\frac{\partial a_s}{\partial p}\frac{\partial q_s}{\partial p}} \tag{III.13}$$

From the definition of proportional loading

$$\frac{\partial q_i}{\partial p} = (q_r)_i \tag{III.14}$$

Then the definition of the current stiffness parameter is

$$S_p = \frac{\frac{d(a_n)_i}{dp}(q_n)_i}{\frac{da_j}{dp}(q_n)_j} \qquad \text{(III.15)}$$

Since this research is based on finite element analysis, the tensors a_i and q_i are of finite dimension n, where n is the number of degrees of freedom. Since these tensors are finite dimensional, they can be represented as vectors. In vector form, the current stiffness parameter is

$$S_p = \frac{\frac{d\{a_n\}^T}{dp}\{q_n\}}{\frac{d\{a\}^T}{dp}\{q_n\}} \qquad \text{(III.16)}$$

The stability state of the structure can be evaluated by examining the sign of the current stiffness parameter as previously explained. This parameter can only be used when proportional loading is used.

VITA

William Paxton Witt,III was born 29 June 1948 in Carrollton, Illinois. He received a Bachelor of Science in Engineering Sciences and a commission in the U. S. Air Force from the U. S. Air Force Academy in June 1970. He earned a Master of Science in Astronautical Engineering from the Air Force Institute of Technology in December 1977 and started work on a PhD in Aerospace Engineering in January 1978.

END

FILMED

1-84

DTIC